# POLYNUCLEAR COORDINATION COMPLEXES OF SOME POLYISOINDOLINES AND POLYPHTHALAZINES



YISHENG ZHANG

# Polynuclear Coordination Complexes of Some Polyisoindolines and Polyphthalazines

by

©Yisheng Zhang, B.Eng., M.Sc.

A thesis submitted to

the School of Graduate Studies

in partial fulfilment of the

requirement for the degree of

Master of Science

Department of Chemistry
Memorial University of Newfoundland

July 1993

St.John's Newfoundland

ISBN 0-315-86665-9

Canada

## Abstract

In an attempt to enhance the bulk extended magnetic properties of antiferromagnetically coupled Cu(II) complexes a series of tetranuclear, hexanuclear and octanuclear Cu(II) coordination complexes of some dendritic polyphthalazine ligands was synthesized and studied. The ligands were obtained by reacting various polyalcohols with 4-nitro-1,2-dicyano-benzene to produce a series of polyphthalonitriles, then condensing with 2-aminopyridine to produce the polyisoindoline intermediates and finally ring expanding with aqueous hydrazine to form the polyphthalazines. Dinuclear complexes were also obtained by reacting two dinucleating polyisoindolines with Cu(II) salts. Analytical spectral, X-ray, and magnetic studies on the complexes reveal that the polyphthalazine ligands are able to bind two pairs, three pairs and four pairs of metal ions in triple bridged, spin-coupled dinuclear centers, one on each branch of the extended polyphthalazine ligands. Two tetranuclear Cu(II) nitrate complexes, $[Cu_4(C\text{-}P)(\mu_2\text{-}OH)_2(\mu_2\text{-}NO_3)_2(NO_3)_2(H_2O)_2](NO_3)_2{\cdot}4H_2O$ and $[Cu_4(O\text{-}P)(\mu_2\text{-}OH)_2(\mu_2\text{-}NO_3)_2(NO_3)_2(H_2O)_2](NO_3)_2{\cdot}10H_2O$, of the tetranucleating polyphthalazines (O-P, C-P) have been characterized by single crystal X-ray diffraction. In these dinuclear centres two,

five or six-coordinate Cu(II) ions are brought into close proximity and bridged by the phthalazine diazine ($N_2$) and hydroxide groups equatorially and by a bidentate nitrate group axially. The overall structure of the tetranuclear Cu(II) complex of O-P reveals that the $Cu_4$ complexes are connected through bridging bidentate nitrates and hydrogen bonding interactions, forming a zig-zag, nanometre scaled, molecular tube with hydrophilic groups inside and hydrophobic groups outside. Variable-temperature magnetic susceptibility measurements on some complexes indicate that strong antiferromagnetic couplings exist within each dinuclear centre, but across the ligand framework coupling is very weak. These polynuclear Cu(II) complexes usually exhibit cyclic voltammograms at positive potentials (V vs SSCE) associated with Cu(II)->Cu(I) reduction.

Preliminary studies have also been carried out on the synthesis of a 'star-like' lithium phthalocyanine peripherally substituted with isoindoline and phthalazine groups in an attempt to generate a system with spin coupled centres linked to a macrocyclic core with extensive $\pi$ conjugation.

## ACKNOWLEDGEMENT

I wish to express my sincere gratitude to my supervisor Prof. L.K. Thompson of the Chemistry Department at Memorial University of Newfoundland, for his patience and valuable advice throughout the course of this study.

My appreciation is extended to Prof. J.N. Bridson, who determined the X-ray structures. Helpful advice and assistance from Drs. S.S. Tandon and S.K. Mandal are also highly appreciated.

Financial Support from Memorial University, in the form of University Graduate Fellowships and Teaching Assistantships, and from Dr. Thompson's Grant from the Natural Sciences and Engineering Research Council of Canada are gratefully acknowledged.

Furthermore, many thanks also go to Dr. P.G. Pickup, Dr. C.R. Jablonski, Dr. B. Gregory, and the Chemistry Department, University of New Brunswick for their help with electrochemistry, NMR, MS and FAB MS studies. I would like especially to thank Ms. Nathalie Brunet for her help with Cosy NMR studies on the characterization of the ligands.

Finally, I am greatly indebted to my parents for their great encouragement.

## TABLE OF CONTENTS

## LIST OF TABLES

## LIST OF FIGURES

# Part 1 INTRODUCTION

# Chapter 1 SUPRAMOLECULAR CHEMISTRY AND MOLECULAR DEVICES

## 1.1. Supramolecules and molecular devices

Most molecules synthesized by traditional synthetic chemists fall into a relatively low molecular weight (< 2,000 amu) and small size (< 10 Å) realm, whereas the macromolecules prepared by polymer chemists have very high molecular weights (>50,000 amu). However, molecules in the midsized range, with molecular weights between 2,000 and 50,000 and nanometre (10 Å) size molecular dimensions have been neglected by synthetic chemists.[1] There has been a recent surge of interest in "supramolecular species" with nanometric dimensions and large molecular weights (nanochemistry). These may have applications in the fields of microlithography and microphysical engineering, where by progressive miniaturization, production of even smaller basic elements may be realized, allowing the development of more powerful and portable devices.

It is now recognized that most of the fascinating properties of supermolecules--e.g. DNA, proteins and enzymes in biological systems, such as selective recognition, fast and reversible information transfer and high catalytic activity, result from the controlled and efficient use of weak non-covalent interactions of these molecules. Nanometre-scale molecules could form their own characteristic shape, mimicking supermolecules in biological systems, due to weak intermolecular electrostatic attractions, van der Waals, and hydrogen-bonding forces between a molecule and its neighbours, so that they arrange themselves in a larger structure with the desired molecular geometry and function.

This kind of organic material has been synthesized and has been found to self-assemble into ordered arrays at low temperature, is capable of molecular recognition and can act as a biomimetic system[2] or organic molecular device. There has been great interest in dendrimers, arborols, cascades and rotaxanes.[3] The largest dendrimer ever reported, $C_{1398}H_{1278}$ (**1**), has a molecular weight of 18,054 and a diameter of 12.5 nm. These kinds of globular molecules not only have exotic tree-like structures but the materials exhibit unusual properties, including high solubility. Among these supramolecular complexes are rotaxanes, which have been prepared recently.[4] These are chemical species in which a cyclic molecular bead is threaded by a linear chain bearing bulky end units which prevents the complex from dissociating into its cyclic and linear molecular components.

Molecular devices have been defined as structurally organized and functionally integrated chemical systems built into supramolecular architectures. The function carried out by a device results from the integration of elementary acts performed by the components. The components may be photoactive, electroactive, or ionoactive depending upon whether they operate with photons, electrons, or ions. Several molecular devices have been reported. Cram[5] produced a molecular tube (**2**) (Fig. 1.1), and found that macrocyclic polyamines bearing suitable side chains do indeed give tubular mesophases that contain stacks of tube-forming macrocycles. Deposition of macrocycles bearing lipophilic side chains at the air-water interface could result in a Langmuir monolayer, thus yielding ion-responsive molecular films.[6]

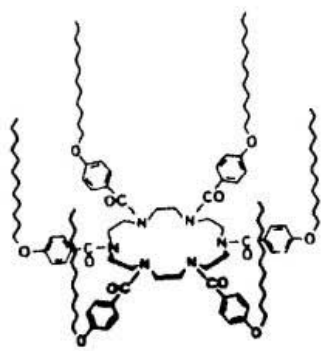

**Fig.1.1** Molecular ionic devices (**2**)

A molecular channel may also be defined by a bundle of transmembrane chains, formed by the spontaneous association of individual molecules ( as in the case of the polymolecular channel formed by the peptide alamethicin).[7] The

synthesis of a "channel" molecule (3) (Fig. 1.2) has been realized, the [18]-$O_6$ macrocyclic annulus possesses selective metal-cation binding properties; it bears two axially oriented bundles of four oxygen-containing chains, which provide binding sites for metal cations and are long enough for the molecule to span a typical lipid membrane; the overall length with the chain in an extended state may be estimated to lie in the 45-50 Å range.[7]

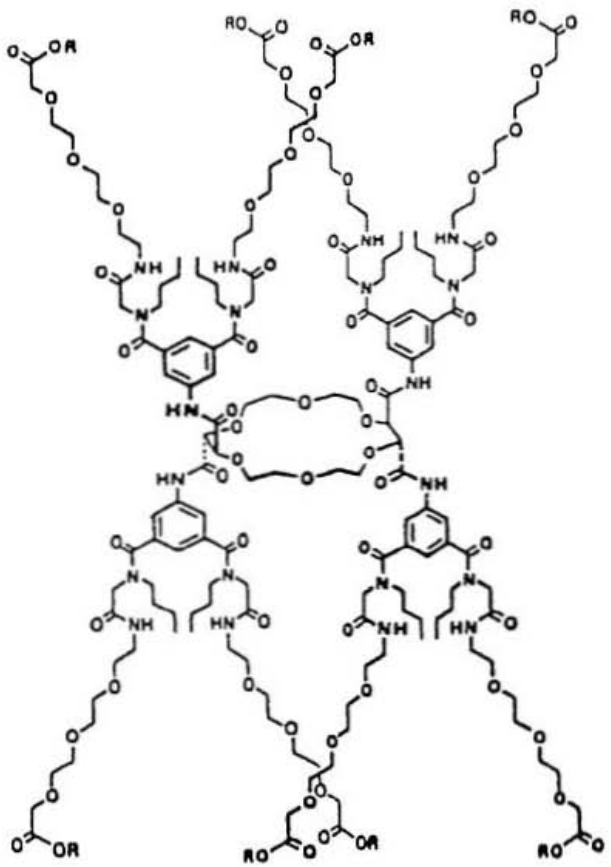

**Fig. 1.2** "Channel" molecule (3)

Correspondingly, advances in synthetic inorganic chemistry have lagged behind organic areas because of the unavailability of suitable molecular building blocks. Most coordination complexes studied today fall into a relatively low molecular weight regime and involve one metal centre per molecule. However, the active sites of most metalloenzymes ( such as the photosynthesis system[9] ) are supramolecular coordination complexes in their own right, in which nanometre scaled subunits assemble or self assemble into the active sites. The enzyme catalyzed reaction can proceed highly effectively and selectively because the substrate molecules can be organized at the active sites at the right time and in the right direction.[10] Hence the study of nanometre scaled polynuclear complexes may result in a new generation of model complexes, which may not only mimic the reactivity of the metalloenzymes like previous model compounds, but also mimic the substrate organization and starting materials selection capabilities of enzymes. However, this category of complexes is rather rare. Polynuclear transition metal complexes of a dendritic nature (**4**) were first described by Balzani et al.[11], but their blocks were not linked exclusively by covalent bonds but also by metal-ligand bonds (Fig. 1.3). Zubieta et al. recently reported the synthesis and structure of an inorganic double helix of a polyvanadium complex which is chiral and strongly magnetic.[12]

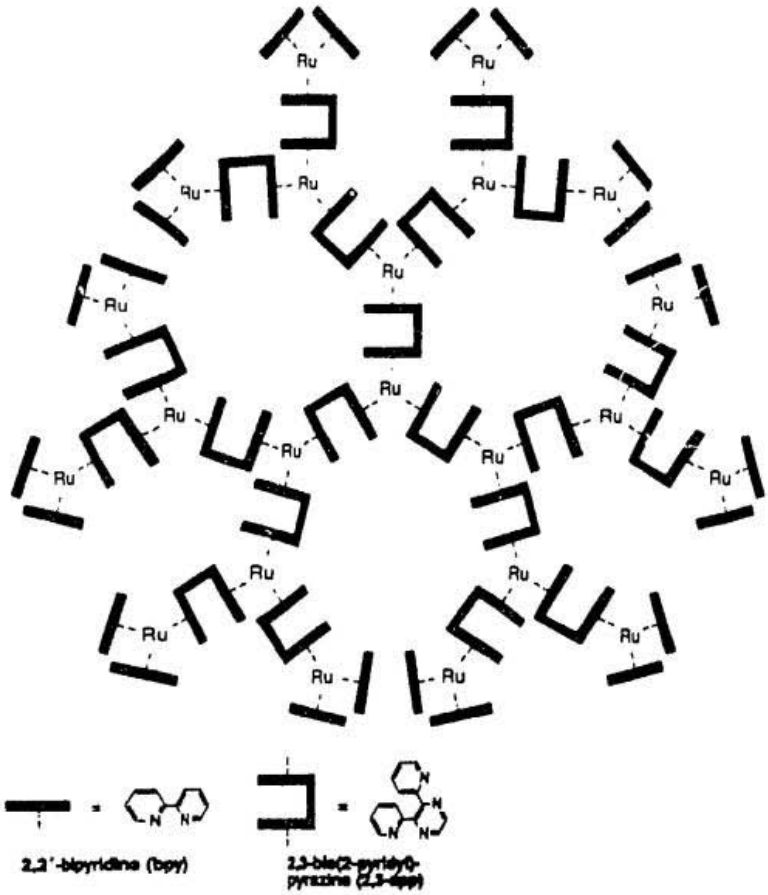


**Fig. 1.3** Dendritic metal complex (**4**) containing 22 ruthenium ions.

Lehn [12-14]et al. used oligobipyridines containing two to five bipyridine units separated by a $CH_2CH_2$ group to yield the corresponding $Cu^I$ double helicate (**5**) (Fig. 1.4). It is of particular interest that the helicate formation process appears to take place with positive cooperativity[12] and with self-recognition,[12] a given ligand forming a double helix preferentially with an identical strand if a mixture of ligands is used. The formation of the double helicate results from the

tetrahedral-like coordination imposed by each $Cu(bpy)^+$ site and from the design of the ligands, which disfavours binding to only a single strand. These two features make up the recognition process and the molecular steric "program" that leads to preferential formation of the double-helical structures respectively. The helicate formation amounts to tetrahedral reading of the molecular information stored in the bpy strands.

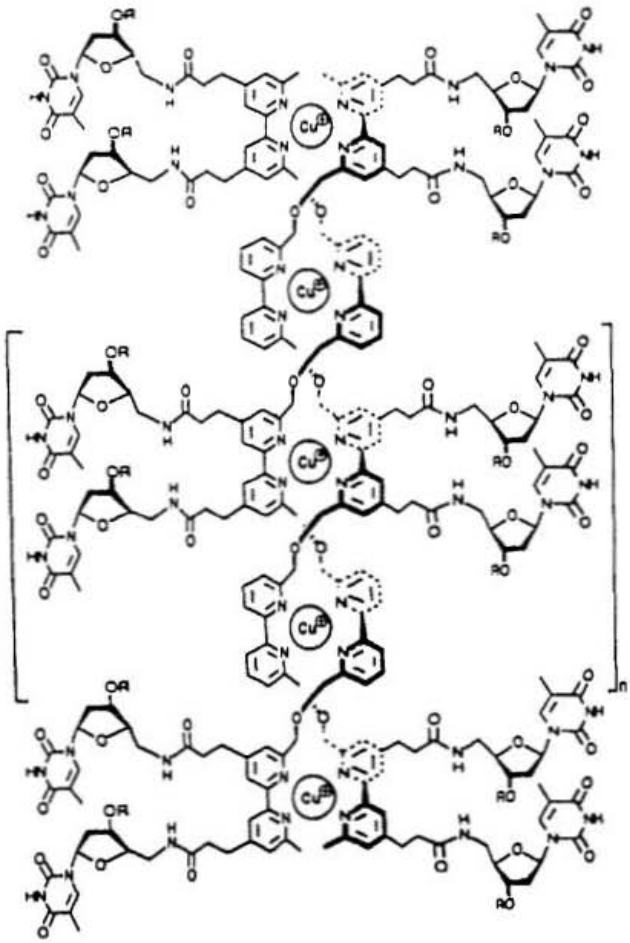

**Fig. 1.4** $Cu^I$ double helicate **(5)**

Usually, binding two metal centres requires some special feature on the part of an organic ligand, which is usually a bidentate bridging group, e.g. $N_2$ diazine (phthalazine, pyridazine, pyrazole, pyrazine, nidazole), alkoxide or hydroxide etc., and is quite common. Extension beyond two metals provides more of a challenge, and frequently requires the use of "templating" techniques, where simple molecular fragments are organised prior to a series of condensation steps. Tetranuclear,[16] hexanuclear,[16] octanuclear $[(Cu_4)_2]$[18] and even dodecanuclear $[(Cu_6)_2]$[17] species can be achieved in this manner, which involve a single, macrocyclic ligand encompassing four and six metals. In the case of the dodecanuclear species two hexanuclear macrocyclic halves are held together by hydroxide bridges, forming a molecule with a molecular weight of about 2700, which would fit into a cylinder with a diameter of approx. 19 Å and a height of approx. 9.7 Å. Newkome[19] reported a single dendritic polynucleating ligand which binds 12 ruthenium(II) ions to form a polynuclear complex (**6**). (Fig. 1.5)

The goals of this study are to design and prepare polynucleating ligands and polynuclear complexes with high molecular weights, high nuclearity and nanometre dimensions, and then to study their structures and properties. Such systems may have importance as nanometre scale molecular devices, as model compounds for multicopper proteins, or as magnetic materials. These systems may undergo self-assembly to give complexes, with molecular magnetic couplings that can be

transmitted from one molecule to another.

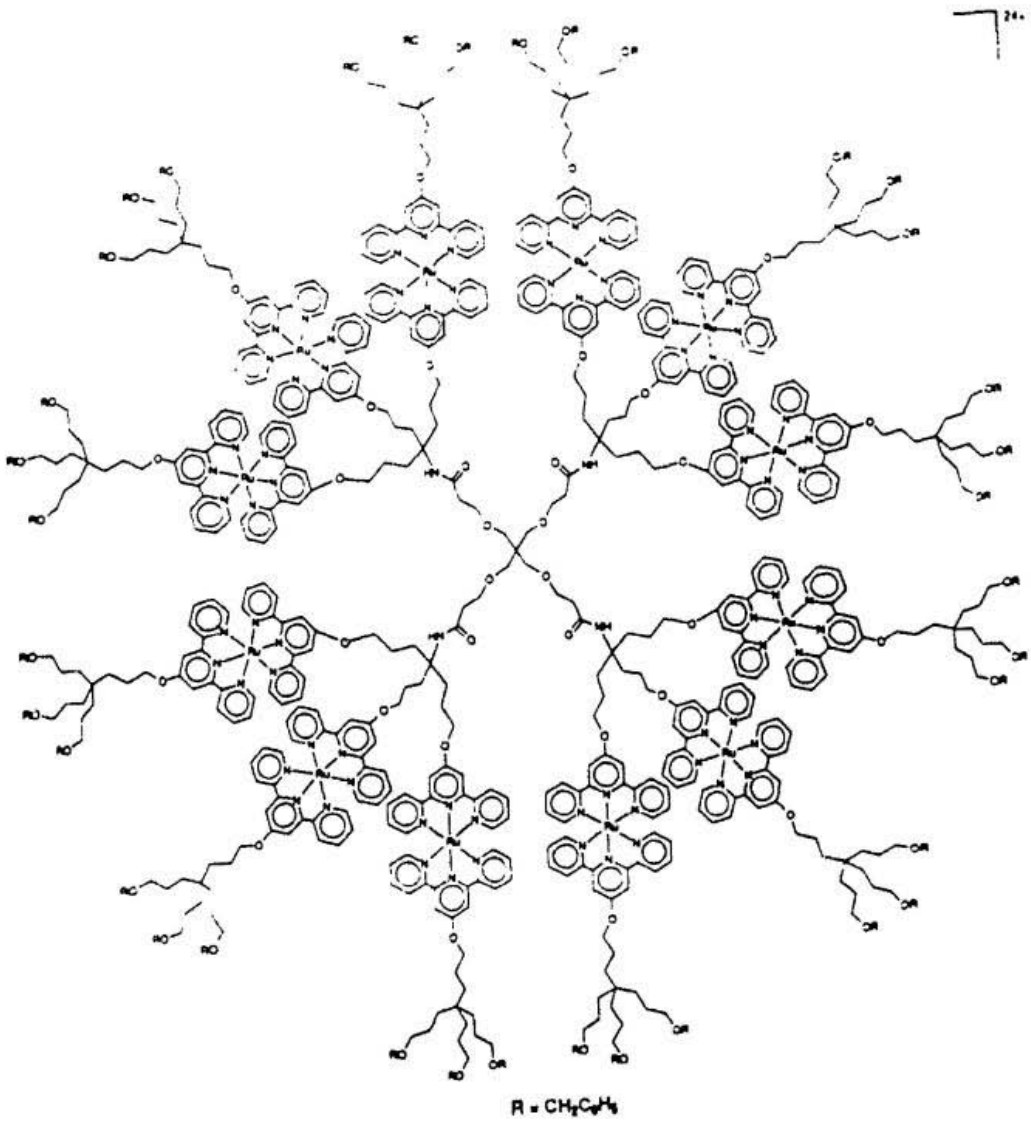

**Fig. 1.5** Dendritic polynuclear Ru(II) complex (**6**)

## 1.2 Magnetic molecular materials

Research in the field of low-dimensional magnetism has been particularly active in the last decade, and major developments have occurred in both the theoretical and practical areas of magnetochemistry. The most remarkable advance is perhaps the preparation and characterization of compounds containing ferromagnetic chains, also called one-dimensional (1-D) ferromagnets.[20] Kahn et al.[21] reported the synthesis of a series of A-B dinuclear complexes ( A: $Fe^{3+}$, $Cr^{3+}$, $VO^{2+}$; B: $Cu^{2+}$ ) (7) (Fig. 1.6) from the dinucleating ligand $(fas)_2en^{4-}$ as 1-D molecular ferromagnets. These A-B complexes have very large intramolecular ferromagnetic exchange because the single electron in the $d_{xy}$ orbital in A couples with the electron in the $d_{x^2-y^2}$ orbital in B. There is no magnetic ordering for 1-D systems, except at absolute zero, and the interchain interactions are very weak compared with the intrachain interactions and the systems exhibit a spontaneous magnetization at a low critical temperature $T_c$, $T_c < 10$ K. It is necessary to increase the dimensionality of the systems in order to obtain a higher $T_c$. The next step is now the search for novel compounds of higher magnetic dimensionality. From the physical point of view, 2-D systems are the most interesting magnetically,[22] since they form the borderline between ordering and non-ordering systems.[23]

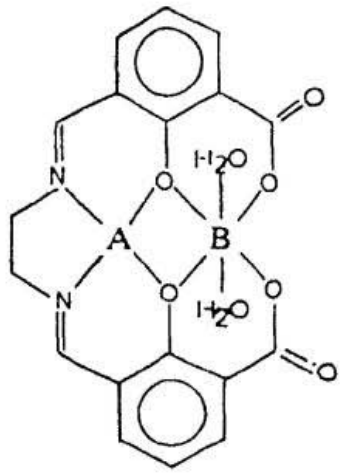


Fig. 1.6 Dinuclear A-B complex of $(fsa)_2en^{4-}$ (7)

High dimensionality magnetically ordered molecular systems require extended interactions linking the molecules within the crystalline lattice. Since the interactions depend on the structural packing of the molecules, the processes by which interactions occur are still not well understood. The engineering of supramolecular structures by assembling molecules in a crystal lattice remains an art rather than a well established technique. The building-block approach to the design and preparation of high spin and high dimensionality molecules and molecular-based ferromagnets requires the assembly of molecules within the crystal lattice in such a way that all the molecular spins align in a parallel fashion. It is very important to prepare high spin molecules developing connectivity in two or

three directions in order to obtain magnetic ordering at relatively high temperatures. High spin molecules are also intrinsically interesting because they have fascinating electronic structures.

## 1.3 Polynuclear Cu(II) complexes

Dinuclear Cu(II) complexes are quite common, and their synthesis was mainly stimulated by interest in model compounds of copper proteins. Trinuclear, tetranuclear, hexanuclear, octanuclear and polynuclear Cu(II) complexes, however, are relatively unusual. There has been significant interest recently in the synthesis and properties of supramolecular complexes of high nuclearity,[10,24,25] and dendritic systems with $Ru_{13}$[25] and $Ru_{22}$[10] clusters have been reported. However in these systems the clusters were built up by synthetic strategies using metal complexes as ligands and metal complexes as metal ion sources, with the result that a large number of ligands is involved in the cluster.

A different approach to high nuclearity species involves the two dimensional extension of porphyrazine[26] or phthalocynaine[27,28] (8) (Fig. 1.7) macrocycles to produce heteropentanuclear systems, involving just one ligand. Template condensation of 2,6-diacetylpyridine with 1,3-diamino-2-propanol produces a tetramanganese complex involving one ligand,[29] while template condensations of

isophthalaldehydes with various diaminoalcohols has produced $Cu_4$,[15,30] and $Cu_6$ (**9**)[16,31] (Fig. 1.8) species with the metals encapsulated by one macrocyclic ligand, within which bridging linkages effectively join all the metal centres. This has led to magnetic properties which, in one case, appear to include all the metals.[16] Octadentate ($N_8$) (**10**) benzodipyridazine ligands have also been shown to bind four copper(II) centres per ligand in a magnetically cross-coupled entity.[17,32](Fig. 1.9)

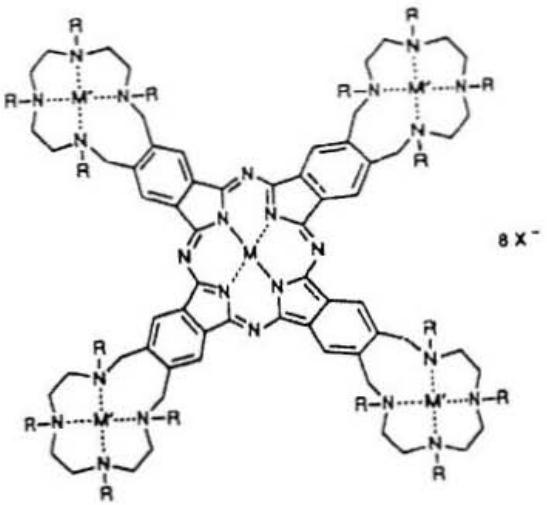


Ts = *p*-$MeC_6H_4SO_3$

| M | M' | R | X |
|---|---|---|---|
| Cu | — | Ts | — |
| Cu | — | H | — |
| Cu | Ni | H | Cl |

**Fig. 1.7** Star-like phthalocynaine (**8**)

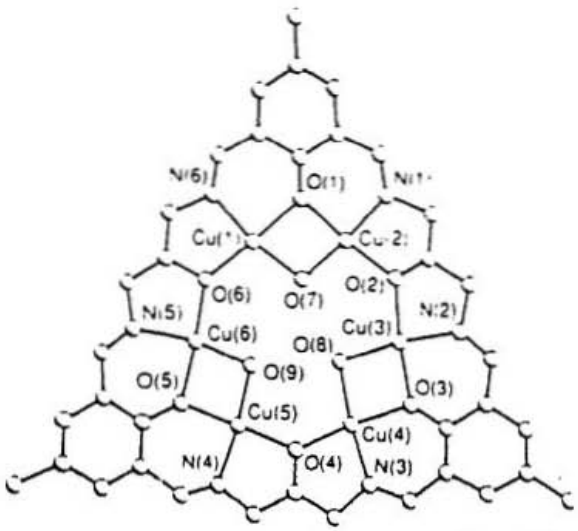


Fig. 1.8 Hexanuclear Cu(II) complex (9)

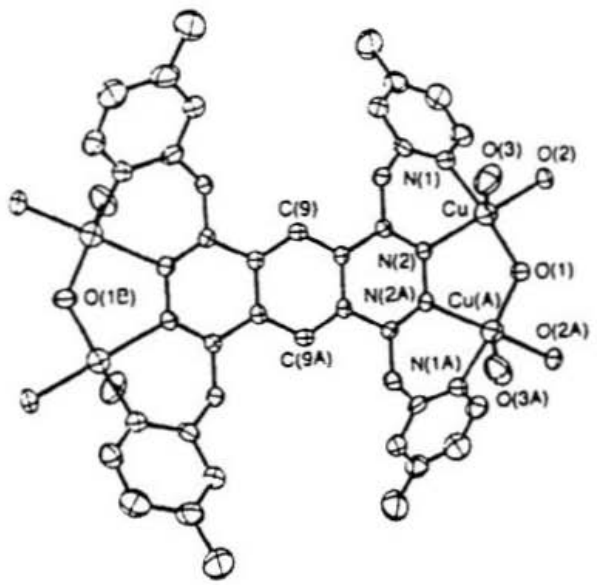


Fig. 1.9 Tetranuclear Cu(II) complex (10)

# Chapter 2 STUDIES OF DINUCLEAR COPPER(II) COMPLEXES OF MONO-PHTHALAZINE LIGANDS

## 2.1 Model compounds for copper proteins

For the last two decades, a large number of dinuclear Cu(II) complexes have been synthesized to mimic the structure and function of the active sites of copper proteins (e.g. haemocyanin and tyrosinase). Haemocyanin is the oxygen transport copper protein in invertebrate species such as crabs, lobsters etc. The previous model compound studies indicate that the Cu(II) ions in oxyhaemocyanin (**11**) reside in a ligand environment composed of three imidazolyl nitrogen donors from the histidine amino acid residue, a bridging dioxygen ligand and an endogenous protein bridge. The Cu-Cu distance is 3.55 Å and each Cu is square planar or square-pyramidal (Fig. 2.1.a). The first peroxo dinuclear Cu(II) complex (**12**) was synthesized by Karlin[33] (Fig. 2.2.a) in 1984 by using a dinucleating ligand

containing a bridging phenoxo group. The detailed Raman study concluded that the peroxide ion is coordinated in an unsymmetric terminal fashion, which is different from the mode suggested for oxy-Hc. The structure of (**13**)[34] (Fig. 2.2.b), another model compound developed by Karlin, was determined by X-ray crystallography as trans-μ-1,2, but the spectroscopic properties of the complex are apparently different from those of oxy-Hc, thereby providing negative evidence that oxy-Hc possesses a trans-μ-1,2 coordination mode. The latest breakthrough work in this field was done by Kitajima.[35-38] The model complexes they synthesized do not contain a bridging ligand other than the peroxide, and they exhibit the following remarkable characteristics: 1. dimagnetism, 2. ν(O-O) stretching frequencies observed at 725-760 $cm^{-1}$, 3. a symmetric coordination mode of the peroxide ion as in oxy-Hc established by resonance Raman spectroscopy, 4. characteristic absorption bands appearing at ca. 350 and 550 nm, 5. Cu-Cu separation of ca. 3.6 Å. All these properties are very similar to those known for oxy-Hc, providing convincing evidence that oxy-Hc likely contains the μ-$\eta^2$:$\eta^2$ coordination mode. Two possible oxygen-binding modes of haemocyanin are summarized in Fig. 2.1.

Recently, the X-ray crystal structure of the first copper-containing oxygen transporting protein (*Panulirus interruptus deoxyhaemocyanin*), has been

determined.[39,40] The structure at 3.2 Å resolution shows that six histidines in the second domain of the subunit ligate the two copper(I) atoms, which are separated by a distance of 3.6 Å. (Fig. 2.3) It was found that a hydrogen-bonding network formed around the dinuclear copper sites of deoxy-haemocyanin (**14**).


a. End-on b. Side-on

**Fig. 2.1** Proposed dinuclear sites in oxyhaemocyanin (**11**)

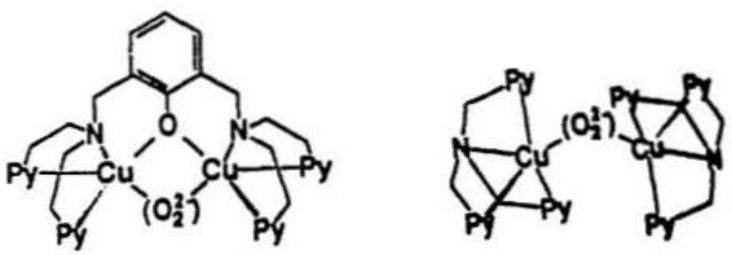


**(12)** **(13)**

**Fig. 2.2** Model complexes prepared by Karlin

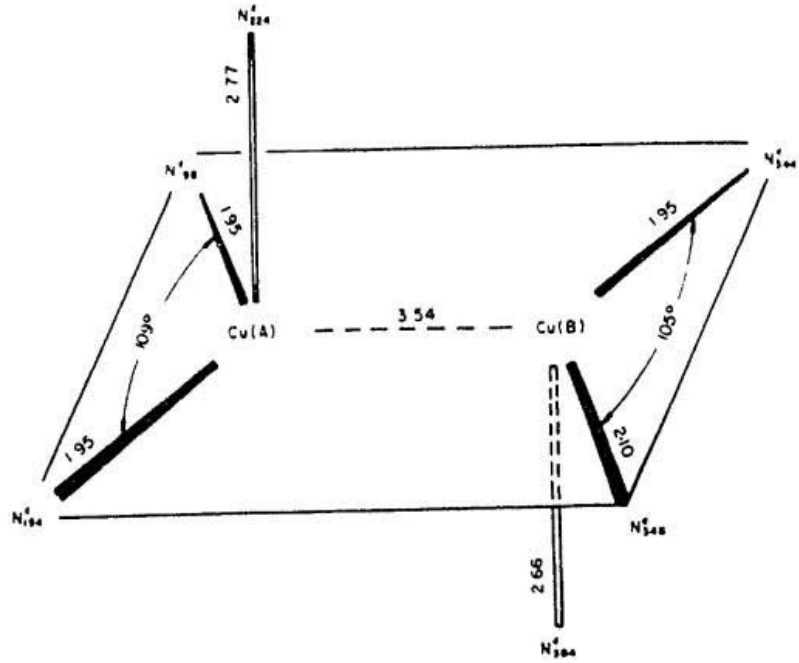


**Fig. 2.3** The dinuclear site in *panulirus interruptus deoxy-haemocyanin* **(14)**

Model compound studies are quite helpful to identify the active site geometry of metalloenzymes and the relationship between the function and the structure of these enzymes. Even when the structures of the dinuclear copper proteins are known from X-ray crystallography, however, well designed model compounds will be useful to probe the fundamental differences in their functions. Several classes of dinucleating ligands and their complexes were synthesized to mimic the structure and function of these copper proteins,[41] in one of which tetradentate phthalazines and pyridazines have produced dinuclear, hydroxy-

bridged Cu(II) complexes with metal-metal separations in the range 3.0-3.5 Å and Cu-OH-Cu bridge angles in the range 100-127°.[42-51] The phthalazine complexes have also demonstrated catalytic activity e.g. for the aerial oxidation of catechol.[52,53]

## 2.2 Structural and magnetochemical properties

Extensive studies have been done on dinucleating ligands containing just nitrogen donor atoms largely based on substituted "diazine" (=N-N=) type units. The transition metal complexes of polyfunctional diazine ligands, derived from a. hydrazine,[54-58] b. triazole,[59-60] c. pyrazole,[61] d. pyridazine,[62,63,65-68] and e. phthalazine,[61,62,64,69-76] have dinuclear centres, in which the metals are brought into close proximity due to the presence of the diazine fragments in these systems. The magnetochemistry and electrochemistry of hydroxy bridged dinuclear copper complexes of mono-phthalazine (PAPR) (Fig. 2.4.a) ligands has been well developed. These dinuclear complexes are strongly antiferromagneticaly coupled due to the spin communication between these two copper ions through a hydroxide and a diazine bridge and have very high redox potentials. The mono-phthalazine (PAP) (Fig. 2.4.b) (**15**) was prepared by Thompson[42] in 1969. Since then, a series

of studies on the coordination chemistry of this ligand have been carried out, and extended to its derivatized analogues as well. X-ray structural studies on these systems reveal that the ligands PAP(R) are capable of forming $\mu$-1,2-diazine bridged bimetallic complexes involving a variety of exogenous bridge groups, e.g., $[Cu_2(PAP6Me)(OH)(\mu_2\text{-}NO_3)_3]\cdot 0.5H_2O$,[77] (**16**) (Fig. 2.5), or $[Cu_2(PAP)(OH)(\mu_2\text{-}SO_4)Cl]\cdot 2H_2O$,[46] (**17**) (Fig. 2.6). A common structural feature in these complexes of the mono-phthalazines includes the hydroxide bridge and the phthalazine diazine bridge. A systematic structural variation has been developed by varying the third anionic bridge. The order of increasing hydroxide bridge angle ($Cl^- \sim Br^- < IO_3^- < NO_3^- < SO_4^{2-}$) is matched by the trend in increasing antiferromagnetic exchange. A linear relationship is demonstrated between the exchange and the hydroxide bridge angle for systems in which the Cu(II) centres have $d_{x^2-y^2}$ ground states.[77]

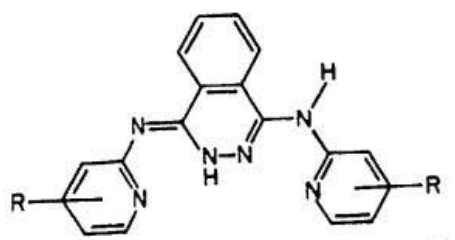

PAP(R = H), PAP4Me (R = 4 methyl), PAP6Me (R = 6 methyl).

(a)

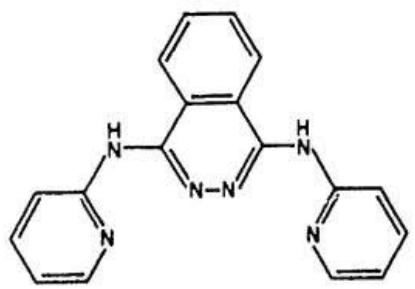

PAP(1,4-di(2'-pyridyl)aminophthalazine)

(b)

Fig. 2.4 Structures of PAPR and PAP

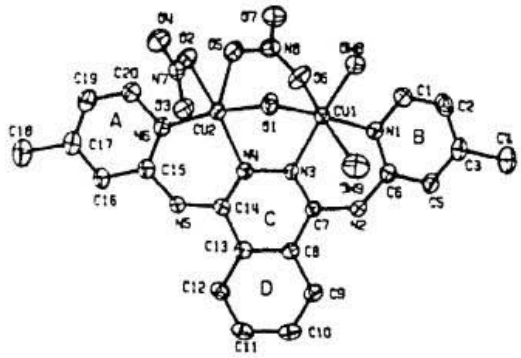

Fig. 2.5 Structure of $[Cu_2(PAP4Me)(OH)(\mu_2\text{-}NO_3)_2(H_2O)_2]^+$ (16)

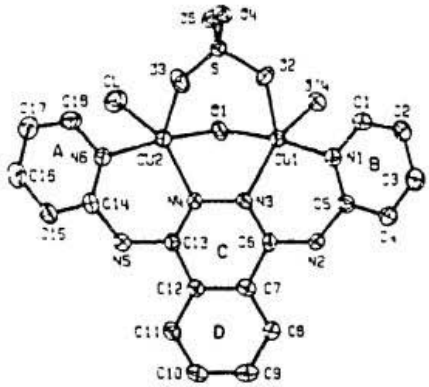

Fig. 2.6 Structure of $[Cu_2(PAP)(OH)(\mu_2\text{-}SO_4)Cl]\cdot 2H_2O$ (17)

Structurally, all of the hydroxo-bridged complexes involve "magnetically symmetric" dinuclear centres with distorted, five-coordinate copper ion stereochemistries. In most cases the distortion approximates a square pyramidal situation with nominally $d_{x^2-y^2}$ ground state copper centres. In these cases each Cu

atom is bound via an equatorial interaction to both the hydroxide bridge and the diazine bridge, which results in a situation where magnetic interactions via these groups are the most relevant, while any axial bridge interaction will be regarded as "non-magnetic".

In these magnetically concentrated dinuclear Cu(II) complexes, the electron spins on adjacent paramagnetic centres are strongly coupled to each other. The coupling between the electron spins leads to antiferromagnetism when the spins in the magnetic ground state are aligned anti-parallel and to ferromagnetism when the spins are aligned parallel.

An intermolecular antiferromagnetic system normally exhibits the characteristic variation of magnetic susceptibility ($\chi$) with temperature (T) shown in Fig. 2.7, curve (2). Starting at high temperature, the magnetic susceptibility increases as the temperature decreases. If the temperature is decreased sufficiently, a quite sharp maximum in the magnetic susceptibility is reached at a temperature, $T_N$ (the Néel point). Then the susceptibility decreases rapidly as the temperature decreases, and will be dependent on the strength of the applied magnetic field. This variation of the $\chi$ with T often leads to a Curie-Weiss law (eq.1) behaviour with appreciable positive values of $\theta$ (Weiss constant). Intermolecular antiferromagnetic systems exhibit many of the general features of intramolecular antiferromagnets, the major differences between them are that the maximum in the

susceptibility is normally much broader, and the susceptibilities are not usually dependent on the strength of the applied field.

$$\chi = C/( T-\theta) \qquad (1)$$

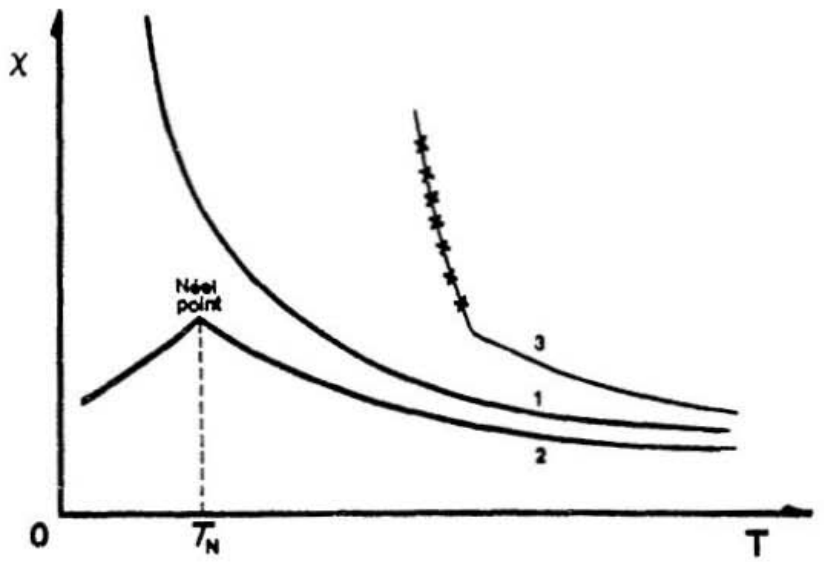


A comparison of the characteristic variation of susceptibility with temperature for normal paramagnetic (1), antiferromagnetic (2) and ferromagnetic (3) materials.

**Fig. 2.7** The characteristic variation of $\chi$ vs T

The antiferromagnetic coupling in these dinuclear Cu(II) complexes involves the interaction between electronic spin on neighbouring atoms. The following two mechanisms are usually used to account for antiferromagnetic exchange: (1.) direct interaction, and (2.) superexchange;

1. Direct interaction. This mechanism involves direct overlap between the orbitals containing the unpaired electrons, leading to mutual pairing in the ground state.

2. Superexchange. This mechanism for antiferromagnetism involves the interaction of electrons with opposite spins on the two interacting ions via an intermediate diamagnetic anion or organic bridge. The mechanism again involves orbital overlap, but instead of only the metal d-orbital being involved, the participation of filled orbitals on the intervening anion must also be considered, e.g., in a linear oxide system $M_2O$ the interaction may occur in two ways, either via a $\sigma$-bonding or a $\pi$-bonding mechanism. The superexchange mechanism may be extended to systems in which more than one anion intervenes between the paramagnetic ions.

In these dinuclear copper(II) complexes, Cu(II) ion has a $d^9$ configuration, S=1/2, and the two interacting copper centres give rise to a molecular spin singlet (S=0) and a molecular spin triplet (S=1) with a singlet-triplet energy gap, conventionally denoted by 2J.[78-81] When the ground state is the singlet state

(2J < 0), the interaction is antiferromagnetic (Fig. 2.8). When the triplet state is the lowest (2J > 0), the interaction is ferromagnetic.

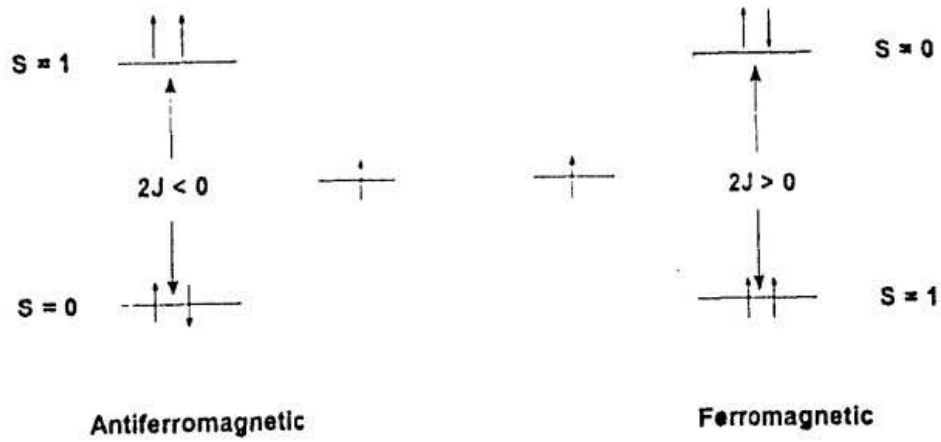


**Fig. 2.8** Magnetic energy levels

The net measured exchange in these dinuclear copper complexes is the sum of any antiferromagnetic ($J_{AF}$) and ferromagnetic ($J_F$) components, i.e.:

$$J = J_{AF} + J_F$$

$J_F$ is usually small and not sensitive to small structural changes, but $J_{AF}$ is found to vary as a function of the following effects:

1. Bridge angle at the superexchange bridge.
2. Ground state of Cu(II) ions.
3. Number of atoms in the bridge ( distance between the copper centres).

4. Electronegativity effects of the bridging and non-bridging atoms bound to copper (II) ions.

5. Spin polarization effects.

The Cu(II) ion can be four, five or six-coordinate in square planar, tetrahedral, square-pyramidal, trigonal-bipyramidal or octahedral geometries. The magnetic orbital for Cu(II) centres in square planar, octahedral and square pyramidal geometries is $d_{x^2-y^2}$, while the magnetic orbital for Cu(II) centres in trigonal bipyramidal geometries is $d_{z^2}$. The interaction of the magnetic orbital of each copper ion with a bridging ligand will generally result in an antiferromagnetic interaction for bridge angles >90°, while the interaction of the magnetic orbital of a copper ion with a non-magnetic orbitals of another ion and the interaction of two non-magnetic copper orbitals via the bridging ligands (orthogonal interactions) result in no antiferromagnetic coupling but leads to ferromagnetic coupling. The effect of the Cu(II)-L-Cu(II) bridge angle on the spin coupling exchange interaction has been extensively studied. Two quantitative calculations by Hatfield et.al[82,83] and Thompson et al.[77] for some singly, doubly and triply bridged Cu(II) dimers predict a large antiferromagnetic coupling for a 180° bond angle when the metal orbital can interact with a bridging ligand orbital of the same symmetry, and a weak ferromagnetic coupling for a 90° bond angle. In a series of dihydroxy bridged copper(II) complexes -2J varies as a function of the hydroxide bridge angle

(θ) according to Hatfield[83] et.al (eq.2)

$$2J=74.53\theta\ (cm^{-1}deg^{-1}) - 7270\ cm^{-1}\ (\theta= 95.6 - 104.4°) \quad (2)$$

A linear relationship between the antiferromagnetic coupling parameter (-2J) and the Cu-OH-Cu bridging angle (α) for a series of phthalazine dinuclear Cu(II) complexes was established by Thomspon et.al[77] (eq.3)

$$-2J=23.06\alpha - 2143\ cm^{-1} \quad (3)$$

In these spin coupled dinuclear complexes of mono-phthalazine ligands the diazine bridge is reasonably assumed to provide a roughly constant contribution to the total magnetic exchange, and the following effects were found to affect the exchange:

1. Terminally bound bromo derivatives have significantly enhanced exchange in comparison with structurally analogous chloro derivatives;

2. The chelate ring size and the size of the nonmagnetic bridge groups profoundly effect binuclear centre dimensions and hence exchange, in the case of hydroxo-bridged derivatives.

The orthogonality generally results in ferromagnetism, not antiferromagnetism in the complexes. The spin polarization effects were demonstrated very well by azide ridged dinuclear Cu(II) complexes. The azide group can act as a 1,1[84] or a 1,3 bridge in its dinuclear complexes. It contains two unpaired electrons at each of the terminal nitrogens, with spins antiparallel. It can

polarize the spin of the unpaired electrons on the two Cu(II) centres to favour either the singlet or the triplet state depending on which way it bridges the two Cu(II) ions. When $N_3^-$ bridges in the 1,3 fashion[84-86] (Scheme 2.1b), the two spin antiparallel electrons localised on the two terminal nitrogen atoms will polarize the electron spin on the two Cu(II) ions with opposite directions, hence, dinuclear Cu(II) complexes with azide bridging in 1,3 fashion are generally strongly antiferromagnetically coupled ($-2J > 800\ cm^{-1}$). If $N_3^-$ bridges two Cu(II) ions in the 1,1 fashion (Scheme 2.1c), the electron on the bridging nitrogen will polarize the electron spin on two Cu(II) ions with the result that the two unpaired electrons on the two Cu(II) ions will have parallel spins, generally resulting in strong ferromagnetic coupling. (e.g. $2J > 200\ cm^{-1}$).

**Scheme 2.1** Spin polarization effect of azide complex

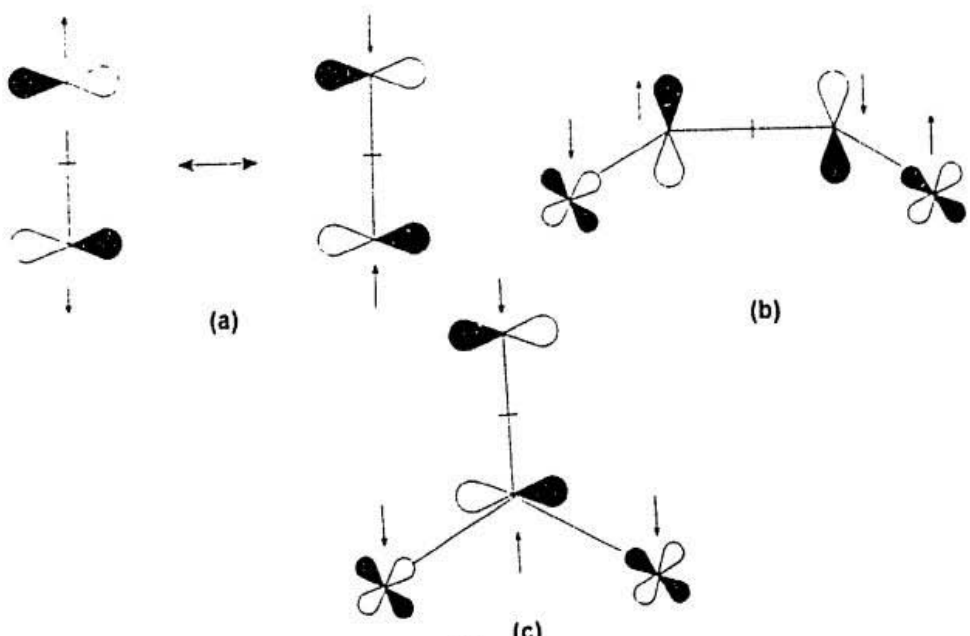

## Part 2 EXPERIMENTAL RESULTS AND DISCUSSION

### EXPERIMENTAL

Commercially available regents were obtained from the Aldrich Chemical Company and used without further purification. Melting points were obtained with a Fisher-Johns melting apparatus and are uncorrected. The IR spectra were obtained by using a Mattson Polaris Fourier Transform spectrophotometer and electronic spectra were obtained with a Cary 5E spectrometer. The NMR spectra were determined on a Varian XL-300 spectrometer using tetramethylsilane as the internal reference. The mass spectral data were obtained with a VG Micromass 7070 HS spectrometer with a direct insertion probe, FAB mass spectra were measured by Mr. Dan Drummond of the Chemistry Department in the University of New Brunswick and C, H and N analyses were carried out by Canadian Microanalytical Service, Delta, Canada.

Variable-temperature magnetic susceptibility data were obtained in the range 5-305K using an Oxford Instruments superconducting Faraday magnetic susceptibility system with a Sartorius 4432 microbalance. A main solenoid field of 1.5T and a gradient field of 10 $Tm^{-1}$ were employed. Calibration data were obtained using $HgCo(NCS)_4$. Cyclic voltammetry was carried out in DMF

(dimethyl formamide) dried by 4 Å molecular sieves. A three-electrode system was used in which both the working and counter electrodes were platinum and the reference electrode was potassium chloride (SCE) calomel electrode. The supporting electrolyte was tetraethylammonium perchlorate (TEAP, 0.1M).

# Chapter 3 SYNTHESIS AND CHARACTERIZATION OF POLYNUCLEATING LIGANDS

## 3.1 Synthesis and characterization of polynucleating ligands

Polynucleating ligands that can bind more than two metals in one molecular entity in more than one binuclear site are relatively uncommon but have received much attention recently.[15,17,87,88] A variety of polyphthalonitriles were prepared by Siegl[89] and Leznoff[87,90,91], and Thompson[92,93] reported the preparation of isoindolines and phthalazines. Based on these preparation methods, we synthesized (Scheme 3.1) a series of extended polyphthalonitriles, polyisoindolines and polyphthalazines (Fig. 3.1) in high yield.

Scheme 3.1 Synthesis of polyisoindolines and polyphthalazines

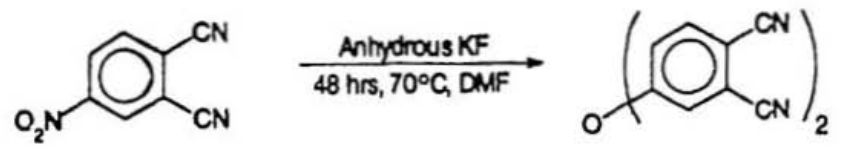


(19) (20)

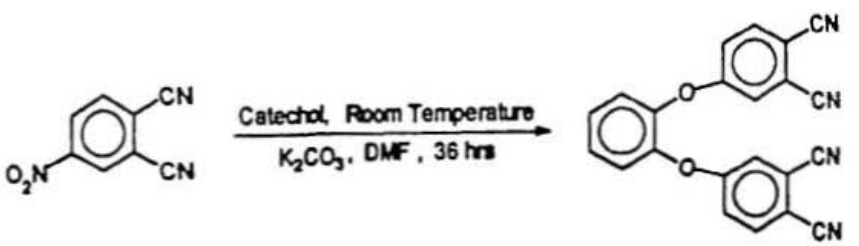


(19) (24)

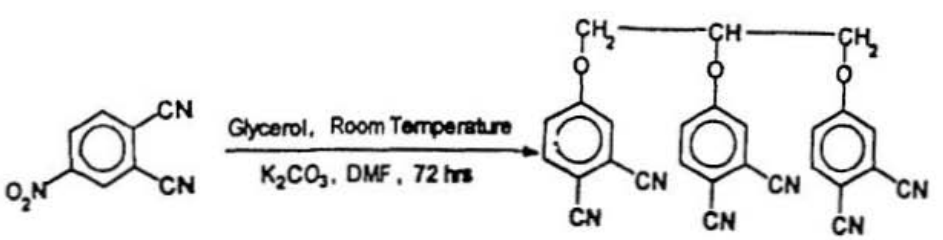


(19) (26)

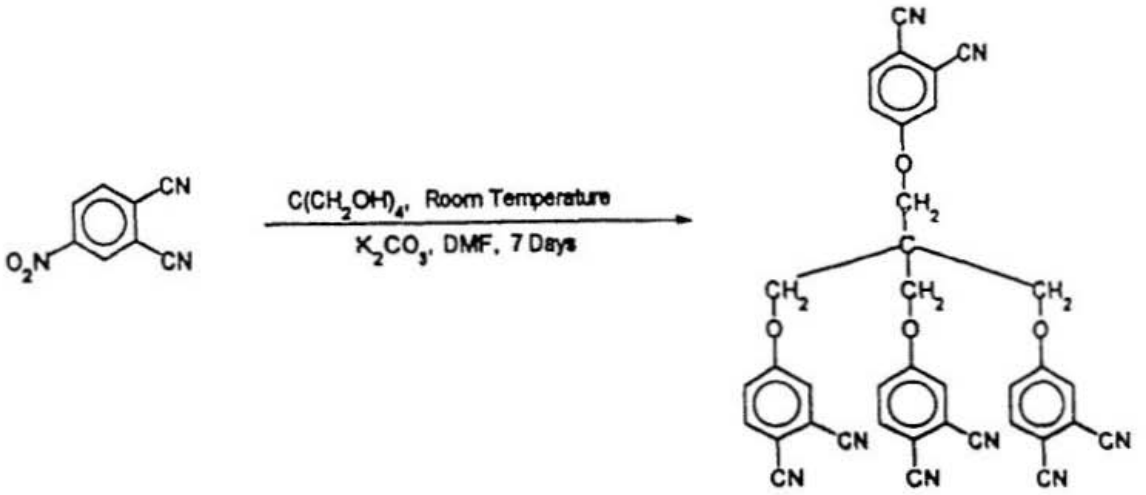


(19) (30)

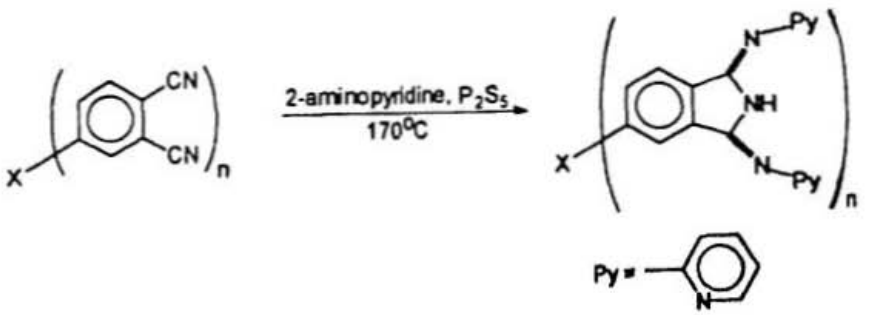


(20),(24),(26),(30) (21),(23),(27),(29)

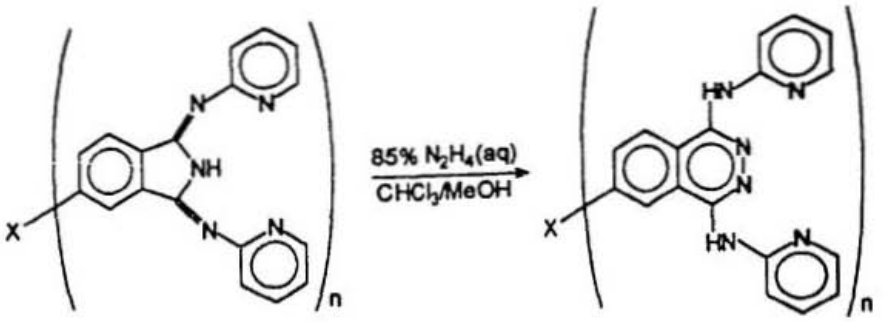


(21),(23),(27),(29) (22),(25),(28),(31)

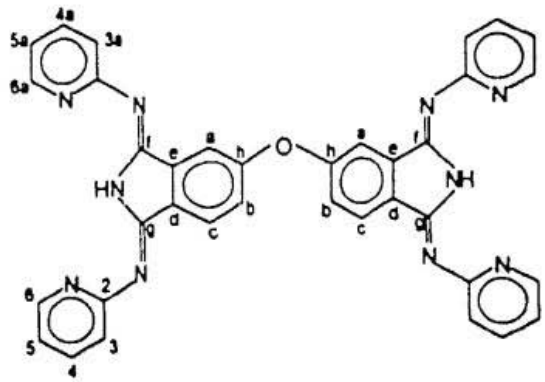

(21)

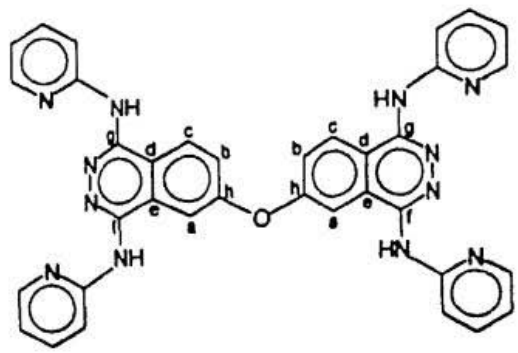

(22)

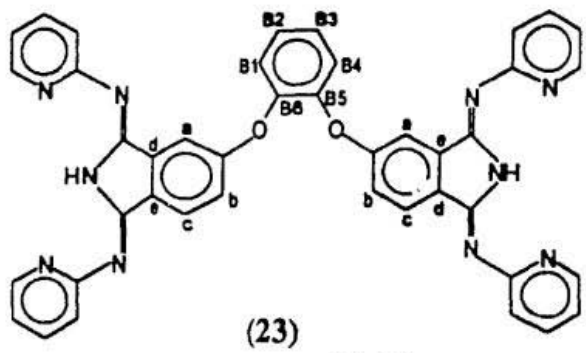

(23)

Fig.3.1.a

Fig. 3.1 Structures of polyisoindolines and polyphthalazines

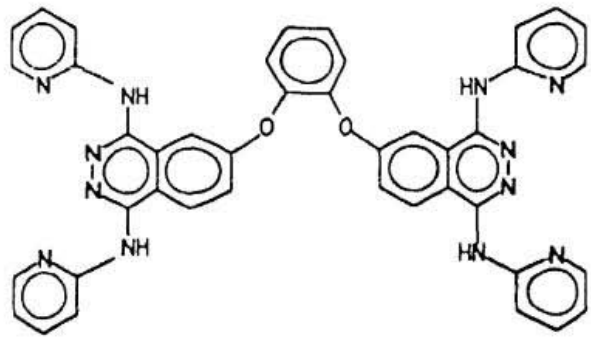

(25)

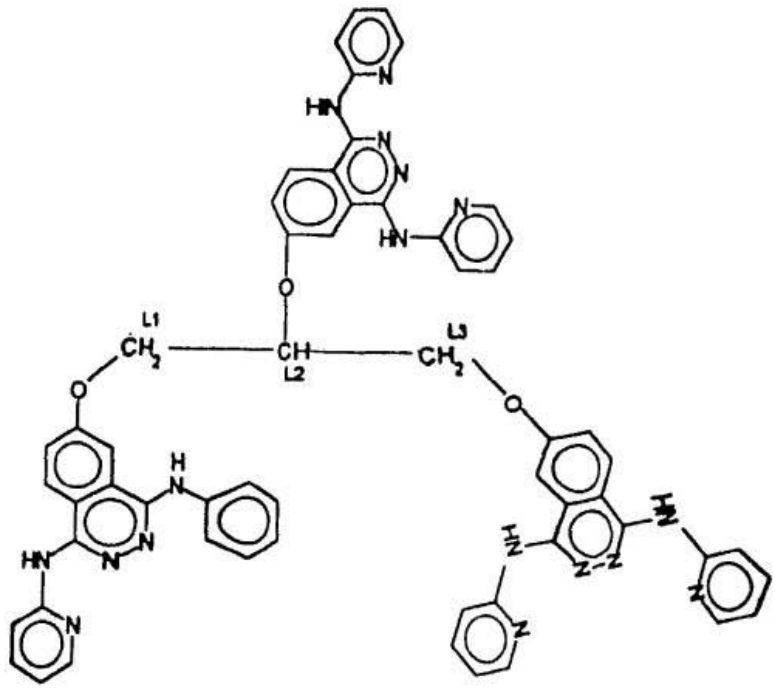

(28)

**Fig.3.1.b**

**Fig. 3.1** Structures of polyisoindolines and polyphthalazines

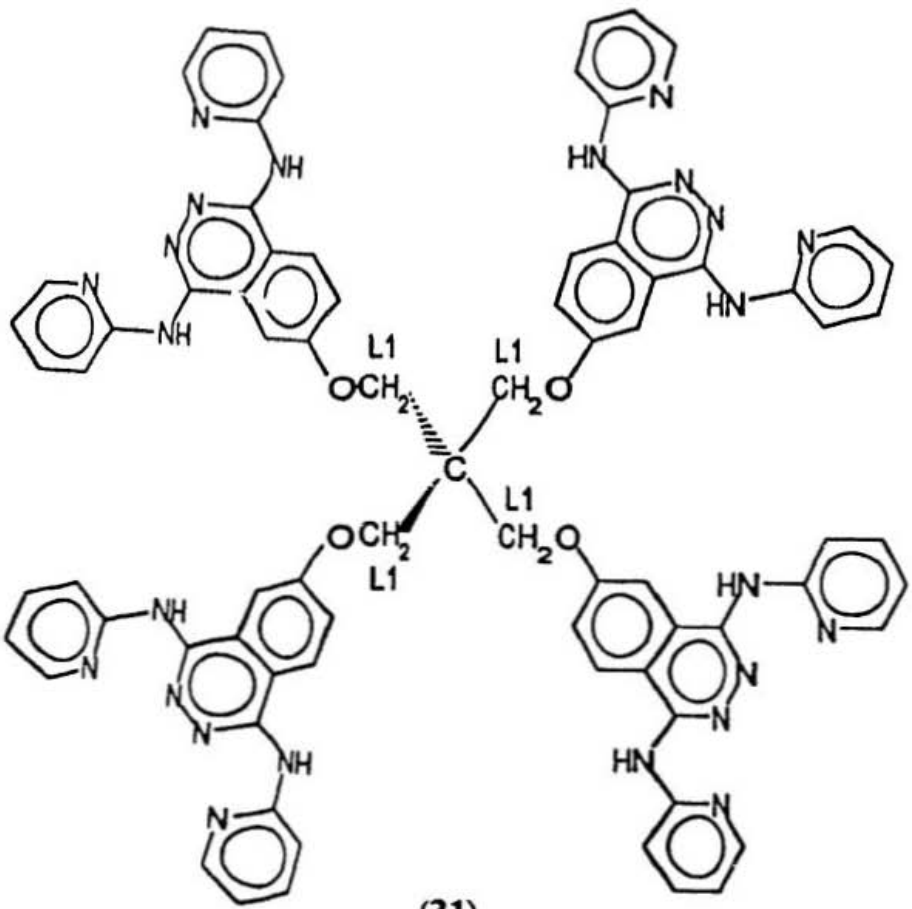

(31)

**Fig.3.1.c**

**Fig.3.1** Structures of polyisoindolines and polyphthalazines

*a. oxy-bis-4,4'-bis-[1,2-dicyanobenzene] (O-CN) (20)*

The starting material, 4-nitrophthalonitrile, was prepared from 4-nitrophthalamide. m.p. 145°C-147°C. (lit. m.p. 142°C). (**20**) was prepared[86] by refluxing 4-nitrophthalonitrile (**19**) with anhydrous potassium fluoride in DMF (dimethyl formamide) solution for 48 hrs. m.p. 260°C-265°C. (lit. m.p. 252°C-256°C).

*b. oxy-bis-5,5'-bis-[1,3-di(2'-pyridylimino)-isoindoline (O-I) (21)*

(**20**) (2.5 g, 9.3 mmol) and a large excess of 2-amino-pyridine were mixed and fused under $N_2$ at 170°C for about 24 hrs, cooled to room temperature, then refluxed with 100 mL diethyl ether, the mixture filtered, and the solid residue washed with diethyl ether and acetone to remove unreacted starting materials and byproducts and dried under vacuum to give a dark yellow solid. The yellow solid was dissolved in $CHCl_3$ (100 mL) and the solution refluxed with activated charcoal for 0.5 hr, filtered, and concentrated to about 30 mL. MeOH (150 mL) was then added and the mixture allowed to stand overnight. Yellow microcrystals were obtained, which were filtered off, washed with MeOH and diethyl ether, and dried under vacuum. ( Yield 1.7g; 29.7% ). m.p. 234°C-236°C. Anal. Calcd for $C_{36}H_{24}N_{10}O$ (612.66): C, 70.58; H, 3.95; N, 22.86. Found: C, 70.52; H, 4.10; N, 22.54. Mass spectrum, major mass peaks (m/e) corresponding to the molecular ion

and reasonable degradation fragments: 613($M^+$, 86.57%), 612(100.00%), 611(30.00%), 534(35.23%), 517(19.62%), 440(79.30%), 363(13.21%), 267(1.37%), 78(100.00%), 51(22.05%). NMR spectra were assigned according to Fig. 3.1.a. $^1H$ NMR spectrum (216 K, DMSO-$d_6$/TMS), (chemical shift, ppm)(relative intensity): 7.26-7.34(4) (multiplet, $H_5$), 7.38-7.48(4) (quartet, $H_3$, $^3J_{H-H}$=8.0 Hz), 7.53-7.58(2) (quartet, $H_b$, $^3J_{H-H}$=8.3 Hz), 7.64(2) (doublet, $H_a$, $^4J_{H-H}$=2.1 Hz), 7.85-7.95(4) (multiplet, $H_4$), 8.10-8.12(2) (doublet, $H_c$, $^3J_{H-H}$=8.3 Hz), 8.72(4) (multiplet, pyridine $H_6$, $^3J_{H-H}$=5.0 Hz). $^{13}C$ NMR (302 K, $CDCl_3$/TMS), (chemical shift, ppm), 112.74($C_a$), 120.28($C_b$), 124.45, 131.11, 138.16, 147.75($C_3$), 153.02, 160.17($C_6$), 160.38($C_2$). $^1H$ NMR (216 K, $CDCl_3$/TMS) (chemical shift, ppm)(relative intensity): 7.20-7.26(4) (multiplet, $H_5$), 7.40-7.53(6) (multiplet, $H_3$, $H_b$), 7.72(2) (doublet, $H_a$, $^3J_{H-H}$=2.1 Hz), 7.80-7.90(4) (multiplet, $H_4$), 8.12-8.14(2) (doublet, $H_c$, $^3J_{H-H}$=8.1 Hz), 8.69-8.71(4) (doublet, $H_6$, $^3J_{H-H}$=4.8 Hz). IR, $cm^{-1}$: 537(s), 794(vs), 1027(vs), 1141(vs), 1219(vs), 1263(vs), 1325(vs), 1366(vs), 1459(vs), 1580(vs), 3253(vs). Cosy NMR spectrum of O-I is shown in Fig. 3.2.

***c. oxy-bis-6,6'-bis-[1,4-di-(2'-pyridylamino)phthalazine] (O-P) (22)***

(**21**) (1.82 g, 2.97 mmol) was dissolved in hot $CHCl_3$/MeOH mixture solvent (25 mL) and a solution of MeOH (125 mL) containing 85% aqueous $N_2H_4$ (5 mL) added and the mixture refluxed for 48 hrs. On standing overnight a pale yellow solid appeared which was filtered off, washed with MeOH and diethyl ether, and

dried under vacuum. Yield 1.4 g; 73.3%. m.p. 283°C-285°C. Anal. Calcd for $C_{36}H_{26}N_{12}O{\cdot}1.5CH_3OH$: C, 65.17; H, 4.63; N, 24.33. Found: C, 65.65; H, 4.33; N, 24.06. Mass spectrum, major mass peaks (m/e) corresponding to the molecular ion and reasonable fragments: 643($M^+$, 24.40%), 642(64.90%), 550(14.20%), 548(12.60%), 455(21.90%), 320(9.40%), 94(23.50%), 78(100.00%), 67(19.30%), 51(10.00%). The $^1H$ nmr of O-P is rather broad and difficult to assign. IR, $cm^{-1}$: 467(m), 641(m), 730(s), 784(vs), 874(s), 961(s), 993(vs), 1161(vs), 1221(vs), 1279(vs), 1316(vs), 1366(vs), 1535(vs), 1624(vs).

C-I (**23**) was prepared in the same manner as O-I from 1,2-bis(3,4-dicyanophenoxy)benzene (**24**), and C-P (**25**) by a similar reaction of the isoindoline intermediate with hydrazine. C-I (Yield 25.7%). m.p. 268-271°C. Anal. Calcd for $C_{42}H_{28}N_{10}O_2{\cdot}H_2O{\cdot}CH_3OH$: C, 68.43; H, 4.50; N, 18.56. Found: C, 68.60; H, 4.03; N, 18.01. Mass spectrum, major mass peaks (m/e): 626 (M-Py, 11.7%), 609(4.6%), 533(11.0%), 532(28.5%), 455(3.1%), 440(2.2%), 352(7.0%), 313(3.0%), 220(1.3%), 170(2.7%), 155(2.3%), 94(2.8%), 79(13%), 78(100%). NMR spectra were assigned according to Fig. 3.1.a. $^1H$ NMR (302 K, $CDCl_3$), (chemical shift, ppm)(relative intensity): 7.01-7.13(8) (multiplet, benzene and pyridine), 7.35(2) (doublet, $H_b$), 7.29-7.46(4) (multiplet, pyridine), 7.63(2) (doublet, $H_a$), 7.61-7.73(4) (multiplet, pyridine), 7.93(2) (doublet, $H_c$), 8.54(4) (multiplet, pyridine). $^{13}C$ NMR ($CDCl_3$/TMS), (chemical shift, ppm): 109.73, 120.27, 123.56, 129.49, 137.60,

147.28, 152.60, 160.29. IR, $cm^{-1}$: 536(m), 664(s), 716(s), 793(s), 882(m), 1026(vs), 1384(vs), 1258(s), 1458(vs), 1578(vs), 1624(vs). Cosy NMR spectrum of C-I is shown in Fig. 3.3. C-P (Yield 45%). m.p. 241°C-244°C. Anal. Calcd for $C_{42}H_{30}N_{12}O_2$: C, 68.66; H, 4.12; N, 22.88. Found: C, 68.55; H, 4.49; N, 22.89. Mass spectrum, major mass peaks (m/e): 642(17.1%), 641 (M-NH-Py, 27.8%), 624(14.5%), 548(18.3%), 547(45.9%), 532(7.3%), 519(2.3%), 455(7.6%), 422(3.9%), 403(2.8%), 367(17.1%), 311(5.3%), 194(2.9%), 155(2.8%), 95.1(12.9%), 79(34.5%), 78(100%). IR, $cm^{-1}$: 734(m), 770(m), 948(m), 980(m), 1103(m), 1140(m), 1207(m), 1265(m), 1314(m), 1351(m), 1377(m), 1425(vs), 1460(vs), 1528(s), 1569(vs), 3600(br). The proton nmr spectrum of C-P is rather broad and ill defined and difficult to assign.

***d. 1,2,3-tris(3,4-dicyanophenoxy)propane (G-CN) (26)***

4-nitrophthalonitrile (6.93 g, 0.04 mol), $K_2CO_3$ (17.0 g), and glycerol (1.26 g, 0.014 mol) were stirred in DMF (80 mL) for 72 hrs at room temperature and the mixture poured into 1 litre of water. A pale yellow solid formed, which was filtered off, washed with water and dried under vacuum. Yield 5.7 g; 91%. m.p. 214-218°C. Mass spectrum, major mass peaks (m/e): 471($M^+$, 3.9%), 470(12.1%), 183(56.5%), 158(12.1%), 157(100%), 155(15.8%), 144(42.9%), 129(12.9%), 127(40.1%), 116.1(11.1%), 100(10.1%). $^1H$ NMR (302 K, DMSO-$d_6$), (chemical shift, ppm)(relative intensity): 4.61(4) (doublet, $CH_2$), 5.52(1) (multiplet, CH),

7.50(3) (multiplet, benzene), 7.85(3) (multiplet, benzene), 8.05(3) (doublet, benzene).

***e. 1,2,3-tris-(1,3-bis(2'-pyridylimino)isoindoline-5'-oxylyl)propane (G-I) (27)***

(**27**) was prepared as above from G-CN. Yield: 54.2%. m.p. 209°C-212°C. Anal. Calcd. for $C_{57}H_{41}N_{15}O_3 \cdot 2H_2O$: C, 66.65; H, 4.45; N, 20.60. Found: C, 66.43; H, 4.53; N, 21.49. Major reasonable fragments (m/e) were found in the FAB mass spectrum: 984($M^+$, 2.1%), 983(5.0%), 982(6.2%), 906(1.0%), 304(3.7%), 260(8.3%), 238(2.4%), 216(11.0%), 194(13.8%), 176(4.3%), 172(16.1%), 162(2.7%), 154(16.4%), 150(100%), 136(14.3%). $^1$H NMR(302 K, $CDCl_3$/TMS), (chemical shift, ppm)(relative intensity): 3.36(4) (multiplet, alkyl), 5.38(1) (multiplet, alkyl), 7.11(6) (multiplet, pyridine), 7.26(3) (multiplet, benzene), 7.44(6) (multiplet, pyridine), 7.64(3) (multiplet, benzene), 7.75(6) (multiplet, pyridine), 8.00(3) (multiplet, benzene), 8.59(6) (multiplet, pyridine). Cosy NMR spectrum of G-I is shown in Fig. 3.4. IR, $cm^{-1}$: 954(m), 1027(s), 1145(s), 1365(m), 1456(vs), 1577(s), 1624(m), 1730(m), 2668(w), 3183(m), 3500(m).

***f. 1,2,3-tris-(1,3-bis(2'-pyridylimino)phthalazine-5'-oxylyl)propane (G-P) (28)***

(**28**) was prepared by reaction of G-I with hydrazine as described previously. Yield: 98.5%. m.p. 188°C-194°C. Anal. Calcd. for $C_{57}H_{44}N_{18}O_3 \cdot 4H_2O$: C, 62.17; H, 4.76; N, 22.90. Found: C, 61.93; H, 4.88; N, 22.75. Major fragments (m/e) were found in the FAB mass spectrum: 1028($M^+$, 3.9%), 1027(3.6%), 514(1.2%),

371(2.9%), 332(1.4%), 331(5.9%), 330(4.1%), 329(8.7%), 314(1.7%), 308(3.7%), 289(10.3%), 273(3.6%), 237(2.3%), 155(24.0%), 153(7.0%), 139(10.9%). $^1$H NMR (302 K, DMSO-$d_6$/TMS), (chemical shift, ppm)(relative intensity): 4.79(4) (multiplet, alkyl), 5.81(1) (multiplet, alkyl), 6.91(6) (multiplet, pyridine), 7.71(12) (multiplet, pyridine), 7.93(3) (multiplet, benzene), 8.05(3) (multiplet, benzene), 8.25(6) (multiplet, pyridine), 8.43(3) (multiplet, pyridine). Cosy NMR spectrum of G-P is shown in Fig. 3.5. IR, cm$^{-1}$: 773(w), 735(m), 992(m), 1096(m), 1147(s), 1226(s), 1318(s), 1376(vs), 1434(vs), 1460(vs), 1532(vs), 1571(vs), 3368(m).

***g. 1,1',1'',1'''-tetrakis-(1,3-bis(2'-pyridylimino)isoindoline-5'-oxymethyl) methane (P-I) (29).***

(**29**) was prepared from tetrakis[(3,4-dicyanophenoxy)methyl] methane (P-CN) (**30**)[84], and ring expanded in the usual way to produce P-P (**31**). Yield: 92%. m.p.>300°C. Anal. Calcd. for $C_{77}H_{56}N_{20}O_4{\cdot}2H_2O$: C, 67.93; H, 4.44; N, 20.58. Found: C, 67.91; H, 5.05; N, 21.16. Major fragments (m/e) were found in the FAB mass spectrum: 1326 ($M^+$, 5.2%), 1324(0.3%), 1249(4.8%), 1173(1.6%), 482(7.0%), 460(14.5%), 329(60.9%), 309(6.3%), 307(100%). $^1$H NMR (302 K, $CDCl_3$/TMS), (chemical shift, ppm)(relative intensity): 4.68(8) (singlet, alkyl), 7.09(8) (multiplet, pyridine), 7.20(4) (multiplet, benzene), 7.45(8) (multiplet, pyridine), 7.70(12) (multiplet, pyridine and benzene), 7.95(4) (doublet, benzene), 8.57(8) (multiplet, pyridine $H_6$). IR, cm$^{-1}$: 534(w), 721(m), 808(m), 1213(s), 1262(w), 1377(vs),

1457(vs), 1578(s), 1626(vs).

***h. 1,1',1",1'"-tetrakis-(1,4-bis(2'-pyridineamino)phthalazines-6'-oxymethyl)methane (P-P) (31).***

Yield: 55%. m.p. 225-230°C. Anal. Calcd. for $C_{77}H_{60}N_{24}O_4 3H_2O$: C, 64.24; H, 4.62; N, 23.36. Found: C, 64.79; H, 4.67; N, 22.88. $^1H$ NMR spectrum is broad and difficult to assign. Major fragments (m/e) were found in the FAB mass spectrum: 1386($M^+$, 3.9%), 1384(15.6%), 1307(8.6%), 1197(2.2%), 979(1.1%), 32964.1%), 237(41.7%), 154(100%). IR, $cm^{-1}$: 722(m), 772(w), 1015(w), 1143(w), 1225(w), 1315(w), 1377(vs), 1461(vs), 1529(w), 1571(vs).

### 3.2 NMR spectra of some ligands

Proton NMR spectra of these polynucleating ligands are rather complex due to overlapping resonances in the benzene and pyridine range, conformational isomerization and presence of a mixture of tautomers due to proton exchange of active hydrogen atoms. Cosy NMR spectra were done and shown in Fig.3.2---Fig.3.5. (most polyisoindolines were recorded in $CDCl_3$ and polyphthalazines were recorded in DMSO-$d_6$). It is very interesting to note that the chemical shift of the two pyridyl groups on the two sides of the polyisoindolines and polyphthalazines are different because of the unsymmetric connection of these polyisoindolines and polyphthalazines with substituted oxygen atoms.

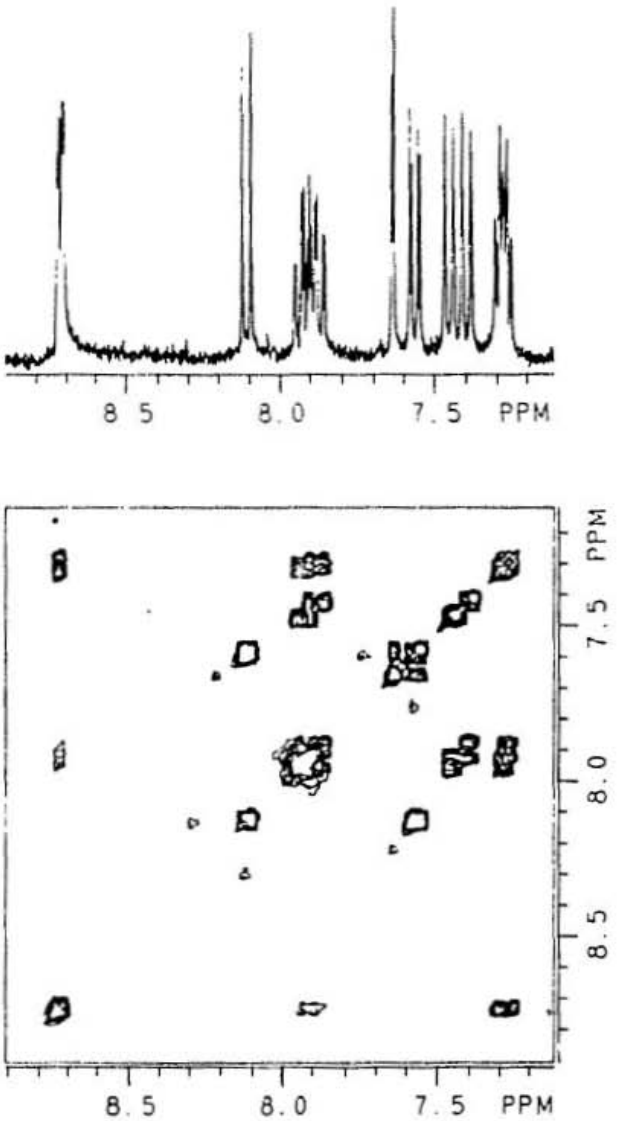


**Fig.3.2** Cosy NMR of O-I

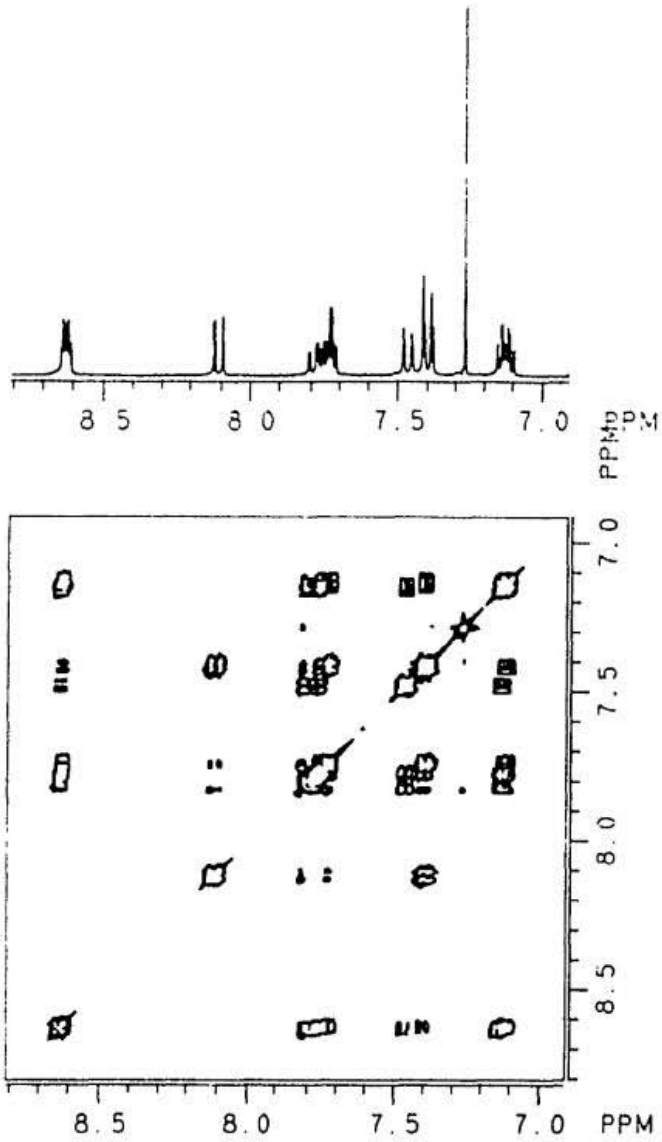


Fig.3.3 Cosy NMR of C-I

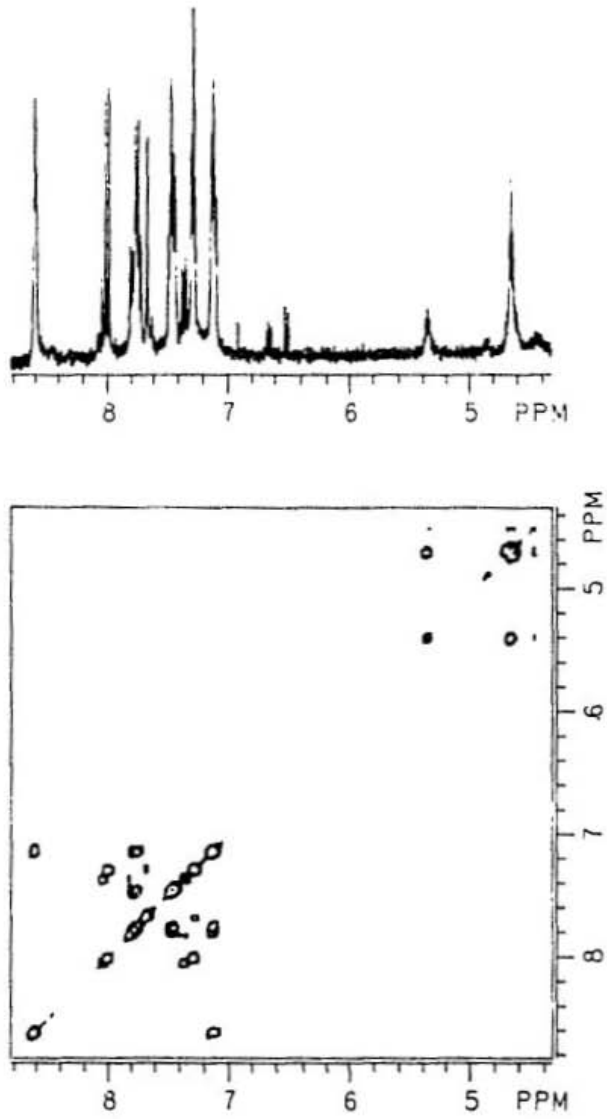


**Fig.3.4** Cosy NMR of G-I

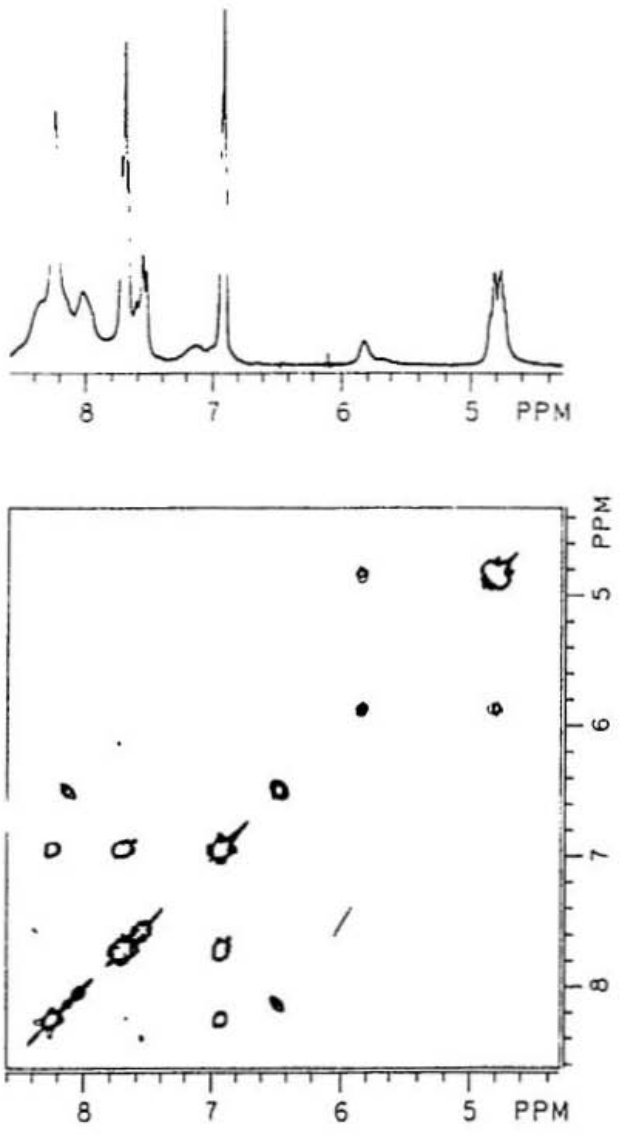


**Fig.3.5** Cosy NMR of G-P

# Chapter 4 SYNTHESIS AND CHARACTERIZATION OF POLYNUCLEAR COMPLEXES

## 4.1 Cu(II) complexes of polyisoindolines

### *$Cu_2$(O-I)$(NO_3)_4$·3$CH_3OH$ (32)*

O-I (0.1 g, 0.16 mmol) was dissolved in chloroform (10 mL), an excess of copper(II) nitrate was dissolved in methanol (40 mL), and the two solutions were mixed, and refluxed for a few hours. A yellow green microcrystalline soiid was formed which was filtered off, washed with methanol and then diethyl ether three times and dried under vacuum. Yield: 0.14g; 87.5%. A portion of the complex was dissolved in DMF solvent and diethyl ether diffused in. Dark green twinned crystals were formed, which were unsuitable for X-ray crystallographic analysis. Anal. Calcd for $C_{39}H_{36}N_{14}O_{16}Cu_2$ (**32**): C, 43.22; H, 3.35; N, 18.10; Cu, 11.74. Found: C, 42.80; H, 2.65; N, 17.81; Cu, 12.34.

### *$Cu_2$(O-I)$(CH_3COO)_4$·4$H_2O$ (33)*

O-I (0.1 g, 0.16 mmol) was dissolved in hot chloroform (15 mL), $Cu(CH_3COO)_2{\cdot}H_2O$ (0.2 g, 1.00 mmol) was dissolved in methanol (80 mL) and the two solutions mixed, and refluxed for 36 hrs. A brown microcrystalline solid

was formed which was filtered off, washed with methanol and then diethyl ether and dried under vacuum. Yield: 0.08 g; 47.7%. Anal. Calcd. for $C_{44}H_{44}N_{10}O_{13}Cu_2$ (**33**): C, 50.43; H, 4.19; N, 13.37; Cu, 12.13. Found: C, 49.80; H, 3.19; N, 14.11; Cu, 11.90.

*$Cu_2$(C-I)$Br_4$·$CH_3OH$ (34)*

Yellow green solid (**34**) was prepared as for (**33**) with 96.0% yield. Anal. Calcd for $C_{42}H_{32}N_{10}O_3Br_4Cu_2$ (**34**): C, 43.64; H, 2.73; N, 11.84. Found: C, 43.63; H, 2.43; N, 11.77.

## 4.2 Polynuclear Cu(II) complexes of polyphthalazines

*[$Cu_4$(C-P)($\mu_2$-OH)$_2$($\mu_2$-$NO_3$)$_2$($H_2O$)$_2$($NO_3$)$_2$]($NO_3$)$_2$·$4H_2O$ (35)*

C-P (0.1 g, 0.14 mmol) was added to an aqueous solution (100 mL) of excess $Cu(NO_3)_2.3H_2O$ and the mixture was refluxed for 24 hrs. The green solution was filtered to remove unreacted ligand and concentrated to about 10 mL. Green crystals formed on standing by adding a small amount of ethanol. The crystals were filtered, washed with EtOH and dried under vacuum. Anal. Calcd for $C_{42}H_{40}N_{18}O_{26}Cu_4$ (**35**): C, 34.39; H, 2.75; N, 17.19. Found: C, 34.42; H,2.67; N, 17.34. The crystals crumble readily on drying, losing lattice solvent. An X-ray

sample was kept in contact with mother liquid prior to crystallographic analysis, and was shown to contain four molecules of water of crystallization.

***$[Cu_4(O\text{-}P)(OH)_2(NO_3)_6]\cdot H_2O$ (36), $[Cu_4(O\text{-}P)(OH)_2(NO_3)_6]\cdot 10H_2O$ (37)***

O-P (0.1 g, 0.16 mmol) was suspended in 25 mL refluxing ethanol. Copper(II) nitrate trihydrate (0.3 g, 1.24 mmol) was dissolved in water (25 mL) and the solution added to ethanol suspension of O-P. The mixture was refluxed for 10 hrs. The unreacted ligand was filtered off and the filtrate allowed to evaporate slowly. Green crystals were obtained which were filtered off, washed with ethanol and dried under vacuum. Anal. Calcd for $C_{36}H_{30}N_{18}O_{22}Cu_4$ (**36**): C, 32.73; H, 2.27; N, 19.09; Cu, 19.24. Found: C, 32.60; H, 2.61; N, 19.61, Cu, 19.72.

Sodium nitrate (0.1 g) was added to the saturated aqueous solution (100 mL) of (**36**) at room temperature, reduced the volume of the solution to about 20 mL on the steambath and then evaporated slowly, green crystals were formed on standing, which were filtered off, washed with ethanol and dried under vacuum. Anal. Calcd for $C_{36}H_{48}N_{18}O_{31}Cu_4$ (**37**): C, 29.16; H, 3.26; N, 17.01; Cu, 17.04. Found: C, 28.03; H, 2.36; N, 17.97; Cu, 17.01. Crystals suitable for X-ray analysis were kept in contact with the mother liquor because of solvent loss on exposure to air.

***$[Cu_4(C\text{-}P)(OH)_2(SO_4)_2]SO_4\cdot 4H_2O$ (38)***

Sodium sulphate (0.1 g) was added to a saturated aqueous solution (100 mL)

of (**35**) at room temperature and the mixture heated on a steambath for a few minutes. A green solid formed, which was filtered off, washed with water and ethyl alcohol and dried under vacuum. Anal. Calcd. for $C_{46}H_{40}N_{12}O_{20}S_3Cu_4$ (**38**): C, 36.48; H, 3.47; N, 12.16; Found: C, 36.33; H, 3.01; N, 12.94.

***$[Cu_4(O\text{-}P)(OH)_2Cl_6]\cdot 4H_2O$ (39), $[Cu_4(C\text{-}P)(OH)_2Br_6]\cdot 2CH_3CH_2OH$ (40)***

O-P (0.1 g, 0.16 mmol) and C-P (0.1 g, 0.13 mmol) were mixed and refluxed for 36 hrs with excess amount of $CuCl_2$ and $CuBr_2$ in aqueous ethanol solution (120 mL) respectively. Green solids that were formed, which were filtered off, washed with methanol and diethyl ether three times and dried under vacuum. Anal. Calcd for $C_{36}H_{36}N_{12}O_7Cl_6Cu_4$ (**39**), C, 35.57; H, 2.99; N, 13.83; Found: C, 35.55; H, 2.59; N, 13.50. Anal. Calcd for $C_{46}H_{44}N_{12}O_6Br_6Cu_4$ (**40**), C, 34.65; H, 2.76; N, 10.55; Cu, 15.03; Found: C, 35.79; H, 2.47; N, 11.62, Cu, 15.94.

***$[Cu_6(G\text{-}P)(OH)_3Cl_9]\cdot 4H_2O$ (41), $[Cu_6(G\text{-}P)(OH)_3Br_9]\cdot 6H_2O$ (42).***

G-P (0.2 g, 0.19 mmol) was added to an aqueous methanol solution (75 mL) of $CuCl_2.2H_2O$ (0.6 g, 3.5 mmol), and the mixture refluxed for 24 hrs. The insoluble green solid formed which was filtered off, washed with water, methanol and diethyl ether and dried under vacuum. Yield 0.2 g; 55.3%. Anal. Calcd. for $C_{57}H_{55}N_{18}O_{10}Cl_9Cu_6$ (**41**): C, 36.95; H, 2.97; N, 13.61; Cu, 20.61; Found: C, 37.00; H, 3.16; N, 13.50; Cu, 19.36. (**42**) Was obtained in a similar fashion as a dark green solid. Anal. Calcd. for $C_{57}H_{59}N_{18}O_{12}Br_9Cu_6$ (**42**): C, 29.90; H, 2.64; N, 11.01;

Cu, 16.64; Found: C, 30.49; H, 2.40; N, 11.09; Cu, 15.94.

***$[Cu_6(G\text{-}P)(OH)_3(NO_3)_9]\cdot 12H_2O$ (43), $[Cu_6(G\text{-}P)(OH)_3(SO_4)_{4.5}]\cdot 11H_2O$ (44)***

G-P (0.25 g, 0.24 mmol) was suspended in ethanol (30 mL) and an aqueous solution (30 mL) of $Cu(NO_3)_2.3H_2O$ (1.0 g, 4.14 mmol) was added. The mixture was refluxed for 72 hrs, forming a deep green solution. The volume of the solution was reduced to about 20 mL with the formation of a green solid which was filtered off, washed with ethanol and dried under vacuum. Yield 0.40 g; 75%. Anal. Calcd. for $C_{57}H_{71}N_{27}O_{45}Cu_6$ (**43**): C, 30.62; H, 3.20; N, 16.92; Cu, 17.06. Found: C, 30.07; H, 2.46; N, 17.45; Cu, 16.82. (**44**) was prepared by treating an aqueous solution of (**43**) with excess of sodium sulphate and obtained as a green, insoluble solid. The product was washed with water and ethanol and dried under vacuum. Anal. Calcd. for $C_{57}H_{69}N_{18}O_{35}S_{4.5}Cu_6$ (**44**): C, 32.74; H, 3.30; N, 12.06: Found: C, 32.74; H, 3.30; N, 12.27.

***$[Cu_8(P\text{-}P)(OH)_4Cl_{12}]\cdot 10H_2O$ (45), $[Cu_8(P\text{-}P)(OH)_4Br_{12}]\cdot 8H_2O$ (46)***

P-P (0.15 g, 0.11 mmol) was added to a solution of $CuCl_2\cdot 2H_2O$ (0.5 g, 2.93 mmol) dissolved in methanol (50 mL) and the mixture refluxed for 36 hrs. A green solid formed which was filtered off, washed with methanol and diethyl ether and dried under vacuum. Anal. Calcd. for $C_{77}H_{84}N_{24}O_{18}Cl_{12}Cu_8$ (**45**): C, 36.02; H, 3.12; N, 13.09; Cu, 20.08. Found: C, 35.96; H, 2.84; N, 12.96; Cu, 20.72. (**46**)

was prepared in a similar manner. Anal. Calcd. for $C_{77}H_{80}N_{24}O_{16}Br_{12}Cu_8$ (46): C, 30.18; H, 2.63; N, 10.97; Cu, 16.59. Found: C, 30.45; H, 2.41; N, 10.89; Cu, 15.93.

*$[Cu_8(P\text{-}P)(OH)_4(NO_3)_{12}]\cdot 8CH_3OH$ (47)*

P-P (0.41 g, 0.30 mmol) was added to an aqueous methanol (v/v = 50/50) (100 mL) solution of $Cu(NO_3)_2\cdot 3H_2O$ (1.0 g, 0.72 mmol) and the mixture refluxed for 36 hrs with the formation of a deep green solution. The solution was filtered and reduced to a small volume and allowed to stand at room temperature. A green crystalline solid formed which was filtered off, washed with methanol and dried under vacuum. Anal. Calcd. for $C_{85}H_{96}N_{36}O_{52}Cu_8$ (47): C, 36.85; H, 2.94; N, 17.03. Found: C, 36.85; H, 2.94; N, 16.99.

## 4.3 Ni(II) and Co(II) complexes of polyphthalazines

*$Ni(O\text{-}P)(NO_3)_2\cdot 8H_2O$ (48)*

O-P (0.8 g, 1.24 mmol) was mixed with excess amount of $Ni(NO_3)_2\cdot 6H_2O$ (1.0 g, 3.44 mmol) in 100 mL aqueous methanol, and the mixture refluxed for 36 hrs. A grey solid formed which was filtered off, washed with methanol and diethyl ether and dried under vacuum. Yield: 1.2 g, 93.5%. Anal. Calcd. for

$C_{36}H_{42}N_{14}O_{15}Ni$ (**48**): C, 44.60; H, 4.33; N, 20.23; Ni, 6.06. Found: C, 43.74; H, 3.41; N, 19.89; Ni, 5.67.

*$Co_3$(G-P)$Cl_6$·10$H_2O$ (49)*

G-P (0.15 g, 0.15 mmol) was refluxed with aqueous ethanol solution (120 mL) of $CoCl_2 \cdot 6H_2O$ (0.15g, 0.63 mmol) for 24 hrs. Unreacted ligand was then filtered off and the volume of solution reduced to about 20 mL. A dark blue solid appeared which was filtered off, washed with methanol and diethyl ether and dried under vacuum. Anal. Calcd. for $C_{57}H_{64}N_{18}O_{13}Cl_6Co_3$ (**49**): C, 42.82; H, 4.03; N, 15.77; Co, 11.06. Found: C, 42.43; H, 3.59; N, 15.35; Co, 11.65.

## 4.4 Infrared, electronic and epr spectra of the complexes

A. The characteristic infrared absorption of the pyridine residue

The infrared spectra of the polyisoindoline and polyphthalazine ligands exhibit a band around 990 $cm^{-1}$, which is associated with a pyridine ring breathing mode of vibration, and which is typically shifted to higher energy by 20-30 $cm^{-1}$ on coordination.[42] The infrared spectra of all the complexes are similar in this region, with a pyridine ring breathing band in excess of 1000 $cm^{-1}$ (Table 4.1)

indicating coordination of all the pyridine residues. Infrared spectra (Table 4.1) of most complexes have characteristic absorptions around 3500 $cm^{-1}$ or above, associated with the bridging OH group, coordinated water and alcohol. Far-infrared spectra for (**34**), (**39**), (**40**), (**41**), (**42**), (**45**), (**46**) and (**49**) are very complex and difficult to assign, but by comparing them with other derivatives, the presence of coordinated halogen is indicated. The nitrate complexes (**32**), (**35**), (**36**), (**37**), (**43**), (**47**) and (**48**) exhibit two characteristic nitrate combination band absorptions ($\nu_1 + \nu_4$) in the range 1725 to 1795 $cm^{-1}$, which can be assigned to a bridging bidentate nitrate group,[94] while the other nitrates appear to be monodentate and ionic, on the basis of the presence of the absorptions around 1764 and 1755 $cm^{-1}$ with the absorption split around 9 $cm^{-1}$, and a shoulder around 1740 $cm^{-1}$. It is very interesting to note that (**37**) exhibits more complicated nitrate combination absorptions at 1726, 1748, 1754, 1764, 1776 and 1787 $cm^{-1}$ compared with (**36**) though they are comprised of the same ligand and anions, which can be explained by the X-ray structure. (**37**) has the zig-zag polymeric structure comprised of (**36**) joined by an unusual bridging bidentate coordinated nitrate group. (**38**) and (**44**) exhibit two characteristic sulphate band absorptions around 1059 and 1110 $cm^{-1}$, which can be assigned to the bridging bidentate sulphate group.[95]

**B.** Electronic and epr spectra of the complexes

Solid-state, mull transmittance electronic spectra for the copper complexes of the polyphthalazines are characterized by the presence of an intense charge transfer absorption in the range 260 nm-480 nm, with a lower energy, less intense band in the range 640 nm-720 nm, which is assigned to a Cu(II) d-d transition band associated with five-coordinated square pyramidal or six-coordinated octahedral Cu(II). The very intense charge-transfer absorptions observed for these complexes seem to be a characteristic feature associated with these ligands with a relatively low energy anti-bonding orbital and so the electronic origin of these intense bands would be assumed to be MLCT and polyphthalazine ligand $\pi$-$\pi^*$ charge transfer absorptions. The copper complexes of the polyisoindolines (**32**), (**33**) and (**34**) show an intense charge-transfer absorption in the range 300 nm-450 nm, and a less intense band in the range 650 nm-680 nm, which is assigned to a Cu(II) d-d transition band associated with five- or six-coordinated square pyramidal or octahedral Cu(II), with the Cu(II) coordinated with nitrogen atoms from two pyridines and with several anions. The very intense charge-transfer absorptions would be assumed to be MLCT and polyisoindoline ligand $\pi$-$\pi^*$ transfer bands. Structurally, (**38**) is expected to be analogous to (**35**), with two axially coordinated

bridging bidentate and one ionic sulphate.[46] (**38**) is clearly a dihydroxo-bridged derivative, involving three bridges (equatorial diazine and hydroxide and axial sulphate) between the copper(II) centres, consistent with its very low magnetic moment. The polyphthalazine ligands can be considered as the duplication of two, three or four PAP fragments connected by polyalcohol frameworks, and each phthalazine-like branch can accommodate one dinuclear Cu(II) centre in an arrangment which resembles the complexes of PAP. The chloride and bromide complexes of the polyphthalazines have d-d absorptions in the range 640 nm-720 nm, and are expected to have analogous structures to the five-coordinate binuclear hydroxo-bridged phthalazine complexes $[Cu_2(PAP)(OH)X_3]$[42] (X = Cl, Br; PAP = 1,4-bis(2'-pyridylamino)phthalazine), which have d-d absorptions at 637 nm and 633 nm respectively in the solid state. (**48**) has an intense absorption at 510 nm, and one weak absorption at 710 nm, which are associated with d-d transition of six coordinate octahedral or pseudo-octahedral Ni(II).[96] (**49**) has an intense absorption at 520 nm and an absorption at 630 nm, which are assigned to $T_{1g}$ and $A_{2g}$ d-d transitions respectively.[96]

Most polynuclear complexes of the polyphthalazines in the solid state are EPR silent at room temperature and 77 K because of strong antiferromagnetic coupling present in the complexes. However, EPR spectra were observed on a

few complexes because of the existence of the paramagnetic impurities. Complex (**32**) at 77 K, g= 2.08; Complex (**33**) at room temperature, g=2.00; Complex (**36**) in solid state at room temperature and 77 K has an isotropic EPR, g=2.03, but in DMF solution, EPR spectra of (**36**) at room temperature become rather complicated and quite different from the solid state spectra, $g_{\parallel}=2.22$, $g_{\perp}=2.07$, which indicates a major structural change; at 77 K, EPR spectra of (**36**) changed slightly, $g_{\parallel}=2.25$, $g_{\perp}=2.05$. EPR spectrum of complex (**43**) changes greatly as temperature changes. In the solid state, no EPR spectrum was observed at room temperature; at 77K, $g_{\parallel}=2.22$, $g_{\perp}=2.04$. In DMF solution at 77 K, $g_{\parallel}=2.41$, $g_{\perp}=2.06$.

**Table 4.1** IR, UV/VIS spectra of complexes

| | Py, $cm^{-1}$ | OH, $H_2O$ $cm^{-1}$ | $NO_3^-$, $cm^{-1}$ $\upsilon_1 + \upsilon_4$ | UV/VIS (nm) solid |
|---|---|---|---|---|
| $Cu_2(O\text{-}I)(NO_3)_4 \cdot 3CH_3OH$ (**32**) | 1011 | 3490 | 1730,1737,1754 1764, 1794 | 680 |
| $Cu_2(O\text{-}I)(CH_3COO)_4 \cdot 4H_2O$ (**33**) | 1012 | 3470 | | 650 |
| $Cu_2(C\text{-}I)Br_4 \cdot CH_3OH$ (**34**) | 1024 | | | 660 |
| $[Cu_4(C\text{-}P)(\mu_2\text{-}OH)_2(\mu_2\text{-}NO_3)_2(H_2O)_2 (NO_3)_2](NO_3)_2 \cdot 4H_2O$ (**35**) | 1025 | 3437 | 1731,1755 1764,1776 | 650 |
| $[Cu_4(O\text{-}P)(OH)_2(NO_3)_6] \cdot H_2O$ (**36**) | 1022 | 3466 | 1726,1758 1789 | 675 |
| $[Cu_4(O\text{-}P)(OH)_2(NO_3)_6] \cdot 10H_2O$ (**37**) | 1024 | 3435 | 1726,1748,1754 1764,1776,1787 | 660 |
| $[Cu_4(C\text{-}P)(OH)_2(SO_4)_2]SO_4 \cdot 4H_2O$ (**38**) | 1029 | 3437 | | 670 |
| $[Cu_4(O\text{-}P)(OH)_2Cl_6] \cdot 4H_2O$ (**39**) | 1028 | 3450 | | 700 |
| $[Cu_4(C\text{-}P)(OH)_2Br_6] \cdot 2CH_3CH_2OH$ (**40**) | 1022 | | | 720 |

Table 4.1 IR, UV/VIS spectra of complexes

| | Py, $cm^{-1}$ | OH, $H_2O$ $cm^{-1}$ | $NO_3^-$,$cm^{-1}$ $\upsilon_1 + \upsilon_4$ | UV/VIS (nm) solid |
|---|---|---|---|---|
| $[Cu_6(G\text{-}P)(OH)_3Cl_9]\cdot 4H_2O$ (**41**) | 1023 | 3440 | | 690 |
| $[Cu_6(G\text{-}P)(OH)_3Br_9]\cdot 6H_2O$ (**42**) | 1024 | 3444 | | 700 |
| $Cu_6(G\text{-}P)(OH)_3(NO_3)_9\cdot 12H_2O$ (**43**) | 1028 | 3535 | 1714,1736 1759 | 650 |
| $[Cu_6(G\text{-}P)(OH)_3(SO_4)_{4.5}]\cdot 11H_2O$ (**44**) | 1025 | 3488 | | 670 |
| $[Cu_8(P\text{-}P(OH)_4Cl_{12}]\cdot 10H_2O$ (**45**) | 1023 | 3520 | | 640 |
| $[Cu_8(P\text{-}P)(OH)_4Br_{12}]\cdot 8H_2O$ (**46**) | 1022 | 3530 | | 650 |
| $[Cu_8(P\text{-}P)(OH)_4(NO_3)_{12}]\cdot 8CH_3OH$ (**47**) | 1023 | 3520 | 1704,1731 1754 | 660 |
| $Ni(O\text{-}P)(NO_3)_2\cdot 8H_2O$ (**48**) | 1013 | 3515 | 1704,1764 | 510,710 |
| $Co_3(G\text{-}P)Cl_6\cdot 10H_2O$ (**49**) | 1023 | 3525 | | 520,630 |

### 4.5 Thermodynamic and kinetic effects

The polynuclear complex formation process is dependent on the structure of the polynucleating ligand and the nature of the metal ions and anions, but also will be affected by thermodynamic, kinetic and solvent effects. Polynuclear Cu(II) complexes gain additional stability by forming OH bridged structures, which is not common for Ni(II) and Co(II) complexes. Cu(II) complexes are likely to be more stable than Ni(II) and Co(II) complexes with coordination numbers 4 and 5, especially since the ligand can only supply 2 nitrogen donors per metal. The maximum number of metal ions a single polynucleating ligand can incorporate is dependent not only on the building blocks of the polynucleating ligands and the nature of the metal ions and anions, but also on the equilibrium of these favourable and unfavourable effects.

Thermodynamic and chelate effects would favour the formation of spin-coupled hydroxide-bridged polynuclear complexes. However, the number of moles decreases greatly during the polynuclear complex formation processes, and if we assume these processes involve the simple association of a large number of individual particles, then, from a simple entropy point of view, the formation of the polynuclear complexes containing large numbers of metals and associated anions and solvent molecules would be unfavourable. (Scheme 4.1).

**Scheme 4.1** Entropy Effect

$4Cu(NO_3)_2$ + C-l· · ·$H_2O$---------->

$Cu_4$(C-P)$(OH)_2(NO_3)_6{\cdot}4H_2O$ + $2H^+$ + $2NO_3^-$

a. assume all the monodentate nitrates dissociate:

$4Cu^{2+}$ + $8NO_3^-$ + C-P + $6H_2O$---------->

$[Cu_4(C-P)(OH)_2(NO_3)_2(H_2O)_4]^{4+}$ + $2H^+$ + $6NO_3^-$

$\Delta n^*$=-10

b. assume no nitrate dissociation:

$4Cu^{2+}$ + $8NO_3^-$ + C-P + $4H_2O$---------->

$[Cu_4(C-P)(OH)_2(\mu_2\text{-}NO_3)_2(NO_3)_2(H_2O)_2]^{2+}$ + $2H^+$ + $4NO_3^-$

$\Delta n$=-10

*$\Delta n$, the change of the number of moles

# Chapter 5 CRYSTAL AND MOLECULAR STRUCTURES OF TWO POLYNUCLEAR COMPLEXES

## 5.1 Crystal structure of $[Cu_4(C\text{-}P)(\mu_2\text{-}OH)_2(\mu_2\text{-}NO_3)_2(NO_3)_2(H_2O)_2](NO_3)_2{\cdot}4H_2O$ (35).

### 5.1.A Collection of X-ray intensity data

Crystals of (35) are green hexagonal plates. The diffraction intensities of an approximately 0.40 X 0.30 X 0.05 mm crystal were collected with graphite-monochromatized Mo Kα radiation by using the ω-2θ scan mode to $2\theta_{max} = 44.9°$ on a Rigaku AFC6S diffractometer at -80°C. Of a total of 10,911 measured reflections, 10,338 were unique and 5958 reflections were observed with $I_{net} > 2.5\sigma(I_{net})$. Data were corrected for Lorentz-polarization absorption effects. The cell parameters were obtained by the least-squares refinement of the setting angles of 24 reflections with $2\theta = 9.12°\text{-}11.23°$. An empirical absorption correction was applied, using the program DIFABS,[97] which resulted in transmission factors ranging from 0.74 to 1.00.

### 5.1.B Solution and refinement of the structure

The structure was solved by direct methods[98,99] and just the copper atoms were refined anisotropically. The final cycle of full-matrix least-squares refinement was based on 5958 reflections and 762 variables and converged with $R = 0.063$ and $R_w = 0.058$, with weights based on counting statistics. The maximum and minimum peaks on the final difference map corresponded to 1.09 and -0.84 $e^-/Å^3$ respectively. Neutral atom scattering factors[100] and anomalous dispersion terms[101,102] were taken from the usual sources. All calculations were performed with the TEXSAN[103] crystallographic software package using a VAX 3100 work station. A summary of crystal and other data is given in Table 5.1 and atomic coordinates are given in Table SI.I.

### 5.1.C Description of the structure of (35)

The structure of (**35**) is shown in Figs. 5.1 and 5.2 (some coordinated water molecules and nitrates are not included for clarity), and interatomic distances and angles relevant to the copper coordination spheres are given in Tables 5.2 and 5.3. There are two chemically equivalent, but structurally slightly different, and not symmetry related, tetranuclear copper(II) complexes present in the unit cell, and

one of these (1) is illustrated in Fig. 5.1 (molecule 1 Cu(1)Cu(2)Cu(3)Cu(4); molecule 2 Cu(5)Cu(6)Cu(7)Cu(8)). The basic structure represents a unique arrangement in which four copper(II) centres are grouped into two pairs on each side of the catechol group, and within each dinuclear unit the copper(II) ions are bridged equatorially by the diazine $N_2$ group and by a hydroxide and axially by a bidentate nitrate. Fig. 5.2 illustrates one dinuclear centre). The dinuclear centre Cu(1)-Cu(2) differs slightly from the rest in that Cu(1) is considered to be six-coordinate with a long axial contact to a water molecule (Cu(1)-O(16) = 2.57(1) Å). The other dinuclear centers involve square-pyramidal copper atoms with additional basal sites occupied by monodentate nitrates and water molecules. Equatorial copper-ligand donor distances are close to 2.0 Å. and compare closely with those in related monomeric dinuclear complexes. Much longer axial distances are found to the bidentate bridging nitrate, which is bound in an asymmetric fashion with a relatively long and short copper-oxygen contact in all cases. The longer Cu(1)-O(32A) distance (2.589(9) Å) is a reflection on the presence of a second axial ligand ($H_2O$(16)) bound to Cu(1). Intradinuclear copper-copper separations fall in the range 3.122(3)-3.188(3) Å, with large Cu-OH-Cu bridge angles in the range 110.4(4)°-116.7(5)°. (**35**) is structurally similar to the binuclear Cu(II) pyridyl-phthalazine complexes [$Cu_2$(PAP4Me)($\mu_2$-OH)($H_2O$)$_2$($\mu_2$-

$NO_3)(NO_3)]NO_3$ (**50**) and $[Cu_2(PAP)(\mu_2\text{-}OH)(\mu_2\text{-}SO_4)Cl]\cdot 2H_2O$ (**51**),[46] which involve square-pyramidal copper(II) centres bridged equatorially by the phthalazine-diazine ($N_2$) and a hydroxy group and axially by a bidentate anion. The pendant pyridine rings are twisted with respect to the phthalazine groups (dihedral angles 38.4°, 28.3°; 32.0°, 41.5° for molecule 1: comparable dihedral angles for molecule 2 are 28.3°, 34.2°; 36.4°, 33.1°) in a *syn* conformation, with a similar twist angle to those found in the monomeric PAP4Me complex.[46] As is usual in complexes of this sort the dinuclear centers are folded along tha Cu-Cu axes, with fold angles between the $Cu_2N_2$ and Cu(OH)Cu least squares planes of 50.1° and 54.1° for molecule 1 and 47.9° and 42.0° for molecule 2.

The two dinuclear centers do not lie close enough to each other for any direct interaction between the dinuclear centers, and the distance between extreme copper atoms is around 10 Å (Cu(1)-Cu(4) 10.475(3) Å). However the folding of the ligand around the connecting 1,2-catecholyl residue does cause some overlay of the two dinuclear centers, with the closest approach associated with two pyridine rings (Fig. 5.3). These rings are essentially parallel (dihedral angles 5.4° (molecule 1), 4.8° (molecule 2)) and quite closely spaced. The average spacings of 3.72 Å (molecule 1) and 4.35 Å (molecule 2). The unit cell packing diagram of (**35**) is shown in Fig. 5.4.

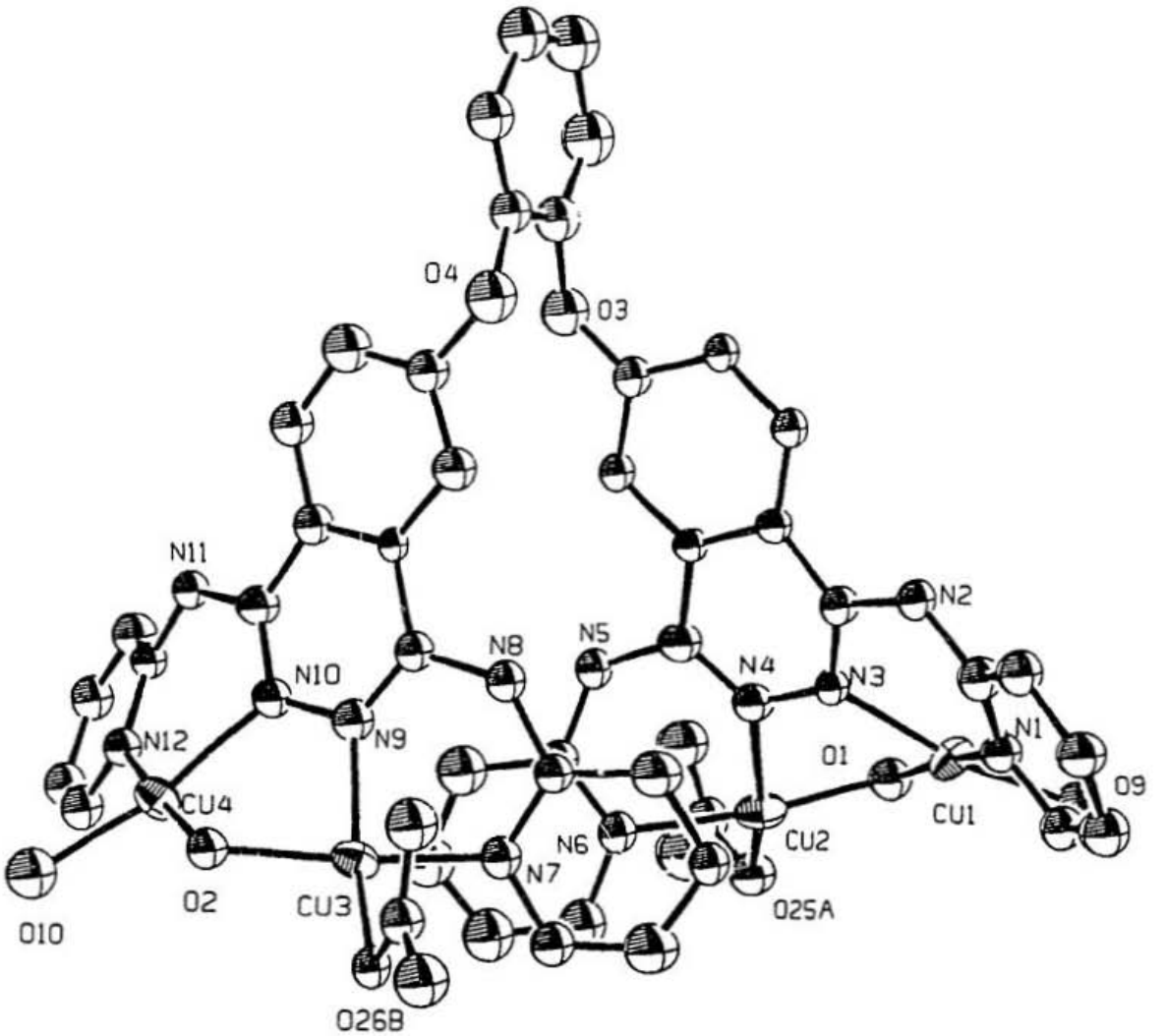


**Fig. 5.1** Crystal structure of one tetranuclear fragment of $[Cu_4(C\text{-}P)(\mu_2\text{-}OH)_2(\mu_2\text{-}NO_3)_2(NO_3)_2(H_2O)_2](NO_3)_2{\cdot}4H_2O$ (**35**).

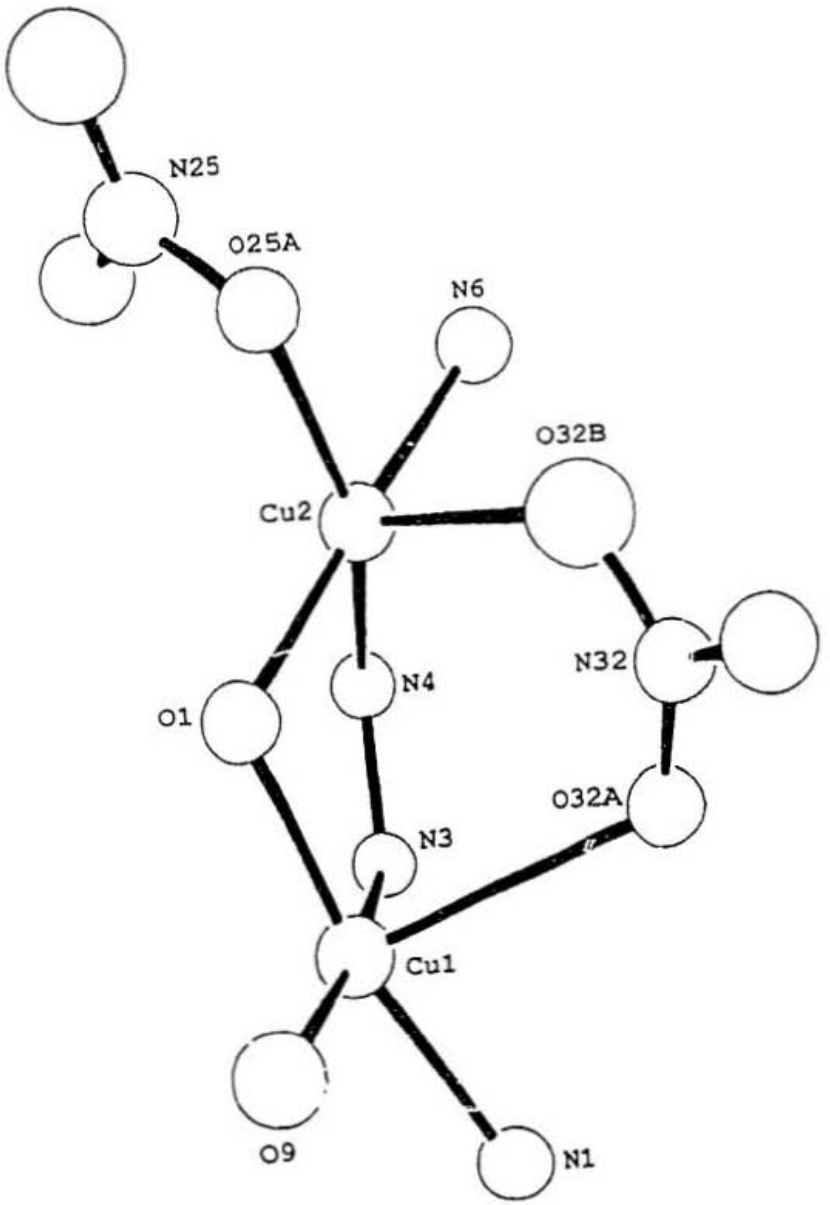


**Fig. 5.2** Structure of a dinuclear centre of (35)

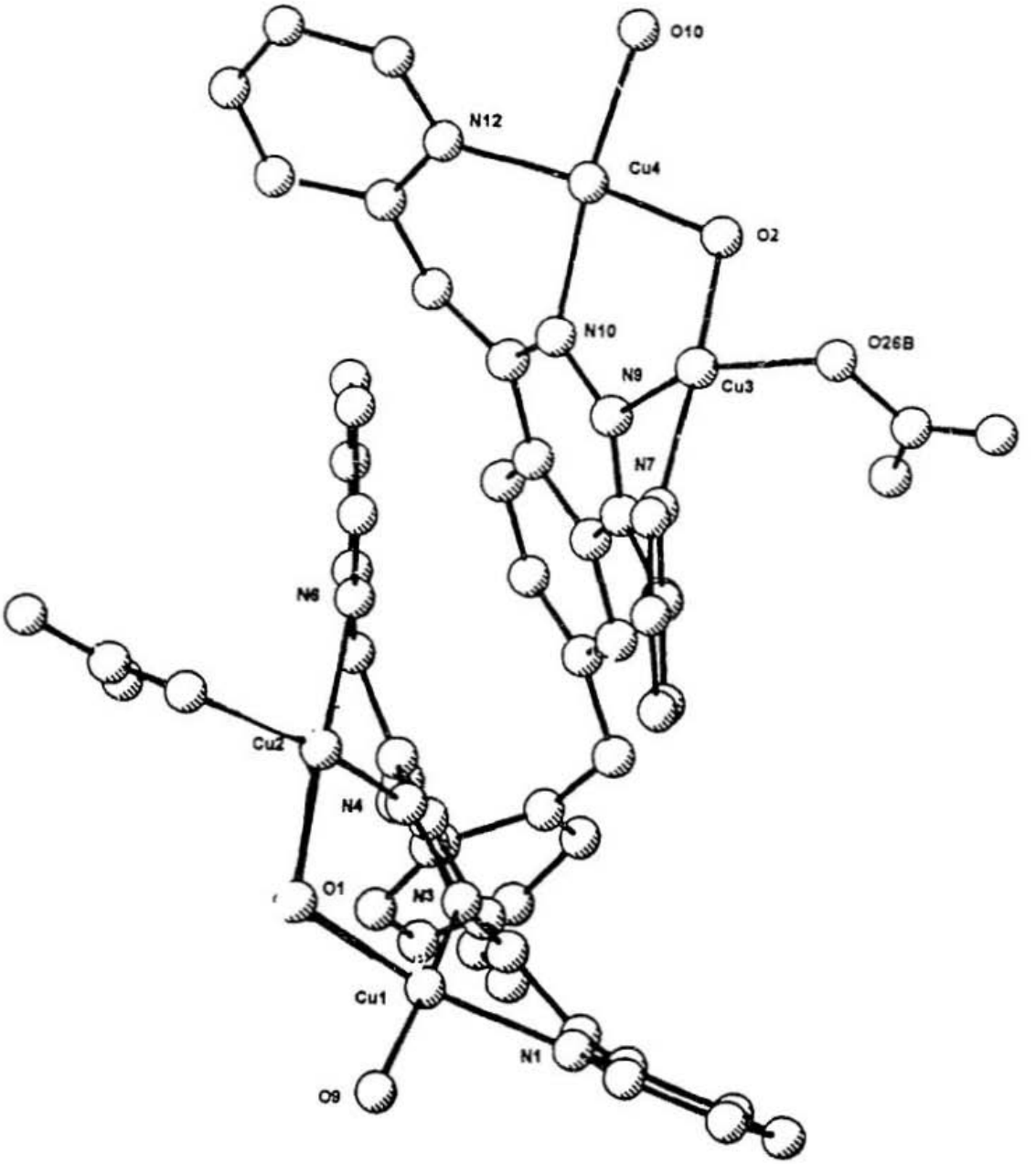


**Fig. 5.3** Overlay of two dinuclear centres of (35)

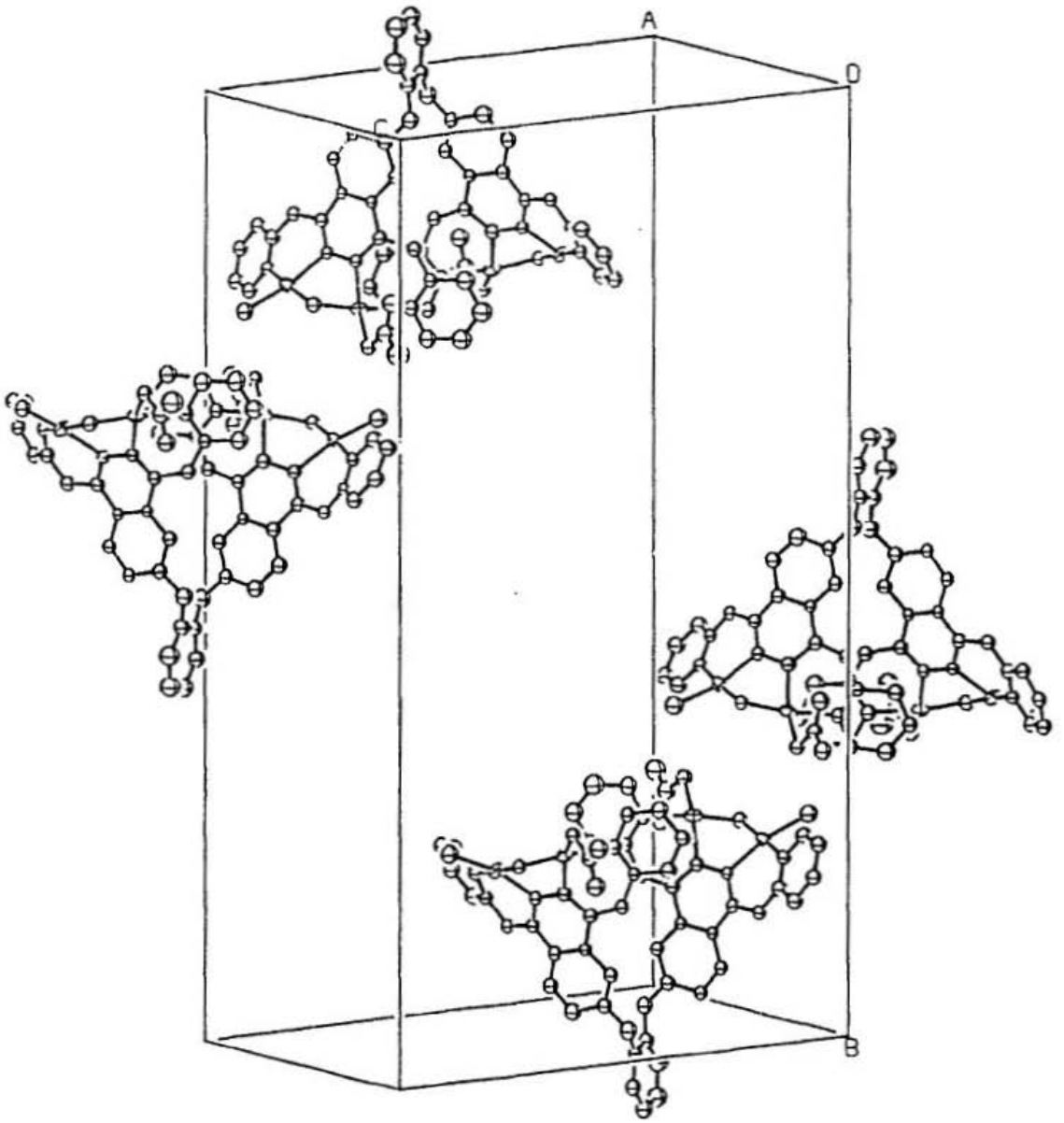


**Fig. 5.4** Packing diagram of (**35**) in one unit cell

**Table 5.1** Crystallographic data for

$[Cu_4(C\text{-}P)(\mu_2\text{-}OH)_2(\mu_2\text{-}NO_3)_2(NO_3)_2(H_2O)_2](NO_3)_2{\cdot}4H_2O$ (**35**).

| | |
|---|---|
| Chemical Formula | Formula weight |
| $C_{84}H_{69}O_{52}N_{36}Cu_8$ | 2923.05 |
| a = 13.346(4)Å | space group $P2_1/c$ |
| b = 37.71(1)Å | T = -80(1)°C |
| c = 21.519(6)Å | $\lambda$ = 0.71069Å (MoK$\alpha$) |
| $\beta$ = 91.04(2)° | $\rho_c$ = 1.793 g.cm$^{-3}$ |
| V = 10829(6)Å$^3$ | $\mu$ = 16.56 cm$^{-1}$ |
| Z = 4 | R = 0.063 |
| $2\theta_{max}$ = 44.9° | $R_W$ = 0.058 |
| Max. shift/$\sigma$ = 0.04 | $F_{000}$ = 5892 |
| Crystal size | GoF 1.96 |
| 0.40x0.30x0.05mm | |

**Table 5.2** Intramolecular distances (Å) relevant to the copper coordination spheres in complex **(35)**

| | | | | | |
|---|---|---|---|---|---|
| Cu(1) | O(1) | 1.904(9) | Cu(7) | O(28A) | 2.010(9) |
| Cu(1) | O(9) | 1.99(1) | Cu(7) | N(19) | 1.93(1) |
| Cu(1) | N(1) | 1.96(1) | Cu(7) | N(21) | 2.01(1) |
| Cu(1) | N(3) | 2.00(1) | Cu(8) | O(6) | 1.880(9) |
| Cu(2) | O(1) | 1.897(9) | Cu(8) | O(12) | 2.01(1) |
| Cu(2) | O(25A) | 2.053(9) | Cu(8) | N(22) | 2.01(1) |
| Cu(2) | O(32B) | 2.26(1) | Cu(8) | N(24) | 1.91(1) |
| Cu(2) | N(4) | 2.02(1) | Cu(2) | N(6) | 1.97(1) |
| Cu(3) | O(2) | 1.906(9) | Cu(3) | O(26B) | 2.038(9) |

**Table 5.2** Intramolecular distances (Å) relevant to the copper coordination spheres in complex **(35)**

| | | | | | |
|---|---|---|---|---|---|
| Cu(3) | N(7) | 1.98(1) | Cu(3) | N(9) | 2.00(1) |
| Cu(4) | O(2) | 1.897(9) | Cu(4) | O(10) | 1.99(1) |
| Cu(4) | O(10) | 2.01(1) | Cu(4) | N(12) | 1.96(1) |
| Cu(5) | O(5) | 1.887(9) | Cu(5) | O(11) | 2.04(1) |
| Cu(5) | N(13) | 1.88(1) | Cu(5) | N(15) | 2.00(1) |
| Cu(6) | O(5) | 1.89(1) | Cu(6) | O(27C) | 2.032(9) |
| Cu(6) | N(16) | 2.02(1) | Cu(7) | O(6) | 1.866(9) |
| Cu(6) | N(18) | 1.98(1) | | | |

**Table 5.3** Intramolecular bond angles in complex (35)

| | | | | | | | |
|---|---|---|---|---|---|---|---|
| O(1) | Cu(1) | O(9) | 92.5(4) | O(10) | Cu(4) | N(12) | 93.4(4) |
| O(1) | Cu(1) | N(1) | 169.5(4) | N(10) | Cu(4) | N(12) | 87.9(5) |
| O(1) | Cu(1) | N(3) | 88.0(4) | O(9) | Cu(1) | N(1) | 93.7(4) |
| O(5) | Cu(5) | N(13) | 171.9(5) | N(1) | Cu(1) | N(3) | 87.4(4) |
| O(11) | Cu(5) | N(13) | 95.2(5) | O(1) | Cu(2) | O(25A) | 95.4(4) |
| O(1) | Cu(2) | O(32B) | 89.2(4) | O(1) | Cu(2) | N(4) | 85.8(4) |
| O(1) | Cu(2) | N(6) | 173.5(4) | O(25A) | Cu(2) | O(32B) | 77.9(4) |
| O(25A) | Cu(2) | N(4) | 156.2(1) | O(25A) | Cu(2) | N(6) | 90.3(4) |
| O(32B) | Cu(2) | N(4) | 125.4(4) | O(32B) | Cu(2) | N(6) | 95.1(4) |

**Table 5.3** Intramolecular bond angles in complex (35)

| | | | | | | | |
|---|---|---|---|---|---|---|---|
| N(4) | Cu(2) | N(6) | 87.7(5) | O(2) | Cu(3) | O(26B) | 96.9(4) |
| O(2) | Cu(3) | N(7) | 173.2(4) | O(2) | Cu(3) | N(9) | 85.5(4) |
| O(26B) | Cu(3) | N(7) | 89.7(4) | O(26B) | Cu(3) | N(9) | 153.3(4) |
| N(7) | Cu(3) | N(9) | 87.8(5) | O(2) | Cu(4) | O(10) | 91.9(4) |
| O(2) | Cu(4) | N(10) | 87.5(4) | O(2) | Cu(4) | N(12) | 174.2(4) |
| O(10) | Cu(4) | N(10) | 165.9(4) | Cu(1) | O(1) | Cu(2) | 112.6(5) |
| Cu(3) | O(2) | Cu(4) | 110.4(4) | Cu(3) | N(7) | C(19) | 121.3(9) |
| Cu(3) | N(9) | N(10) | 116.2(8) | Cu(3) | N(9) | C(24) | 122(1) |

Table 5.3 Intramolecular bond angles in complex (35)

| | | | | | | | |
|---|---|---|---|---|---|---|---|
| Cu(2) | O(25A) | N(25) | 110.4(8) | Cu(4) | N(10) | N(9) | 115.4(8) |
| Cu(3) | O(26B) | N(26) | 109.6(8) | Cu(4) | N(10) | C(31) | 123(1) |
| Cu(2) | O(32B) | N(32) | 123.8(9) | Cu(4) | N(12) | C(32) | 124(1) |
| Cu(1) | N(1) | C(1) | 118.7(9) | Cu(4) | N(12) | C(36) | 118(1) |
| Cu(1) | N(1) | C(5) | 124(1) | C(32) | N(12) | C(36) | 117(1) |
| C(1) | N(1) | C(5) | 117(1) | Cu(1) | N(3) | N(4) | 116.2(8) |
| Cu(1) | N(3) | C(6) | 120.8(9) | Cu(2) | N(4) | N(3) | 115.7(8) |
| Cu(2) | N(4) | C(13) | 121(1) | Cu(2) | N(6) | C(14) | 122(1) |
| Cu(2) | N(6) | C(18) | 119(1) | Cu(5) | O(5) | Cu(6) | 111.4(5) |
| Cu(7) | O(6) | Cu(8) | 116.7(5) | | | | |

## 5.2 CRYSTAL STRUCTURE OF $\{[Cu_4(O\text{-}P)(\mu_2\text{-}OH)_2(\mu_2\text{-}NO_3)_2(H_2O)_7]_2(\mu\text{-}NO_3)\}(NO_3)_7.xH_2O$ (37)

### 5.2.A collection of X-ray intensity data

Structural data were collected for a green irregular plate-like crystal of (**37**) with approximate dimensions 0.400 x 0.250 x 0.150 mm at -90(1)° C by the same procedure outlined for (**35**). The structure was solved by direct methods[91,92] with the non-hydrogen atoms set anisotropically except C(16), C(17), and C(18), which showed unusual thermal motion. No hydrogen atoms were found belonging to any water molecules. A summary of crystal and other data is given in Table 5.4 and atomic coordinates are given in Table SI.II.

### 5.2.B Description of structure

Structural representations of (**37**) as a tetranuclear monomer and a nitrate bridged octanuclear dimer are shown in Figs 5.5, 5.6 and 5.7 (some coordinated water molecules and nitrates are not included for the clarity), and interatomic distances and angles relevant to the copper coordination spheres are given in

Tables 5.4 and 5.5. The structural solution for (**37**) was hampered somewhat by our inability to successfully locate many of the water molecules in the lattice. However the main molecular fragments are clearly identified, despite the less than ideal refinement. The structure (Figs. 5.5 and 5.6) consists of a tetranuclear arrangement with six-coordinate copper(II) centers bridged by phthalazine ($N_2$) and hydroxide in the equatorial plane and by an axial bridging nitrate. Other coordination sites are occupied by water molecules, with the exception of O(17C) and O(17A), bound to Cu(3) and Cu(2), which is part of a bridging nitrate, and connects two tetranuclear units forming an octanuclear dimer (Fig. 5.7). Intradinuclear copper-copper separations (Cu(1)-Cu(2) 3.206(3) Å, Cu(3)-Cu(4) 3.135(3) Å), and Cu-(OH)-Cu angles (Cu(1)-O(1)-Cu(2) 113.1(8)°, Cu(4)-O(6)-Cu(3) 114.3(6)°) are comparable with those in (**35**). In plane copper-ligand distances are all 2.06 Å, or less, with contacts to the bridging hydroxide substantially shorter than the others. The axial copper-oxygen distances fall in the range 2.45-2.62 Å, typical for tetragonal, six-coordinate copper, with the bridging nitrate bound to Cu(2) with copper-oxygen distances of 2.46(1) Å.

The two halves of the tetranuclear species are twisted about the oxygen (O(7)) atom connecting the two phthalazine subunits in such a way that the two dinuclear centers do not approach each other closely enough for any possible

contact between the copper atoms, thus creating a complex with large external dimensions. Within the same tetranuclear entity copper-copper separations are quite long (Cu(1)-Cu(3) 8.862(5) Å, Cu(1)-Cu(4) 11.098(5) Å, Cu(2)-Cu(3) 10.988(4) Å, Cu(2)-Cu(4) 13.294(5) Å), and the length of the species is estimated to be about 20 Å, placing it squarely in the nanometre scale range. The dimeric complex cation (Fig. 5.7) is even longer, with a length of approximately 32 Å. H-bonding was found to play an important role in joining these tetranuclear Cu(II) complexes together. The Cu1Cu2 centres are alternatively linked by the N17 nitrate ( on a 2-fold axis ) and through H-bonding from O3 on Cu2 to an oxygen of the N13 nitrate bridging a neighbouring Cu1Cu2 pair. The Cu3Cu4 centres are linked by extended H-bonding from the O4 bridge between coppers, to O18, a water molecule additionally H-bonded to the other two oxygen atoms from water molecules. O18 in turn H-bonds to an oxygen of the N16 nitrate bridging Cu3 and Cu4 of the next molecule. There are no links between Cu1Cu2 and Cu3Cu4. Packing diagrams viewed down the 'c' and 'a' axes (Figs. 5.7-8) indicate a stacked, zig-zag arrangement of octanuclear species, but there is no direct evidence for any intermolecular linkages other than nitrate N(17), which might cause intermolecular associations between octanuclear units.

The overall structure of (**37**) is a polymeric structure in which four chains

of dicopper centres are held together by the tetradentate organic ligand in a "cable". The cable analogy can be extended, with the dicopper centres and their associated oxygen and nitrogen atoms forming the core, and the predominantly aromatic carbon groups surrounding the core as "insulation". Each cell contributes components to two such cables. This unique structure of the complex inspires us to explore its potential application as a model compound for nanometre scale magnetic materials and a selective binding molecular cell membrane.

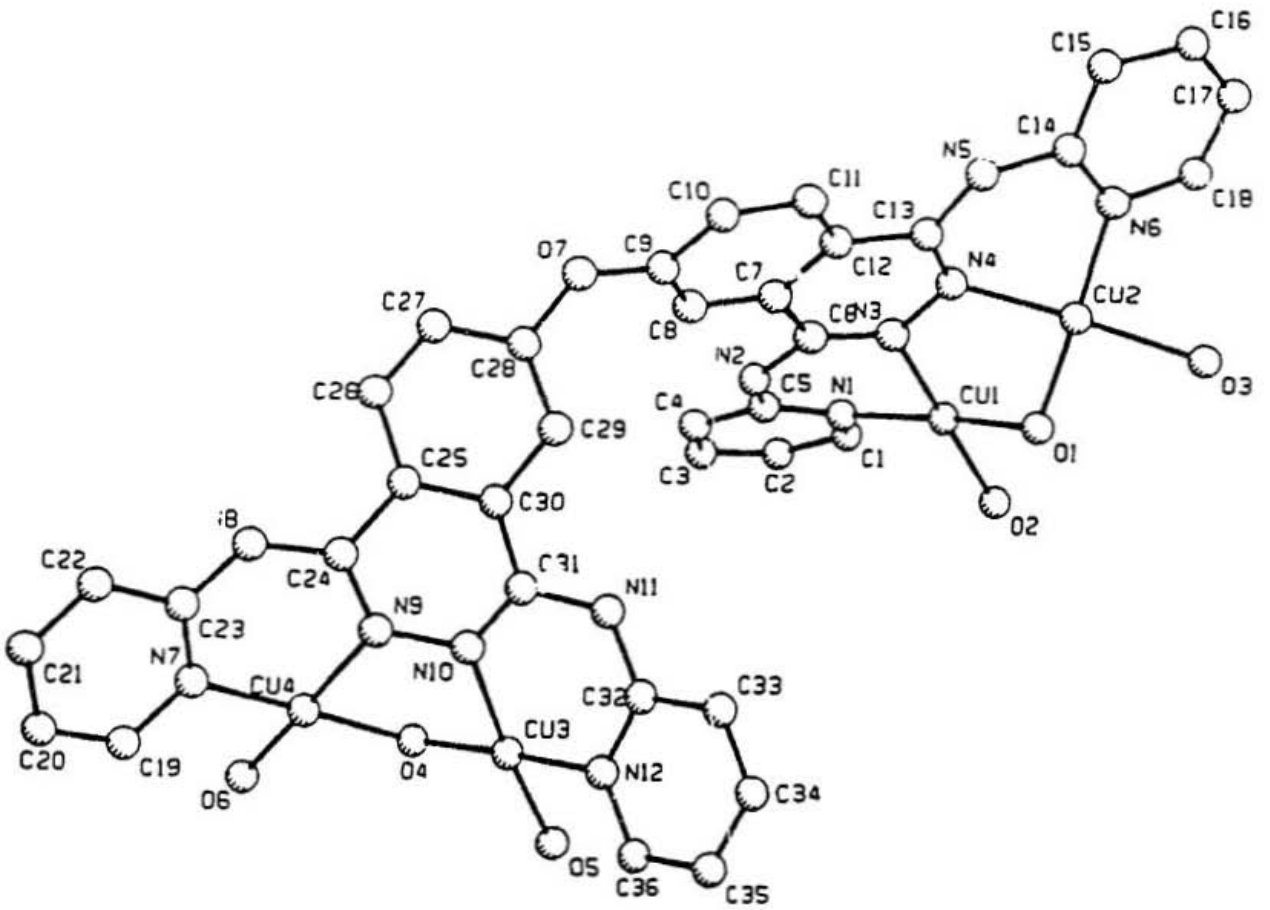


**Fig.5.5** Crystal structure of $[Cu_4(O\text{-}P)(\mu_2\text{-}OH)_2(\mu_2\text{-}NO_3)_2(NO_3)_2(H_2O)_2](NO_3)_2 \cdot 10H_2O$ **(37)**

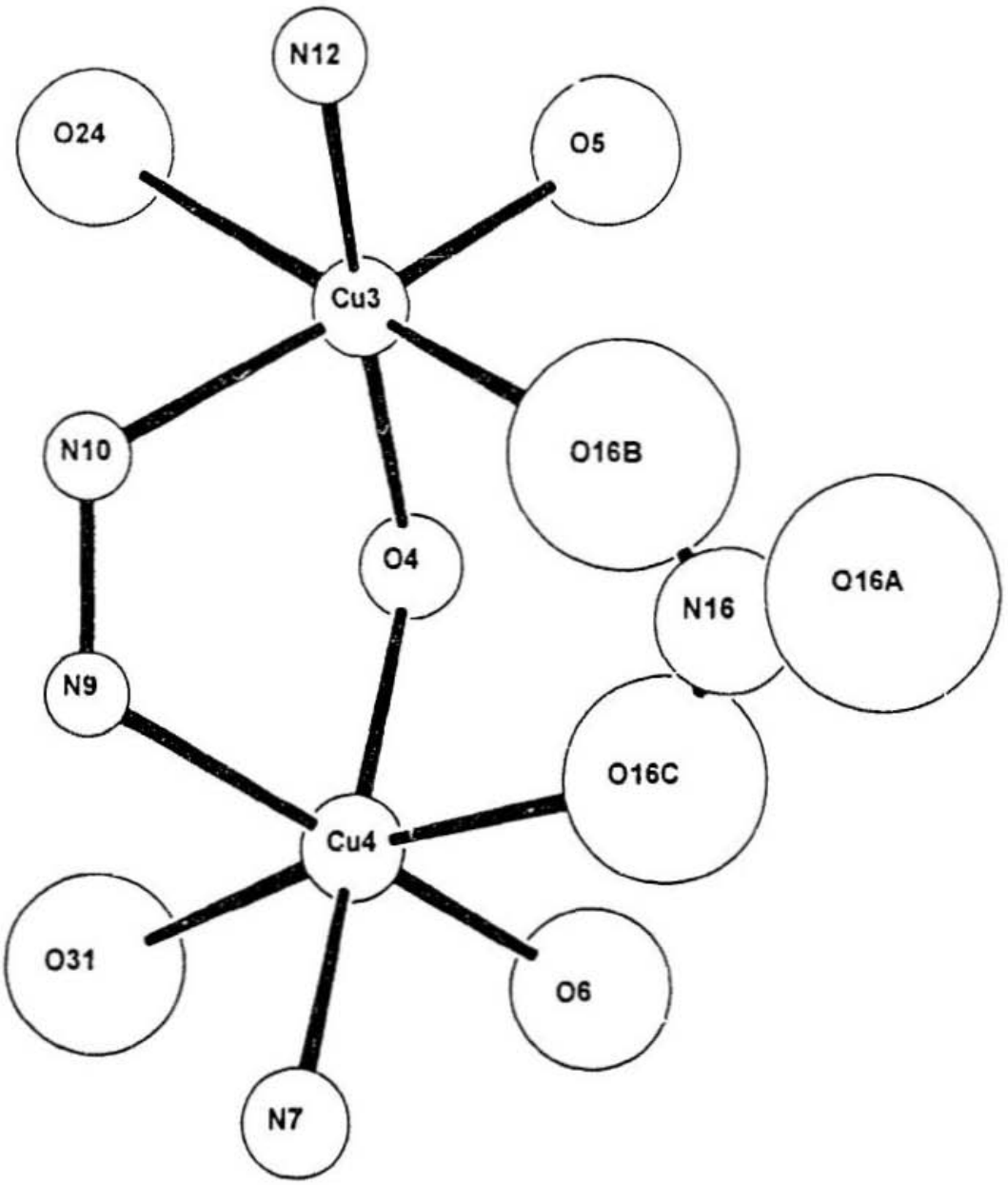


**Fig.5.6** Structure of a dinuclear centre of (37)

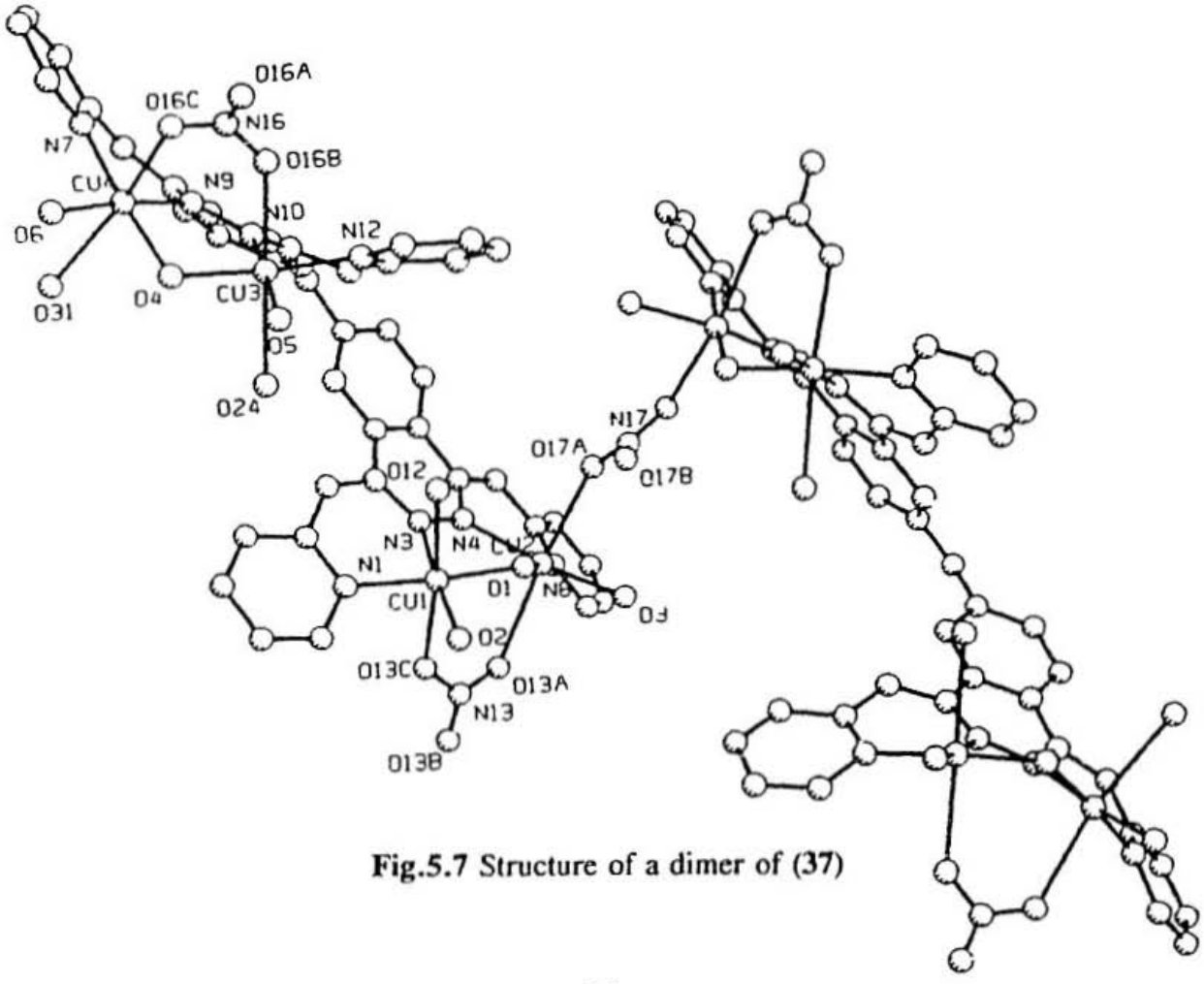


**Fig.5.7** Structure of a dimer of **(37)**

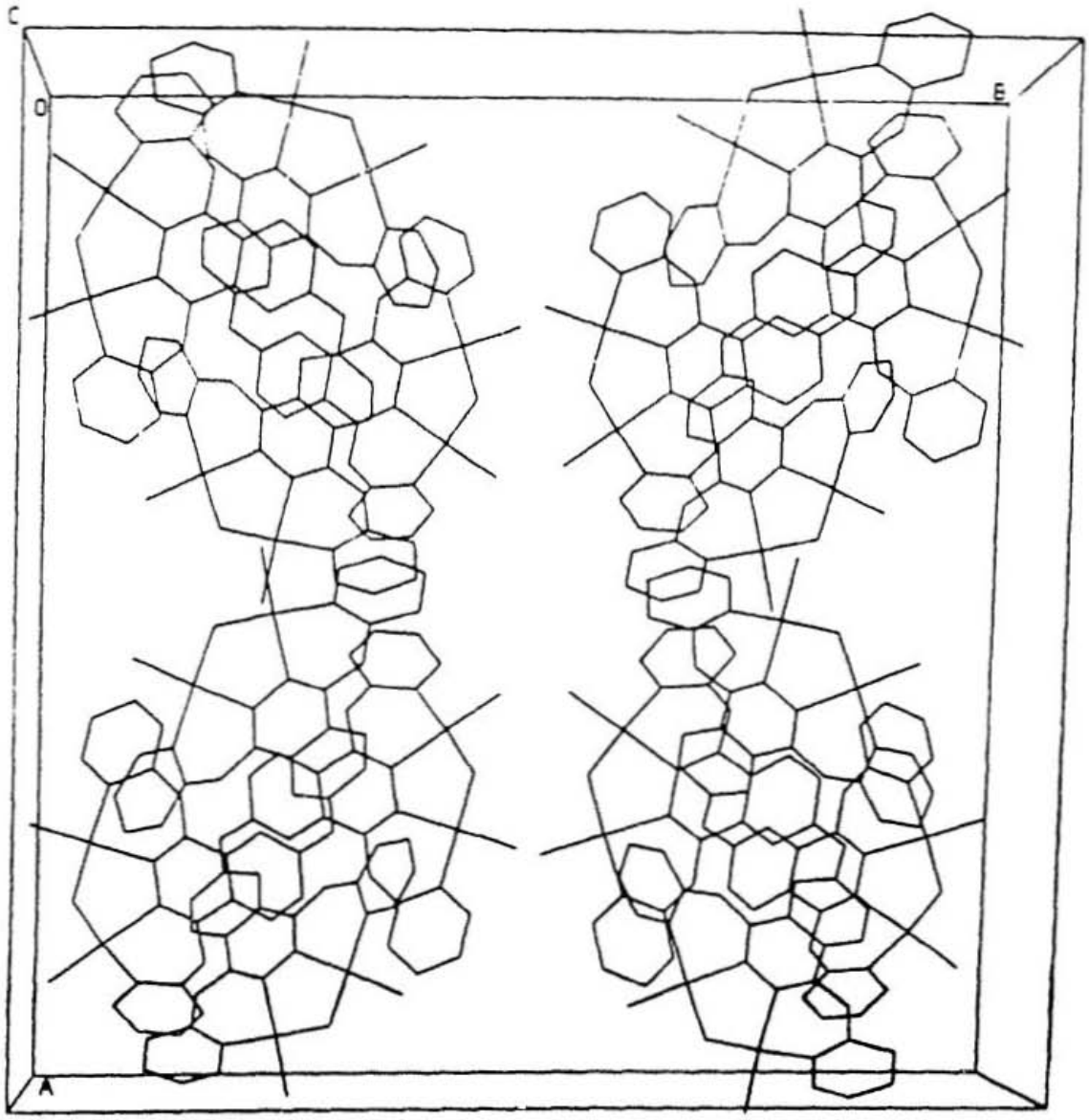


**Fig. 5.8** Packing diagram of (37) in one unit cell

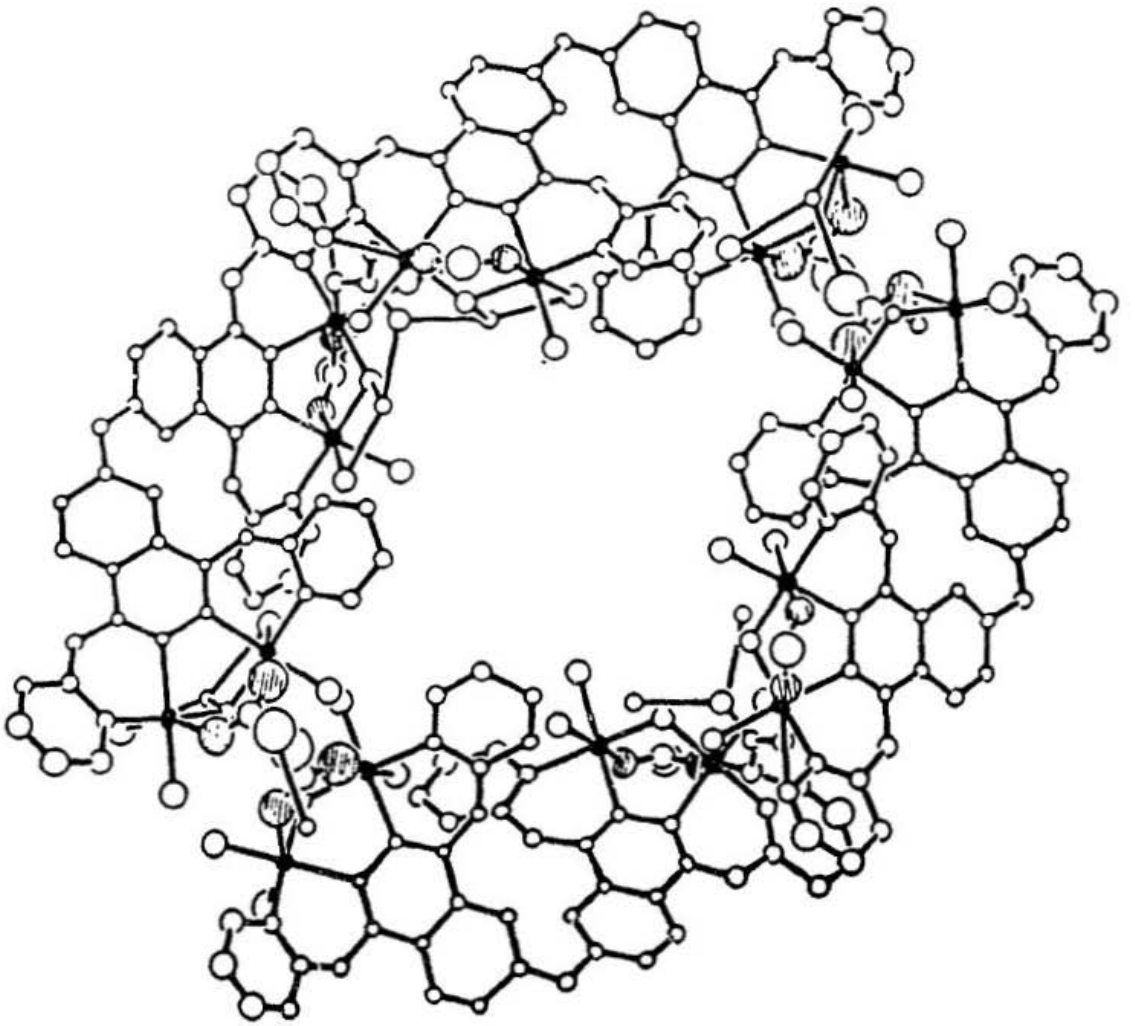

**Fig. 5.9** Packing diagram of (37) viewed down 'c' and 'a' axis

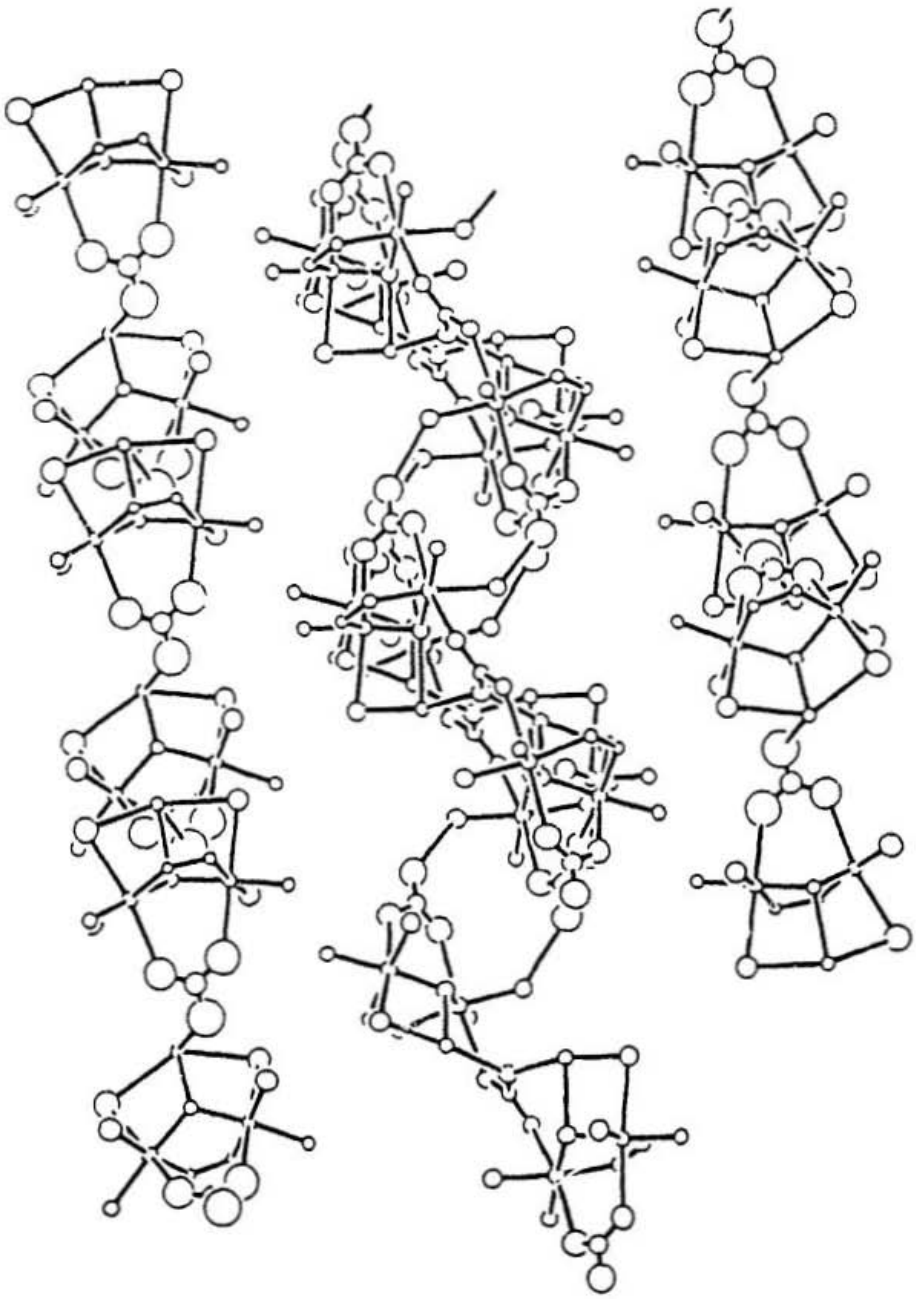

**Fig.5.10** Packing diagram of **(37)** viewed down 'b' axis

Table 5.4 Crystallographic data for $[Cu_4(O\text{-}P)(\mu_2\text{-}OH)_2(\mu_2\text{-}NO_3)_2(NO_3)_2H_2O)_2](NO_3)_2 \cdot 10H_2O$ (37).

| | |
|---|---|
| Chemical Formula | Formula weight |
| $C_{40}H_{40}O_{25}N_{15}Cu_4$ | 1385.03 |
| a = 31.948(5)Å | space group C2/c(#15) |
| b = 30.900(1)Å | T = -90°C |
| c = 12.683(6)Å | $\lambda$ = 0.71069Å (MoK$\alpha$) |
| $\beta$ = 96.22(2)° | $\rho_c$ = 1.478 g.cm$^{-3}$ |
| V = 12446(6)Å$^3$ | $\mu$ = 14.34 cm$^{-1}$ |
| Z = 8 | R = 0.108 |
| $2\theta_{max}$ = 50.0° | $R_w$ = 0.118 |
| Max. shift/$\sigma$ = 4.54 | $F_{\infty\infty}$ = 5892 |
| Crystal size | GoF 4.96 |
| 0.400x0.250x0.150mm | |

**Table 5.5** Intramolecular distances relevant to the coordination spheres in complex (37)

| | | | | | |
|---|---|---|---|---|---|
| Cu(1) | O(1) | 1.89(1) | Cu(3) | O(4) | 1.88(1) |
| Cu(3) | O(5) | 1.97(1) | Cu(3) | N(10) | 2.02(1) |
| Cu(3) | N(12) | 1.94(2) | Cu(4) | O(4) | 1.93(1) |
| Cu(4) | O(6) | 1.98(2) | Cu(4) | N(7) | 2.01(2) |
| Cu(1) | O(2) | 2.04(1) | Cu(1) | N(1) | 1.97(2) |
| Cu(1) | N 3) | 2.02(2) | Cu(2) | O(1) | 1.87(2) |
| Cu(2) | O(3) | 2.03(1) | Cu(1) | Cu(2) | 3.138(4) |
| Cu(2) | N(6) | 1.89(2) | Cu(1) | Cu(3) | 8.826(5) |
| Cu(4) | N(9) | 2.06(1) | Cu(1) | Cu(4) | 11.098(5) |
| Cu(2) | N(4) | 2.03(1) | Cu(2) | Cu(3) | 10.988(4) |
| Cu(2) | Cu(4) | 13.294(5) | Cu(3) | Cu(4) | 3.206(4) |

**Table 5.6** Intramolecular bond angles relevant to the coordination spheres in complex (37)

| | | | | | | | |
|---|---|---|---|---|---|---|---|
| O(1) | Cu(1) | O(2) | 89.7(6) | O(1) | Cu(1) | N(1) | 175.3(7) |
| Cu(1) | N(1) | C(1) | 119(2) | O(1) | Cu(1) | N(3) | 87.8(6) |
| Cu(1) | N(1) | C(5) | 122(1) | O(2) | Cu(1) | N(1) | 92.5(7) |
| O(2) | Cu(1) | N(3) | 177.0(7) | N(1) | Cu(1) | N(3) | 89.9(6) |
| Cu(1) | N(3) | N(4) | 116(1) | O(1) | Cu(2) | O(3) | 90.5(6) |
| Cu(1) | N(3) | C(6) | 120(1) | O(1) | Cu(2) | N(4) | 89.9(6) |
| O(1) | Cu(2) | N(6) | 176.0(7) | Cu(2) | N(4) | N(3) | 115(1) |
| O(3) | Cu(2) | N(4) | 171.1(6) | Cu(2) | N(4) | C(13) | 123(1) |
| O(3) | Cu(2) | N(6) | 91.4(7) | N(4) | Cu(2) | N(6) | 88.7(7) |
| O(4) | Cu(3) | O(5) | 90.4(6) | Cu(2) | N(6) | C(14) | 125(1) |
| O(5) | Cu(3) | N(10) | 172.3(7) | Cu(4) | N(7) | C(19) | 117(2) |
| O(5) | Cu(3) | N(12) | 92.7(6) | Cu(4) | N(7) | C(23) | 125(2) |
| N(10) | Cu(3) | N(12) | 88.4(6) | O(4) | Cu(4) | O(6) | 88.8(6) |
| O(4) | Cu(4) | N(7) | 174.7(7) | Cu(1) | O(1) | Cu(2) | 113.1(8) |
| Cu(3) | O(4) | Cu(4) | 114.3(6) | O(4) | Cu(3) | N(10) | 89.1(6) |
| Cu(2) | N(6) | C(18) | 112(2) | O(4) | Cu(3) | N(12) | 175.0(6) |

**Table 5.7** Intermolecular distances relevant to the coordination spheres of complex (**37**)

| | | | | | |
|---|---|---|---|---|---|
| Cu(1) | O(13C) | 2.46(2) | Cu(1) | O(12) | 2.57(1) |
| O(1) | O(18A) | 3.43(3) | Cu(1) | O(13) | 3.29(1) |
| Cu(1) | N(13) | 3.38(2) | O(2) | O(11) | 2.94(5) |
| Cu(2) | O(17A) | 2.46(1) | O(2) | O(18B) | 2.97(3) |
| Cu(2) | O(13A) | 2.57(2) | O(2) | O(13C) | 3.14(3) |
| Cu(2) | N(17) | 3.351(4) | O(2) | O(12) | 3.25(2) |
| Cu(2) | N(13) | 3.41(2) | O(3) | O(13B) | 2.61(2) |
| Cu(2) | O(13C) | 3.48(2) | O(3) | O(18A) | 2.83(3) |
| Cu(2) | O(17B) | 3.501(8) | O(3) | O(17A) | 3.04(2) |
| Cu(3) | O(16B) | 2.47(3) | O(3) | O(13A) | 3.33(3) |
| Cu(3) | O(24) | 2.61(2) | O(3) | O(18B) | 3.39(3) |
| Cu(3) | N(16) | 3.42(3) | O(3) | O(17B) | 3.42(2) |
| Cu(3) | O(18) | 3.45(1) | O(3) | O(14A) | 3.42(2) |
| Cu(4) | O(16C) | 2.49(3) | O(3) | N(17) | 3.42(2) |
| Cu(4) | O(31) | 2.57(2) | O(3) | C(22) | 3.43(3) |

**Table 5.7** Intermolecular distances relevant to the coordination spheres of complex (37)

| | | | | | |
|---|---|---|---|---|---|
| Cu(4) | N(16) | 3.30(3) | O(3) | N(18) | 3.47(4) |
| Cu(4) | O(16B) | 3.38(3) | O(3) | N(13) | 3.60(3) |
| Cu(4) | O(18) | 3.58(1) | O(3) | O(14B) | 3.60(2) |
| Cu(1) | Cu(1) | 12.240(6) | Cu(1) | Cu(2) | 14.377(5) |
| Cu(1) | Cu(3) | 8.699(4) | Cu(1) | Cu(4) | 11.077(4) |
| Cu(2) | Cu(2) | 16.423(7) | Cu(2) | Cu(3) | 11.804(4) |
| Cu(2) | Cu(4) | 14.187(4) | Cu(3) | Cu(4) | 7.924(4) |
| Cu(3) | Cu(3) | 7.516(4) | Cu(4) | Cu(4) | 8.030(4) |

# Chapter 6 MAGNETOCHEMISTRY AND ELECTROCHEMISTRY OF POLYNUCLEAR COMPLEXES

## 6.1 Magnetic studies of complexes

Room temperature magnetic moment measurements were recorded on dried samples and are given in Table 6.1. The copper complexes of the polyisoindolines have room temperature magnetic moment around 1.73 B.M., which indicates that very weak magnetic coupling exists in these complexes, in contrast to the very low magnetic moments for the polynuclear copper complexes of the polyphthalazines, among which strong antiferromagnetic coupling exists.

Variable temperature magnetic studies were performed on dried, powdered samples of complexes (**35**) and (**37**) in the temperature range 5-300 K. Fitting of the magnetic data for (**35**) to the Bleaney-Bowers equation[104] (eq. [1]) for a copper dimer:

$$\chi_m = \frac{N\beta^2 g^2}{3k(T-\theta)}\,[1+1/3\exp(-2J/kT)]^{-1}(1-\rho) + \frac{[N\beta^2 g^2]\,\rho}{4kT} + N\alpha \quad \text{------(1)}$$

gave best fit parameters g = 2.05(2), -2J = 537(7)$cm^{-1}$, $\rho$ = 0.02, N$\alpha$ = 58x$10^{-6}$ cgsu and $\theta$ = 0 K ($10^2$R = 1.1; R=$[\Sigma(\chi_{obs}-\chi_{calc})^2/\Sigma(\chi_{obs})_2]^{1/2}$) ($\theta$ is a corrective, Weiss-like term for possible intermolecular magnetic interactions;[86] $\rho$ represents the fraction of a possible magnetically dilute copper(II) impurity; other terms have their usual meaning). Fig. 6.1 illustrates a plot of $\chi_m$ vs temperature for (**35**), with the solid line corresponding to the best fit using the derived parameters quoted above. The exchange integral for (**35**) is entirely consistent with that observed for the complex $[Cu_2(PAP4Me)(\mu_2\text{-}OH)(\mu\text{-}NO_3)(NO_3)(H_2O)_2]\cdot NO_3$ (**19**), (-2J = 497 $cm^{-1}$), which has a comparable hydroxide bridge angle of 115.3(1)° [46]. The rise in $\chi_m$ at low temperature is indicative of the presence of a small amount of paramagnetic impurity. The $\theta$ value of 0 indicates no interdinuclear spin interactions, and no magnetic connection through the catechol bridge linking the two halves of the molecule together. This is confirmed by an analysis of the variable temperature magnetic data for the catechol-isoindoline derivative $[Cu_2(C\text{-}I)Br_4].CH_3OH$ (g = 2.147(6), -2J = 1.4(4) $cm^{-1}$) (Fig. 6.2). In the absence of structural details for this

compound it is not clear how the weak exchange is propagated, but it might occur through the catechol bridge.

Variable temperature magnetic data for (**37**) are quite different from (**35**). A maximum in the $\chi$ vs. temperature plot occurs at about 225K (Fig.6.3), in contrast to (**35**), which has a maximum in excess of 300 K, in agreement with the data analysis. Dimensions at each dinuclear center in (**37**) are similar to those in (**35**), and in particular comparable hydroxide bridge angles, and dinuclear center fold angles would suggest an exchange integral (-2J) of around 500 $cm^{-1}$. A meaningful fit of the data cannot be achieved using the Bleaney-Bowers equation for a simple dinuclear species, and after testing a variety of models the only one (Fig. 6.4) that gave anything approaching a reasonable fit involved two dinuclear centres, with different exchange integrals, and adjusted for a significant paramagnetic impurity correction ($g = 2.04(3)$, $-2J_1 = 509(25)$ $cm^{-1}$, $-2J_2 = 198(10)$ $cm^{-1}$, $\rho = 0.065$) (Fig. 6.3). To rationalise such a magnetic difference between dinuclear centers would require some rather more marked structural differences than is apparent in the structure of (**37**). (**37**) has a polymeric structure comprised of octanuclear units resulting from two tetranuclear complexes joined by a bridging nitrate, and linked by bridging bidentate nitrate groups and H-bonds. In one of these octanuclear units the pyramidal nitrate bridge between two Cu(II)

ions causes an electronic perturbation at the dinuclear centres leading to reduced antiferromagnetic coupling between these two nitrate bridged centres.

The simple dimer magnetic model may not be adequate to give a good magnetic data fit for the tetranuclear and hexanuclear complexes, in which trinuclear and pentanuclear impurities exist. These impurities could include incompletely metallated complexes of the tetranucleating and hexanucleating ligands or possibly fully metallated complexes involving mixed phthalazine-isoindoline ligands resulting from incomplete reaction with hydrazine during ligand ring expansion. These species would behave effectively as a "monomeric" impurity. Resonable dinuclear impurities would correspond to two possible derivatives, one with two coppers bound on one side of the ligand framework and the other with one copper on each side of the ligand system. It is very unusual for tetranuclear Cu(II) complexes (**35**) and (**37**) to have different dinuclear centres with different Cu-OH-Cu bridge angles with the difference around 6° and hence have two antiferromagnetic couplings with the -2J difference around 100 $cm^{-1}$.[77] This -2J difference could become larger in the magnetochemistry of tetranuclear halogen coordinated complexes because of the possibility that we may obtain two dinuclear centres with a Cu-OH-Cu bridge in one centre and a Cu-X-Cu bridge in another centre, which will result in a large -2J difference. $[Cu_2(PAP46Me)Cl_4]$ (**50**)[65]

exhibits rather weak antiferromagnetic coupling, $-2J = 55.2\ cm^{-1}$, in contrast to the $[Cu_2(PAP6Me)(OH)Cl_3]\ 3H_2O$ (**51**)[105] with $-2J = 432\ cm^{-1}$. This -2J difference would not appear as paramagnetic impurity, but if -2J in one spin coupled dinuclear centre is close to zero then a portion of the complex would appear to be paramagnetic impurity. However, only a simple dimer model was applied to these complicated magnetic systems, and it is no surprise that good data fits were not obtained in all cases, which suggests that more complicated magnetic models should be built to fit these magnetic data, creating a difficult theoretical problem.

Table 6.1 Magnetic data for the Cu(II) complexes

| Complexes | $\mu_{eff}$(BM)* | g | -2J($cm^{-1}$) | N$\alpha$ X $10^6$ | $\rho$ | R |
|---|---|---|---|---|---|---|
| $Cu_2$(O-I)$(NO_3)\cdot 3CH_3OH$ (32) | 1.74 | | | | | |
| $Cu_2$(O-I)$(CH_3COO)_4\cdot 4H_2O$ (33) | 1.74 | | | | | |
| $Cu_2$(C-I)$Br_4\cdot CH_3OH$ (34) | 1.72 | 2.15 | 1.40 | 119 | 0.00 | 3.2 |
| $[Cu_4$(C-P)$(\mu_2$-OH$)_2(\mu_2$-$NO_3)_2$ $(H_2O)_2(NO_3)_2](NO_3)_2\cdot 2H_2O$ (35) | 0.98 | 2.05 | 537.0 | 58 | 0.02 | 1.1 |
| $[Cu_4$(O-P)$(OH)_2(NO_3)_6\cdot H_2O$ (36) | 1.28 | | | | | |
| $[Cu_4$(O-P)$(OH)_2(NO_3)_6]\cdot 10H_2O$ (37) | 1.04 | 2.04 | $-2J_1=509$ $-2J_2=198$ | 60 | 0.065 | 3.2 |
| $Cu_4$(C-P)$(OH)_2(SO_4)_2]SO_4\cdot 4H_2O$ (38) | 0.74 | | | | | |
| $[Cu_4$(O-P)$(OH)_2Cl_6]\cdot 4H_2O$ (39) | 1.05 | | | | | |
| $[Cu_4$(C-P)$(OH)_2Br_6]\cdot 2CH_3CH_2OH$ (40) | 1.52 | 2.03 | 472.4 | 73 | 0.17 | 10.6 |
| $Cu_6$(G-P)$(OH)_3Cl_9]\cdot 4H_2O$ (41) | 1.32 | | | | | |
| $[Cu_6$(G-P)$(OH)_3Br_9]\cdot 6H_2O$ (42) | 1.27 | 2.01 | 409.3 | 76 | 0.21 | 9.8 |
| $[Cu_6$(G-P)$(OH)_3(NO_3)_9]\cdot 12H_2O$ (43) | 1.10 | 2.01 | 222.6 | 70 | 0.32 | 10.0 |
| $[Cu_8$(P-P)$(OH)_4Cl_{12}]\cdot 10H_2O$ (45) | 0.72 | | | | | |
| $[Cu_8$(P-P)$(OH)_4Br_{12}]\cdot 8H_2O$ (46) | 0.59 | | | | | |
| $[Cu_8$(P-P)$(OH)_4(NO_3)_{12}]\cdot 8CH_3OH$ (47) | 0.81 | | | | | |

* At room temperature.

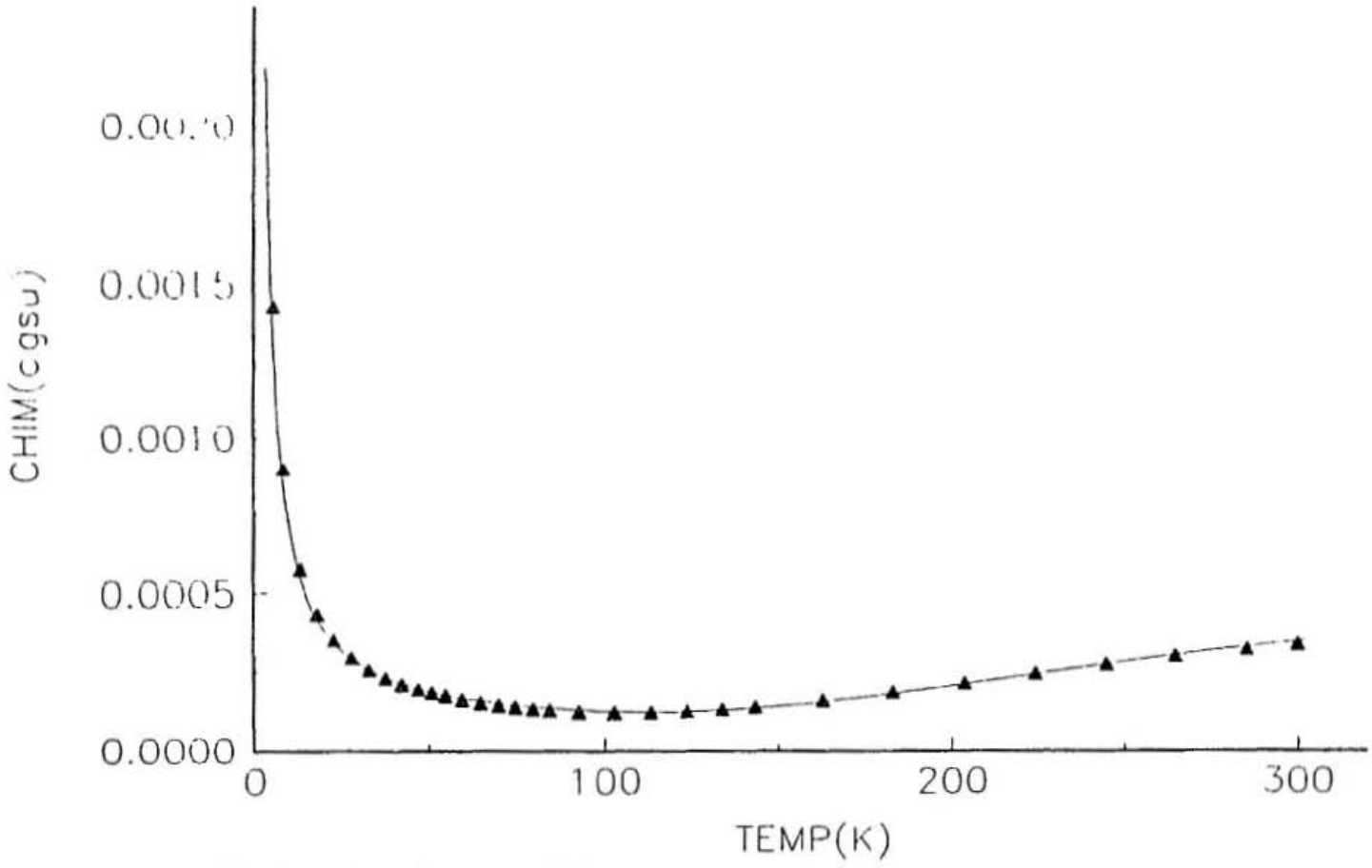


**Fig.6.1** Magnetic susceptibility data for

$[Cu_4(C\text{-}P)(\mu_2\text{-}OH)_2(\mu_2\text{-}NO_3)_2(NO_3)_2(H_2O)_2](NO_3)_2{\cdot}4H_2O$ **(35)**

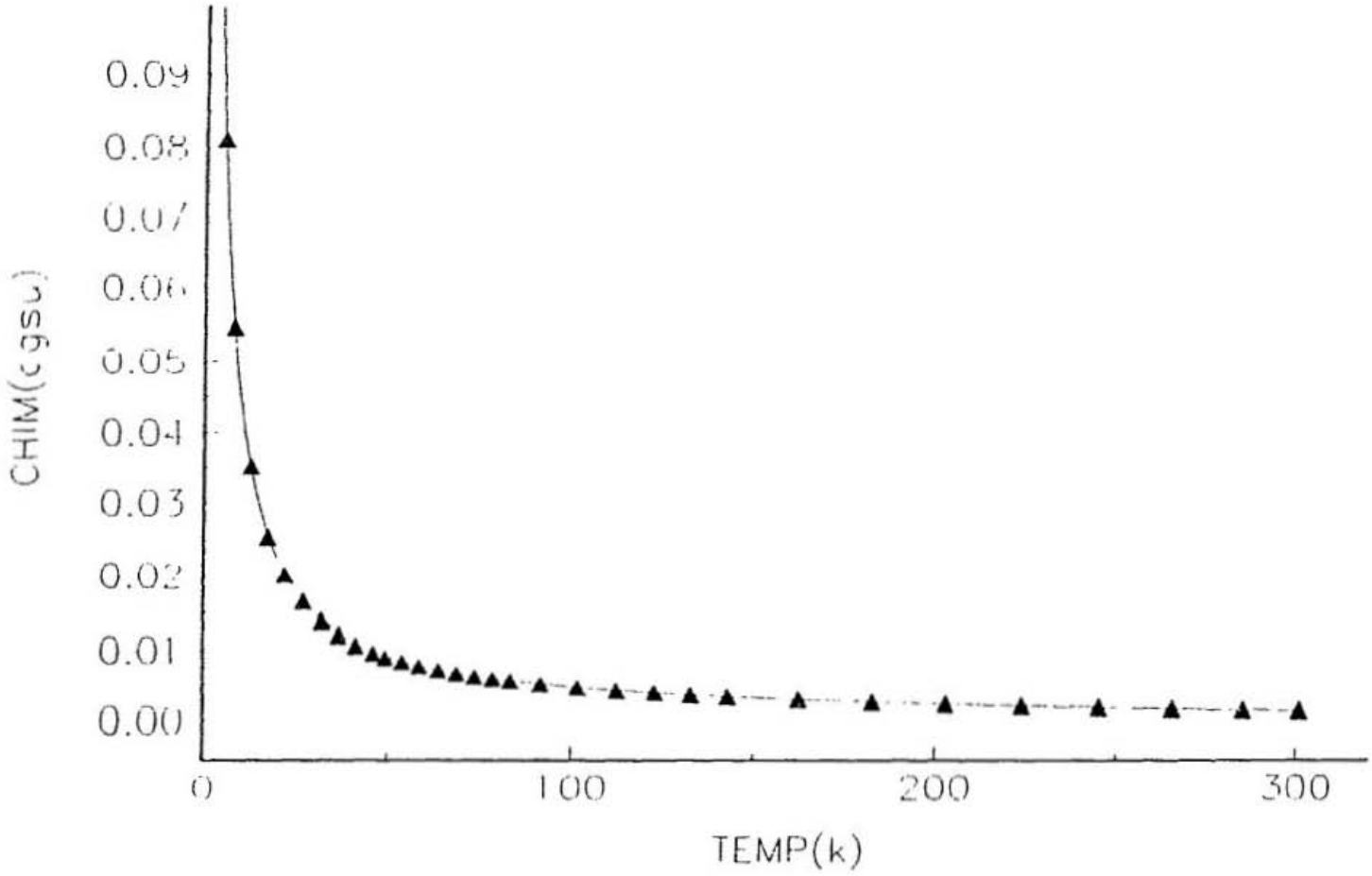


**Fig.6.2 Magnetic susceptibility data for $[Cu_2(C\text{-}I)Br_4].CH_3OH$ (34)**

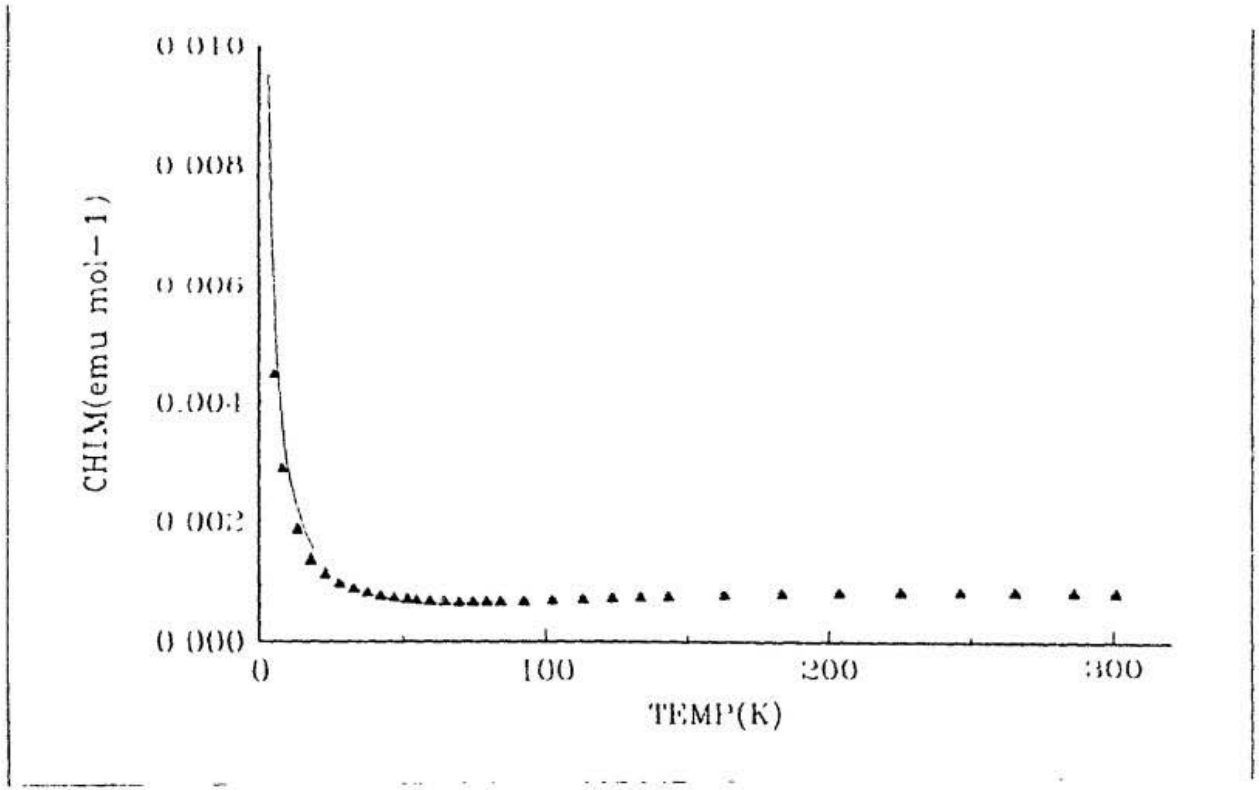


**Fig 6.3** Magnetic susceptibility data 1 for $[Cu_4(O\text{-}P)(\mu_2\text{-}OH)_2(\mu_2\text{-}NO_3)_2(NO_3)_2(H_2O)_2](NO_3)_2{\cdot}10H_2O$ **(37)**

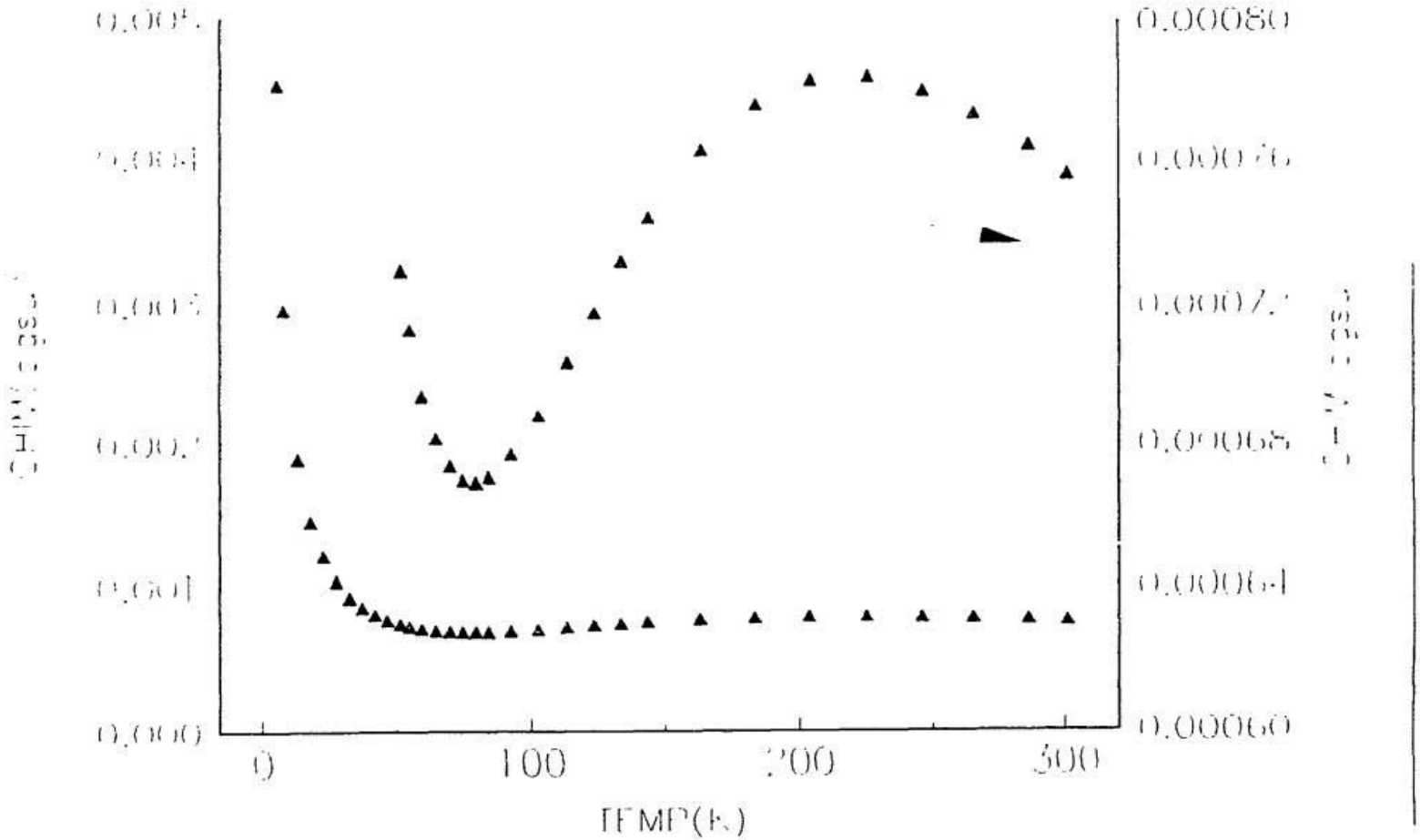


**Fig 6.3** Magnetic susceptibility data 2 for $[Cu_4(O\text{-}P)(\mu_2\text{-}OH)_2(\mu_2\text{-}NO_3)_2(NO_3)_2(H_2O)_2](NO_3)_2{\cdot}10H_2O$ **(37)**

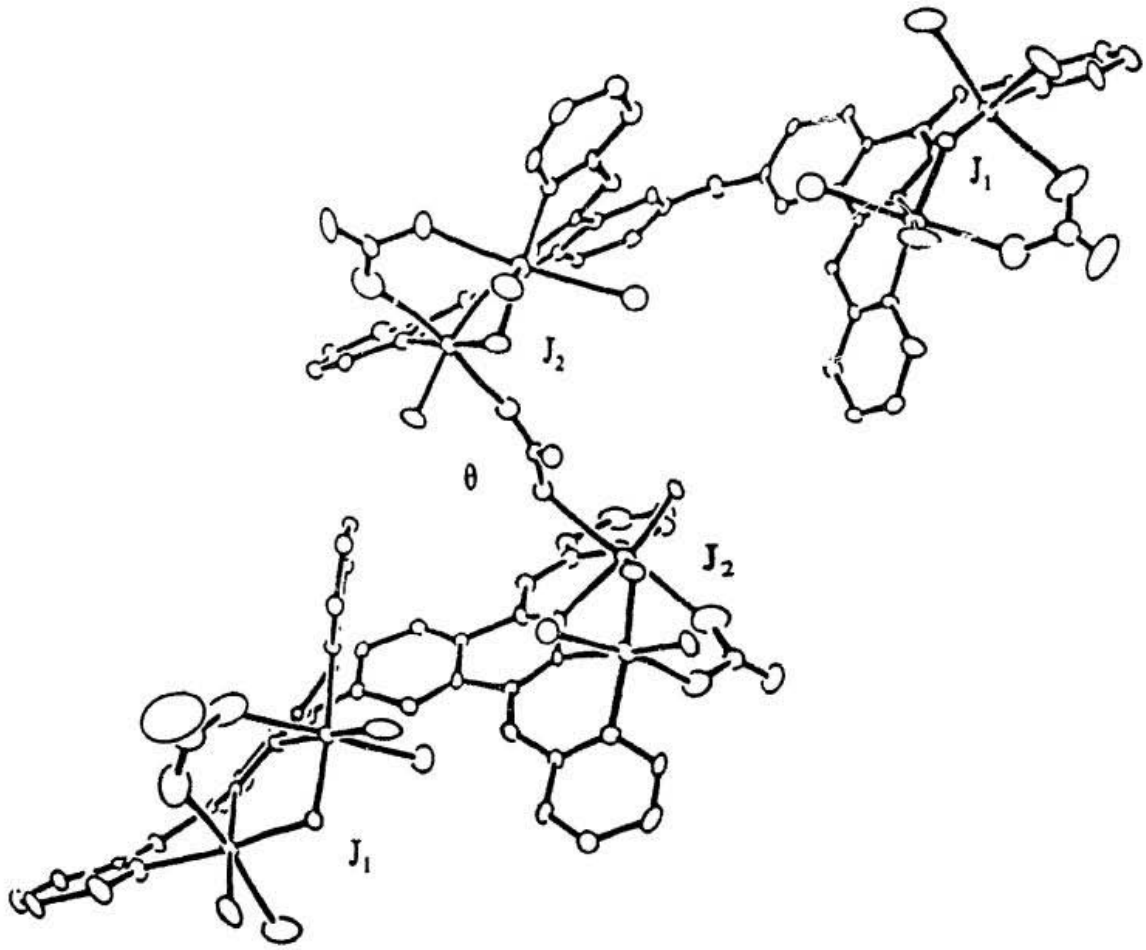


**Fig.6.4** Magnetic model for

$[Cu_4(O\text{-}P)(\mu_2\text{-}OH)_2(\mu_2\text{-}NO_3)_2(NO_3)_2(H_2O)_2](NO_3)_2 \cdot 10H_2O$(**37**)

## 6.2 Electrochemistry of the complexes

The redox chemistry of some complexes has been studied by cyclic voltammetry in dried dimethylformamide (DMF-tetraethylammonium perchlorate, Pt, SSCE) at a scan rate 200 mV/s and the results are presented in Table 6.2. They exhibit highly non-reversible redox waves at positive potentials, which are associated with $Cu^{II}/Cu^{I}$ redox processes. The positive $E_{1/2}$ is consistent with other dinuclear copper(II) complexes with similar $N_4$ monomeric diazine ligands.[52,105] These antiferromagnetically coupled, hydroxide bridged polynuclear Cu(II) complexes, involving heterocyclic nitrogen donors which exhibit multi-electron transfer at high positive potentials, have application as model compounds of Type III multi-copper enzymes, which also exhibit electrochemical processes at positive potentials.

Table 6.2 Electrochemical data of complexes

| Compounds | $E_{1/2}$(V) | $\Delta E_p$(V) |
|---|---|---|
| $[Cu_4(C\text{-}P)(\mu_2\text{-}OH)_2(\mu_2\text{-}NO_3)_2(H_2O)_2(NO_3)_2]$ | | |
| $(NO_3)_2 \cdot 4H_2O$ (**35**) | 0.377 | 0.542 |
| $[Cu_4(O\text{-}P)(OH)_2(NO_3)_6] \cdot H_2O$ (**36**) | 0.371 | 0.334 |
| $[Cu_4(O\text{-}P)(OH)_2Cl_6] \cdot 4H_2O$ (**39**) | 0.385 | 0.770 |
| $[Cu_4(C\text{-}P)(OH)_2Br_6] \cdot 2CH_3CH_2OH$ (**40**) | 0.42 | 0.380 |
| $[Cu_6(G\text{-}P)(OH)_3Br_9] \cdot 6H_2O$ (**42**) | 0.364 | 0.727 |
| $[Cu_6(G\text{-}P)(OH)_3(NO_3)_9] \cdot 12H_2O$ (**43**) | 0.290 | 0.400 |
| $[Cu_8(P\text{-}P)(OH)_4(NO_3)_{12}] \cdot 8CH_3OH$ (**47**) | 0.195 | 0.330 |

# Chapter 7 STAR-LIKE SYSTEM

In an attempt to link groups of spin-coupled dinuclear copper centres in such a way that the spin-exchange effects might be extended to produce "polymagnets", we have designed ligands in which phthalazine-like ($N_4$) groups are attached peripherally to a phthalocyanine core (Scheme 7.1). Having two metals attached to each phthalazine moiety and with all four dinuclear centres attached to the highly conjugated phthalocyanine ring could create a possibility that all eight copper(II) ions would be coupled together magnetically. Also, with a metal coordinated in the phthalocyanine cavity, the creation of nonanuclear species could lead to unusual magnetic effects involving the central metal as well, depending on its identity.

A new category of highly conjugated polyphthalazine ligands has been synthesized by starting with octacyanophthalocyanine, conversion to the corresponding tetraisoindoline and finally to the tetraphthalazine on reaction with hydrazine. (Scheme 7.1)

Scheme 7.1 Synthesis of Star-like Polyisoindoline and Polyphthalazine

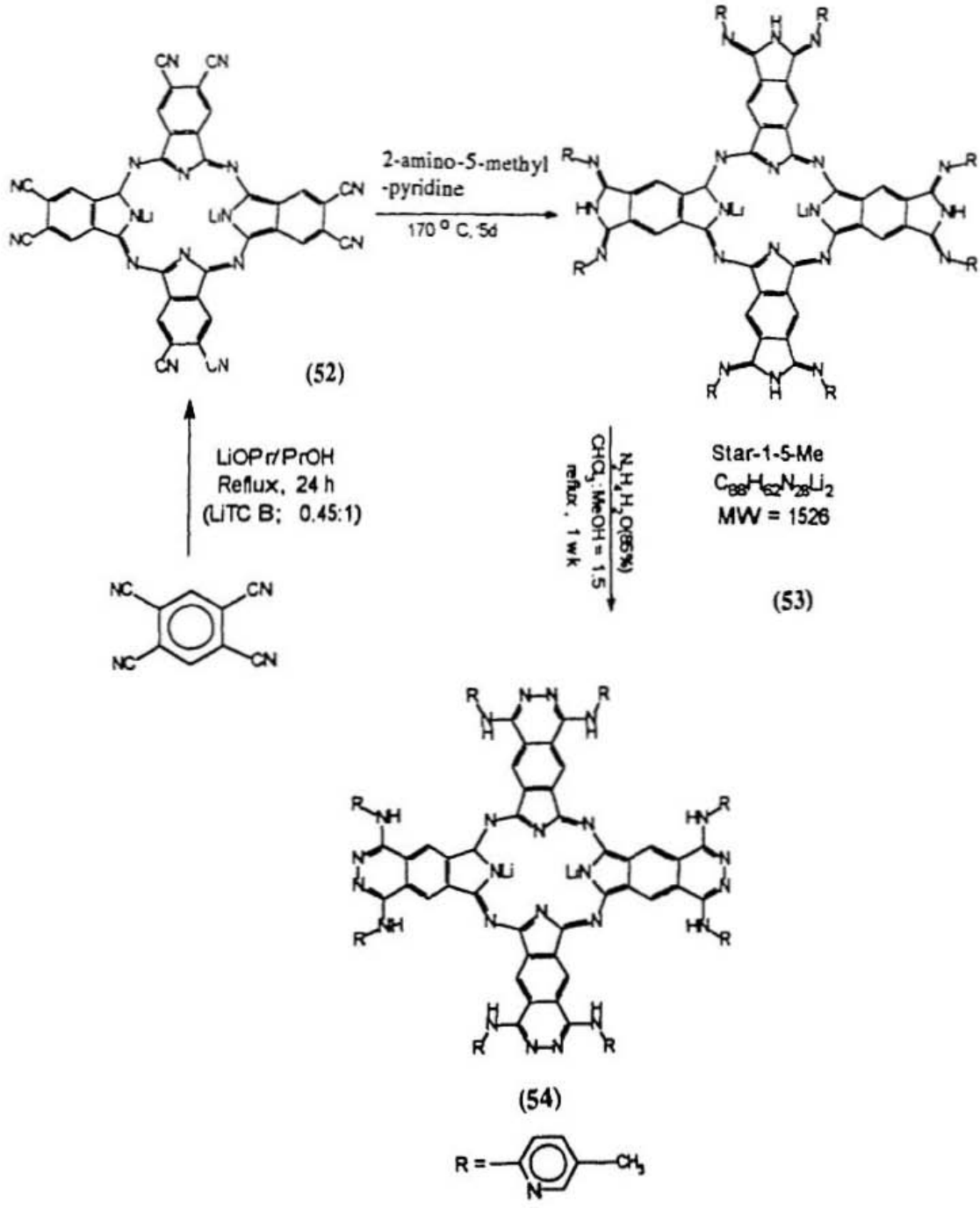

## 7.1 Synthesis and characterization of star-like polyphthalonitrile (S-CN) (52)

A solution of lithium (99.7mg, 14.4 mmol) dissolved in 1-propanol (380 mL) under a dry nitrogen atmosphere, was added dropwise very slowly to a refluxing solution of tetracyanobenzene (4.3 g, 24.2 mmol) in 1-propanol (1.0 L) over a period of 24 hrs. The solvent was then removed leaving a dark blue solid (3.5 g), which was soxhlet extracted in carbon tetrachloride (300 mL) to remove impurities. Yield 80.0%. IR($cm^{-1}$): 2231(s)($\gamma_{CN}$), 722.3(s), 906.5(s), 1052.1(s), 1116.7(s), 1303.8(s), 1377.1(vs), 1462.0(vs), 1596.0(s), 1665.4(s). UV/VIS spectrum: $\lambda_{max}$=700 nm (in dimethyl sulfoxide solution).

## 7.2 Star-like polyisoindoline (S-I) (53)

An excess of 2-amino-5-methyl-pyridine (11.00 g, 0.1 mol) was mixed with S-CN (1.00 g, 1.38 mmol) and fused at 170°C in the presence of a catalytic amount of $P_2S_5$ under nitrogen, for 120 hrs, then refluxed with 200 mL diethyl ether. The unreacted starting material was removed by filtration (soluble) and the remaining solid washed thoroughly with acetone to remove further impurity. A dark solid (1.90 g) was obtained, which was soxhlet extracted with chloroform

(150 mL) for 24 hrs. The solvent was evaporated leaving 0.9 g (0.59 mmol) of a dark solid, which was washed thoroughly with methanol and dried under vacuum. Yield 42.8%. mp > 290°C. IR($cm^{-1}$): 1048.5(s), 590.2(s), 722.3(s), 834.2(m), 1117.7(s), 1244.0(s), 1303.8(s), 1377.1(vs), 1464.0(vs), 1583.5(s), 1586.4(s), 1621.1(s), 1716.6(s), 1768.6(s). UV/VIS spectrum: $\lambda_{max}$=620 nm. The Cosy NMR spectrum of star-like polyisoindoline is shown in Fig.7.1. Anal. Calcd for $C_{98}H_{102}N_{28}O_{10}Li_2$ $10CH_3OH$: C, 63.77; H, 5.57; N, 21.25. Found: C, 64.92; H, 4.68; N, 20.43.

### 7.3 Star-like polyphthalazine (54)

S-I (0.70 g, 0.46 mmol) was dissolved in a mixture of chloroform/methanol (50 mL/120 mL), 12 mL aqueous hydrazine (85%) was added and the reddish solution refluxed for 120 hrs. A small amount of black starting material was filtered off and the volume of the filtrate reduced to about 20 mL. A dark yellow solid appeared, which was filtered off, washed with methanol and dried under vacuum. Yield 0.4 g, 54.3%. $\lambda_{max}$=730 nm, 430 nm in DMF solution. Anal. Calcd for $C_{92}H_{102}N_{32}O_{14}Li_2 \cdot 8H_2O \cdot 8CH_3OH$: C, 58.05; H, 5.79; N, 22.57. Found: C, 58.29; H, 4.59; N, 22.74. Molecular ion and reasonable fragments were found

in the FAB mass spectrum: 1587($M^+$, 0.2%; calcd 1586.8), 1488 (0.2%), 1419 (0.2%), 1327 (0.4%), 1286 (0.4%), 580 (6.3%), 306 (0.4%), 243 (6.8%), 176 (12%), 154 (97.2%), 136 (100%). Cyclic voltammogram (Fig. 7.2) was recorded in DMF (dimethyl formamide) and tetraethylammonium perchlorate as electrolyte by using Pt/C/SCE electrochemical system. The EPR spectrum of S-P in DMSO (dimethyl sulfoxide) was recorded at room temperature and at 77 K and is shown in Fig. 7.3. g=2.00, which indicates that this highly conjugated molecule is a stable weak radical similar to the lithium phthalocyanine radical.[106,107]

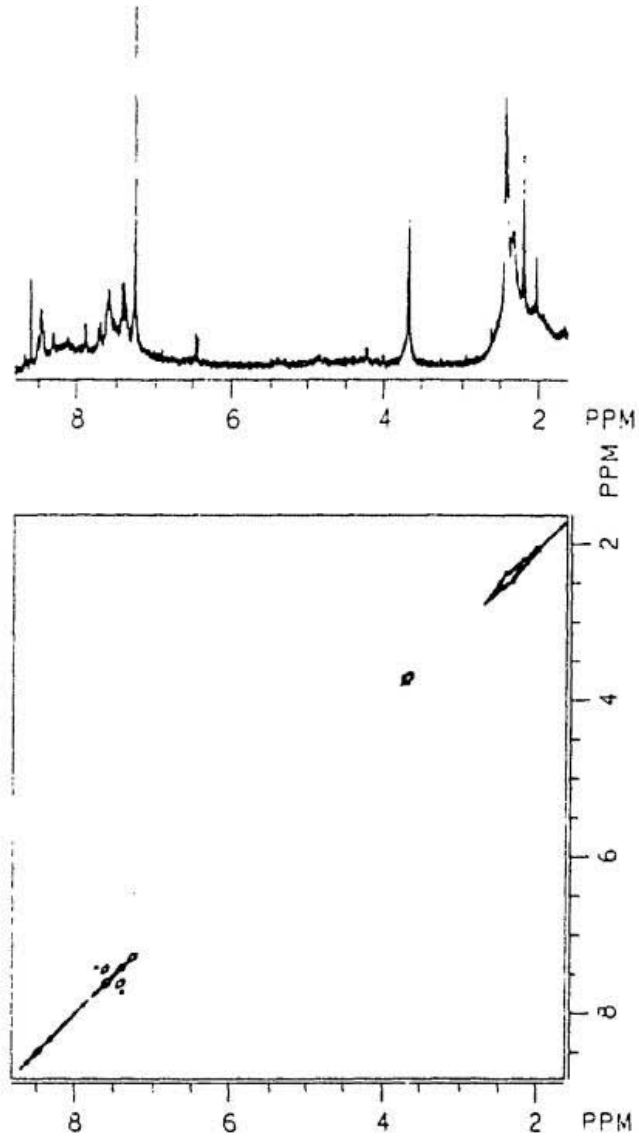


**Fig.7.1** Cosy NMR of S-I **(53)**

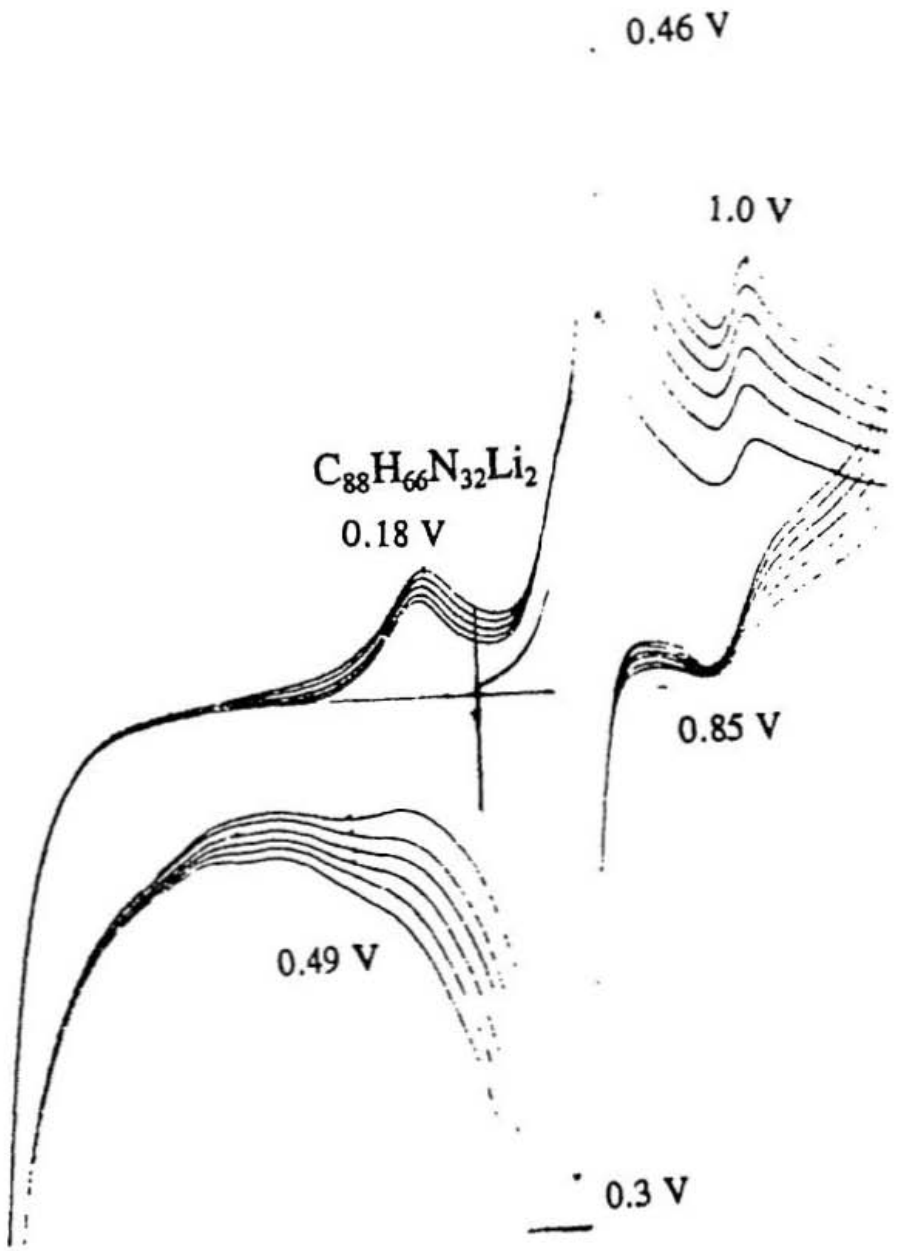


Fig.7.2 Cyclic voltammogram of S-P (54)

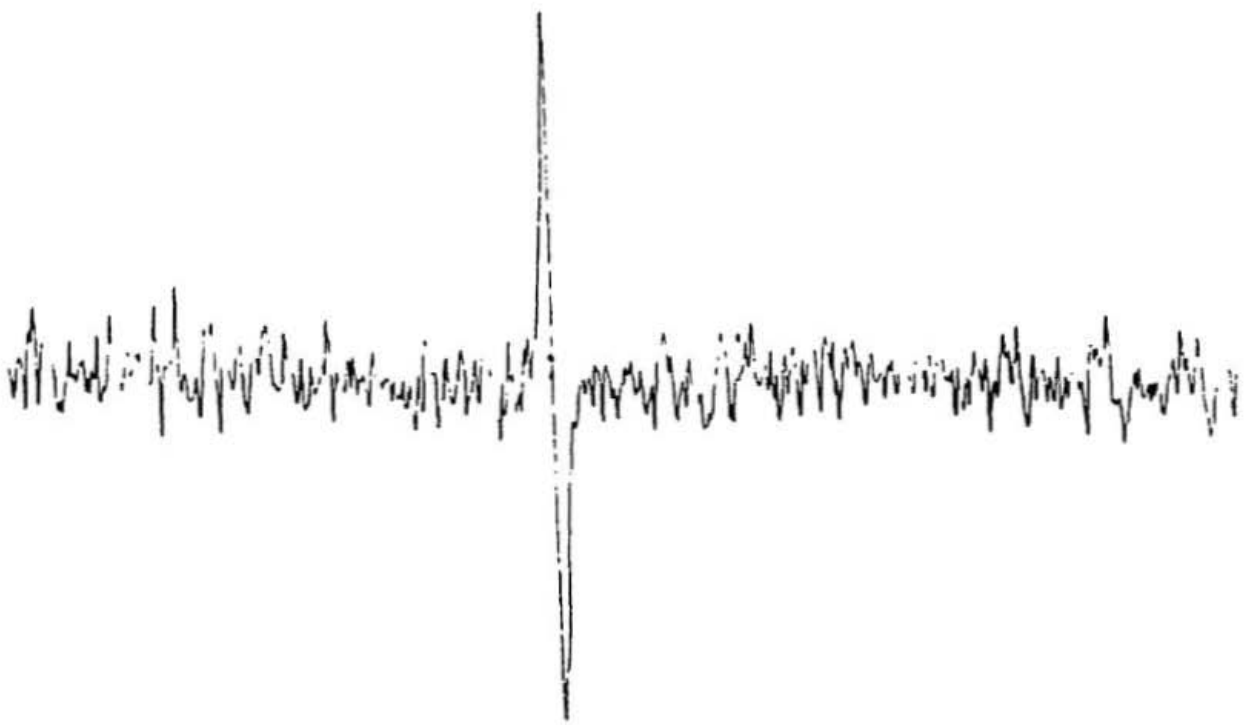

**Fig.7.3** X-Band ESR spectrum of S-P (**54**) in DMSO at 77 K (9.52 GHz)

## Part 3 CONCLUSION

1. Two new polyphthalonitriles and ten novel polyisoindolines and polyphthalazines have been synthesized and characterized.
2. A variety of binuclear, tetranuclear, hexanuclear and octanuclear Cu(II) complexes have been successfully synthesized by the reaction of polynucleating ligands with Cu(II) salts and their structure, magnetochemistry and electrochemistry have been studied.
3. These polynuclear complexes are antiferromagnetically coupled within the binuclear units but electron communication across the ligand framework is non-existent.
4. A new star-like lithium phthalocyaninate peripherally substituted with isoindoline and phthalazine fragments has been synthesized.

## REFERENCES


1. R. Dagani, C&EN, April 12, **1993**, 26.
2. J.S. Lindsay, New. J. Chem., **1991**, 15, 153.
3. H.-B. Mekelburger, W. Jaworek, and F. Vögtle, Angew. Chem., Int. Ed. Engl., **1992**. 31, 12.
4. H.-J. Schneider, H. Durr in "Frontiers in Supramolecular Organic Chemistry and Photochemistry", VCH, 1991.
5. D.J. Cram, Angew. Chem.Int. Ed. Engl., **1986**, 25, 1039.
6. J.-M. Lehn, J. Malthete, A.-M. Levelut, J. Chem. Soc., Chem. Commun., **1985**, 1794.
7. R.O. Fox. Jr., F.M. Richards, Nature, **1982**, 300, 325.
8. L. Jullien, J.-M. Lehn, Tetrahedron Lett., **1988**, 3803.
9. M.R. Wasielewski, Chem. Rev., **1992**, 92, 435-461.
10. D.H. Busch, Chem. Rev., **1993**, 93, 847-860.
11. S. Serroni, G. Denti, S. Campagna, A. Juris, M. Ciano and V. Balzani, Angew. Chem. Int. Ed. Engl. **1992**, 31, 1493.
12. V. Soghomonian, Q. Chen, R.C. Haushalter, J. Zubieta, C.J. O'Connor, Sience, **1993**, 259, 1596.

13. J.-M. Lehn, A. Rigault, J. Siegel, J. Harrowfield, B. Chevrier, D. Moras, Proc. Natl. Acad. Sci. USA, **1987**, 84, 2565.

14. J.-M. Lehn, A. Rigault, Angew. Chem., **1988**, 100, 1121.

15. J.-M. Lehn, A.Rigault, Angew. Chem.,Int. Ed. Engl., **1988**, 27, 1095.

16. V. McKee and S.S. Tandon, Inorg. Chem., **1989**, 28, 2901.

17. S.S. Tandon, L.K. Thompson and J.N. Bridson, J. Chem. Soc., Chem. Commun., **1992**, 911.

18. S.S. Tandon, S.K. Mandal, L.K. Thompson and R.C. Hynes, Inorg.Chem., **1992**, 31, 2215.

19. G.R. Newkome, F. Cardullo, E.C. Constable, C.N. Moorefield and M.W.C. Thompson, J. Chem. Soc., Chem. Commun., **1993**, 925.

20. C.P. Landee in "Organic and Inorganic Low Dimensional Crystalline Materials" (Eds.: P.Delhaes, M.Drillon) (NATO ASI Ser. 1987), p168.

21. O. Kahn in D. Gatteschi, O. Kahn, J.S. Miller and F. Palacio (Eds.), "Magnetic Molecular Materials", NATO ASI Series 198; Kluwer, Dordrecht, The Netherlands, 1991.

22. L.J.de Jongh in "Magnetic Properties of Layered Transition Metal Compounds" Vol.9 (Ed.: L.J.de Jongh), Kluwer, Dordrecht, 1990.

23. J.J. Borras-Almenar, E. Coronado, C.J. Gomez-Garcia, and L. Ouahab, Angew. Chem. Int. Ed. Engl., **1993**, 32, 561.

24. H-B. Mekelburger, W. Jaworek and F. Vögtle, Angew. Chem. Int. Ed. Engl., **1992**, 31, 1571.

25. S. Campagna, G. Denti, S. Serroni, M. Ciano, A. Juris and V. Balzani, Inorg. Chem., **1992**, 31, 2982 and references therein.

26. C.S. Veláquez, G.A. Fox, W.E. Broderick, K.A. Anderson, O.P. Anderson, A. G.M. Barrett and B.M. Hoffman, J. Am. Chem. Soc., **1992**, 114, 7416.

27. M. Koçak, A. Cihan, A.İ. Okur and Ö. Bekâroğlu, J. Chem. Soc., Chem. Commun., **1991**, 577.

28. A. Gürek, V. Ahsen, A. Gül and Ö. Bekâroğlu, J. Chem. Soc., Dalton Trans., **1991**, 3367.

29. V. McKee and W.B. Sheppard, J. Chem. Soc., Chem. Commun., **1985**, 158.

30. V. McKee and S.S. Tandon, J. Chem. Soc., Dalton Trans., **1991**, 221.

31. B.F. Hoskins, R.R. Robson and P.D. Smith, J. Chem. Soc., Chem. Commun., **1990**, 488.

32. S.S. Tandon, S.K. Mandal, L.K. Thompson and R.C. Hynes, J. Chem. Soc., Chem. Commun., **1991**, 1572.

33. K.D. Karlin, R.W. Cruse, Y. Gultneh, A. Farooq, J.C. Haynes, J. Zubieta, J. Am. Chem. Soc., **1987**, 109, 2668-2679.

34. R.R. Jacobson, I. Tyklár, A. Farooq, K.D. Karlin, S. Liu and J. Zubieta, J Am. Chem. Soc., **1988**, 110, 3690.

35. N. Kitajima, T. Koda, S. Hashimoto, T. Kitagawa, Y. Moro-oka, J. Chem. Soc., Chem. Commun., **1988**, 151-152.

36. N. Kitajima, K. Fujisawa, C. Fujimoto, Y. Moro-oka, S. Hashimoto, K. Toriumi and A. Nakamura, J. Am. Chem. Soc., **1992**, 114, 1277-1291.

37. N. Kitajima, T. Koda, Y. Iwata, Y. Moro-oka, J. Am. Chem. Soc., **1990**, 112, 8833-8839.

38. N. Kitajima, T. Koda, S. Hashimoto, T. Kitagawa, Y. Moro-oka, J. Am. Chem. Soc., **1991**, 113, 5664-5671.

39. W.P.J. Gaykema, A. Volbeda and W.G.J. Hol, J. Mol. Biol., **1985**, 187, 255-275.

40. A. Volbeda and W.G.J. Hol, J. Mol. Biol., **1989**, 209, 249-279.

41. P.A. Vigato, S. Tamburini, Coord. Chem. Rev., **1990**, 29.

42. L.K. Thompson, V.T. Chacko, J.A. Elvidge, A.B.P. Lever and R.V. Parish, Can. J. Chem., **1969**, 47, 4141.

43. G. Marongiu and E.C. Lingafelter, Acta Crystallogr., Sect. B, **1982**, 38, 620.

44. L.K. Thompson, Can. J. Chem., **1983**, 61, 579.

45. L.K. Thompson, F.W. Hartstock, P. Robichaud, and A.W. Hanson,

Can. J. Chem., **1984**, 62, 2755.

46. L.K. Thompson, A.W. Hanson, and B.S. Ramaswamy, Inorg. Chem., **1984**, 23, 2459.

47. L.K. Thompson, T.C. Woon, D.B. Murphy, E.J. Gabe, F.L. Lee, and Y. Le Page, Inorg. Chem., **1985**, 24, 4719.

48. M. Ghedini, G.De Munno, G. Bruno, A.M.Manotti Lanfredi, and A. Tiripicchio, Inorg. Chim. Acta, **1982**, 57, 87.

49. P. Dapporto, G.De Munno, G.Bruno, and M. Romeo, Acta Crystallogr., Sect. C, **1983**, 39, 718.

50. P. Dapporto, G.De Munno, A. Sega and L. Mealli, Inorg. Chim. Acta, **1984**, 83, 171.

51. G. De Munno, and G. Denti, Acta Crystallogr., Sect. C, **1984**, 40, 616.

52. T.C. Woon, R. McDonald, S.K. Mandal, L K. Thompson, S.P. Connors and A.W. Addison, J. Chem. Soc., Dalton Trans., **1986**, 2381.

53. A.B.P. Lever, B.S. Ramaswamy and S.R. Pickens, Inorg. Chim. Acta, **1980**, 46, L59.

54. W.J. Stratton, D.H. Busch, J. Am. Chem. Soc., **1960**, 82, 4834.

55. W.J. Stratton, Inorg. Chem., **1970**, 9, 517.

56. W.J. Stratton, P.J. Ogren, Inorg. Chem., **1970**, 9, 2588.

57. C.J. O'Connor, R.J. Romananch, D.M. Robertson, E.E. Eduok, F.R. Fronczek, Inorg. Chem., **1983**, 22, 449.

58. T.C. Woon, L.K. Thompson, P. Robichaud, Inorg. Chim. Acta., **1984**, 90, 201.

59. F.S. Keij, R.A.G.de Graaff, J.G. Haasnoot, J. Reedijk, J. Chem. Soc. Dalton Trans., **1984**, 2094.

60. R. Prins, P.J.M.W.L. Birker, J.G. Haasnoot, G.C. Verschoor, J. Reedijk, Inorg. Chem., **1985**, 24, 4128.

61. P.W. Ball, A.B. Blake, J. Chem. Soc. A, **1969**, 1415.

62. P.W. Ball, A.B. Blake, J. Chem. Soc., Dalton Trans., **1974**, 852.

63. A.M.Manotti Lanfredi, A. Tiripicchio, M. Ghedini, G. De Munno, Acta Crystallogr. Sect. B, **1982**, 38, 1165.

64. S.S. Tandon, L.K. Thompson and R.C. Hynes, Inorg. Chem., **1992**, 31, 2210.

65. S. K. Mandal, L. K. Thompson, M. J. Newlands, F. L. Lee, Y. Le Page, J-P. Charland and E. J. Gabe, Inorg. Chim. Acta, **1986**, 122, 199.

66. L. K. Thompson, S. K. Mandal, E. J. Gabe, F. L. Lee and A. W. Addison, Inorg. Chem., **1987**, 26, 657.

67. L. K. Thompson, S. K. Mandal, L. Rosenberg, F. L. Lee and E. J. Gabe, Inorg. Chim. Acta, **1987**, 133, 81.

68. S. K. Mandal, L. K. Thompson, E. J. Gabe, F. L. Lee and J-P. Charland, Inorg. Chem., **1987**, 26, 2384.

69. J.C. Dewan and L.K. Thompson, Can. J. Chem., **1982**, 60, 121.

70. D.V. Bautista, J.C. Dewan and L.K. Thompson, Can. J. Chem., **1982**, 60, 2583.

71. Y. Zhang, L.K. Thompson, M. Bubenik and J.N. Bridson, J. Chem. Soc., Chem. Commun., in press.

72. G. Bullock, F.W. Hartstock and L.K. Thompson, Can. J. Chem., **1983**, 61, 57.

73. L.K. Thompson, Can. J. Chem., **1983**, 61, 579.

74. F.W. Hartstock and L.K. Thompson, Inorg. Chim. Acta, **1983**, 72, 227.

75. P. Robichaud and L.K. Thompson, Inorg. Chim. Acta, **1984**, 85, 137.

76. L.K. Thompson, F.W. Hartstock, L. Rosenberg and T.C. Woon, Inorg. Chim. Acta, **1985**, 97, 1.

77. L. K. Thompson, F. L. Lee and E. J. Gabe, Inorg. Chem., **1988**, 27, 39.

78. M. Melnik, Coord. Chem. Rev., **1982**, 42, 259.

79. M. Kato and Y. Muto, Coord. Chem. Rev., **1988**, 92, 45.

80. C.J. O'Connor, Prog. Inorg. Chem., **1983**, 29, 203.

81. O. Kahn, Angew. Chem. Int. Ed. Engl., **1985**, 24, 834.

82. D.J. Hodgson, Prog. Inorg. Chem., **1975**, 19, 173.

83. V.H. Crawford, H.W. Richardson, J.R. Wasson, D.J. Hodgson and W.E. Hatfield, Inorg. Chem., **1976**, 15, 2107.

84. O. Kahn, S. Sikorav, J. Gouteron, S. Jeannin and Y. Jeannin, Inorg. Chem., **1983**, 22, 2877.

85. J. Comarmond, P. Plumiere, J.-M. Lehn, Y. Agnus, R. Louis, R. Weiss, O. Kahn and I. Morgenstern-Badarau, J. Am. Chem. Soc., **1982**, 104, 6330.

86. S. Sikorav, I. Bkouchewaksman, O. Kahn, Inorg. Chem., **1984**, 23, 490.

87. W.A. Nevin, W. Liu, S. Greenberg, M.R. Hempstead, S.M. Marcuccio, M. Melnik, C.C. Leznoff, A.B.P. Lever, Inorg. Chem., **1987**, 26, 891.

88. M. Bell, A.J. Edwards, B.F. Hoskins, E.H. Kachab, R. Robson, J. Am. Chem. Soc., **1989**, 111, 3603.

89. W.O. Siegl, J. Heterocyclic Chem., **1981**, 18, 1613.

90. C.C. Leznoff, P.I. Svirskaya, B. Khouw, R.L. Cerny, P. Seymour, A.B.P. Lever, J. Org. Chem., **1991**, 56, 82.

91. S.M. Marcuccio, P.I. Svirskaya, S. Greenberg, A.B.P. Lever, and C.C.

Leznoff and K.B. Tomer, Can. J. Chem., **1985**, 63, 3057.

92. S.K. Mandal, L.K. Thompson and S. Ray, J.Heterocyclic Chem., **1992**, 29, 1671.

93. D.V. Bautista, G. Bullock, F.W. Harstock and L.K. Thompson, J. Heterocyclic. Chem., **1983**, 20, 345.

94. A.B.P. Lever, E. Mantovani, B.S. Ramaswamy, Can. J. Chem., **1971**, 49, 1957.

95. D.M. Adams and A. Squire, J. Organometal. Chem., **1973**, 63, 381.

96. G. Bullock, A. Cook, A. Foster, L. Rosenberg and L.K. Thompson, Inorg. Chim. Acta., **1985**, 103, 207-215.

97. N. Walker and D. Stuart, Acta. Crystallogr., **1983**, A39, 158.

98. C.J. Gilmore, J. Appl. Crystallogr., **1983**, A39, 158.

99. P.T. Beurskens, Dirdif: Technical Report 1984/1, Crystallography Laboratory, Toernooiveld, 6525 Ed Nijmegen, Netherlands.

100. D.T. Cromer and J.T.Waber, J.T. "International Table for X-ray Crystallography". Vol. IV. The Kynoch Press, Birmingham, U.K., 1974, Table 2.2A.

101. J.A. Ibers and W.C. Hamilton, Acta Crystallogr., **1974**, 17, 781.

102. D.T. Cromer, "International Table for X-ray Crystallography". Vol. IV.

The Kynoch Press, Birmingham, U.K., 1974, Table 2.3.1.

103. Texsan-Texray structure analysis package, Molecular Structure Corporation, 1985.

104. B. Bleaney, K.D. Bowers, Proc. R. Soc. London, **1952**, A214, 451.

105. S.K. Mandal, T.C. Woon, L.K. Thompson, M.J. Newlands and E.J. Gabe, Aust. J. Chem., **1986**, 39, 1007.

106. P. Turek, M. Moussavi, and J.-J. Andre, Europhysics Letters, **1989**, 8, 275-280.

107. P. Turek, J.-J. Andre, M. Moussavi and G. Fillion, Mol. Cryst. Liq. Cryst., **1989**, 176, 535-546.

## APPENDIX A

## SOME X-RAY DATA FOR COMPLEXES

Table SI.I Atomic positional parameters X, Y, Z and B(eq) values for complex (35)

| atom | x | y | z | B(eq) |
|---|---|---|---|---|
| Cu(1) | 0.6502(1) | 0.18917(5) | 0.96651(9) | 2.9(1) |
| Cu(2) | 0.4533(1) | 0.20831(5) | 0.88968(9) | 2.8(1) |
| Cu(3) | 0.5231(1) | 0.18859(5) | 0.57223(9) | 2.6(1) |
| Cu(4) | 0.3267(1) | 0.16651(5) | 0.50120(9) | 2.8(1) |
| Cu(5) | 0.0931(2) | 0.08075(5) | -0.0203(1) | 3.7(1) |
| Cu(6) | -0.0759(2) | 0.05617(5) | 0.06848(9) | 3.3(1) |
| Cu(7) | 0.0911(1) | 0.05621(5) | 0.39744(8) | 2.5(1) |
| Cu(8) | -0.1045(1) | 0.07227(4) | 0.47558(9) | 2.5(1) |
| O(1) | 0.5126(7) | 0.2022(2) | 0.9698(4) | 2.9(2) |
| O(2) | 0.4642(6) | 0.1781(2) | 0.4930(4) | 2.4(2) |
| O(3) | 0.4273(7) | 0.0136(3) | 0.7943(5) | 3.5(2) |
| O(4) | 0.5605(8) | -0.0008(3) | 0.6983(5) | 4.0(2) |
| O(5) | -0.0374(7) | 0.0619(2) | -0.0152(4) | 3.3(2) |

| | | | | |
|---|---|---|---|---|
| O(6) | 0.0320(7) | 0.0599(2) | 0.4751(4) | 2.8(2) |
| O(7) | -0.1054(7) | 0.2498(3) | 0.1850(4) | 3.4(2) |
| O(8) | 0.0618(7) | 0.2436(2) | 0.2678(4) | 3.2(2) |
| O(9) | 0.6826(7) | 0.2137(2) | 1.0460(4) | 3.4(2) |
| O(10) | 0.2930(7) | 0.1862(2) | 0.4178(5) | 3.7(2) |
| O(11) | 0.0955(8) | 0.0668(3) | -0.1119(5) | 4.7(3) |
| O(12) | -0.1173(7) | 0.0560(2) | 0.5641(4) | 3.5(2) |
| O(13) | 0.9033(8) | 0.0665(3) | 0.8440(5) | 4.7(3) |
| O(14) | 0.4229(8) | 0.1646(3) | 0.3390(5) | 5.1(3) |
| O(15) | 0.5590(9) | 0.1816(3) | 0.1253(5) | 6.0(3) |
| O(16) | 0.6605(8) | 0.1361(3) | 0.0416(5) | 4.8(3) |
| O(25A) | 0.3389(7) | 0.2403(2) | 0.9187(4) | 2.9(2) |
| O(25B) | 0.1758(9) | 0.2397(3) | 0.9280(5) | 5.4(3) |
| O(25C) | 0.2546(7) | 0.1913(3) | 0.9072(5) | 3.7(2) |
| O(26A) | 0.8011(8) | 0.2125(3) | 0.5253(5) | 3.8(2) |
| O(26B) | 0.6408(7) | 0.2174(2) | 0.5405(4) | 2.5(2) |
| O(26C) | 0.7152(7) | 0.1666(3) | 0.5567(5) | 3.7(2) |
| O(27A) | -0.339(1) | 0.0184(3) | 0.0281(6) | 6.4(3) |
| O(27B) | -0.2579(9) | 0.0682(3) | 0.0425(6) | 6.1(3) |

| | | | | |
|---|---|---|---|---|
| O(27C) | -0.1781(7) | 0.0179(2) | 0.0474(4) | 3.2(2) |
| O(28A) | 0.2021(7) | 0.0260(2) | 0.4332(4) | 2.9(2) |
| O(28B) | 0.356(1) | 0.0321(3) | 0.4617(6) | 6.4(3) |
| O(28C) | 0.2743(8) | 0.0773(3) | 0.4262(5) | 5.2(3) |
| O(29A) | 0.2971(7) | 0.2231(3) | 0.5565(4) | 3.3(2) |
| O(29B) | 0.3249(8) | 0.2796(3) | 0.5570(5) | 4.0(3) |
| O(29C) | 0.4497(8) | 0.2438(2) | 0.5670(5) | 3.5(2) |
| O(30A) | -0.1074(7) | -0.0351(3) | 0.4138(5) | 3.7(2) |
| O(30B) | 0.0029(9) | 0.0015(3) | 0.3851(5) | 4.7(3) |
| O(30C) | -0.1450(7) | 0.0201(3) | 0.4100(5) | 3.6(2) |
| O(31A) | 0.7378(8) | 0.0880(3) | 0.7428(5) | 4.0(2) |
| O(31B) | 0.7685(8) | 0.0869(3) | 0.6440(5) | 5.1(3) |
| O(31C) | 0.8784(8) | 0.0668(2) | 0.7100(4) | 3.4(2) |
| O(32A) | 0.6757(7) | 0.2557(2) | 0.3968(4) | 2.8(2) |
| O(32B) | 0.5235(9) | 0.2372(3) | 0.3849(5) | 4.8(3) |
| O(32C) | 0.6380(7) | 0.1996(3) | 0.4039(5) | 3.8(2) |
| O(33A) | 0.1841(8) | -0.0103(3) | 0.0963(5) | 4.1(3) |
| O(33B) | 0.1570(8) | 0.0432(3) | 0.0641(5) | 4.7(3) |
| O(33C) | 0.0319(8) | 0.0062(3) | 0.0795(5) | 3.7(2) |
| O(34A) | 0.119(1) | 0.0729(3) | 0.7442(6) | 6.8(3) |

| | | | | |
|---|---|---|---|---|
| O(34B) | 0.2160(8) | 0.0971(3) | 0.8099(5) | 4.6(3) |
| O(34C) | 0.256(1) | 0.0969(3) | 0.7148(6) | 6.9(3) |
| O(35A) | 0.695(1) | 0.1459(4) | 0.3039(7) | 8.1(4) |
| O(35B) | 0.713(1) | 0.1601(3) | 0.2068(6) | 6.2(3) |
| O(35C) | 0.5897(9) | 0.1799(3) | 0.2565(5) | 5.3(3) |
| O(36A) | 0.381(1) | 0.1730(4) | 0.1906(7) | 9.0(4) |
| O(36B) | 0.249(2) | 0.1529(5) | 0.155(1) | 14.2(7) |
| O(36C) | 0.270(1) | 0.1590(3) | 0.2492(7) | 7.0(4) |
| N(1) | 0.7913(8) | 0.1798(3) | 0.9480(5) | 2.2(2) |
| N(2) | 0.7556(8) | 0.1222(3) | 0.9092(5) | 2.4(3) |
| N(3) | 0.6141(8) | 0.1568(3) | 0 8961(5) | 1.9(2) |
| N(4) | 0.5218(8) | 0.1625(3) | 0.8677(5) | 2.2(2) |
| N(5) | 0.3919(8) | 0.1472(3) | 0.8002(5) | 2.6(3) |
| N(6) | 0.3981(8) | 0.2093(3) | 0.8041(5) | 2.7(3) |
| N(7) | 0.5739(8) | 0.1950(3) | 0.6584(5) | 2.6(3) |
| N(8) | 0.5880(8) | 0.1326(3) | 0.6709(5) | 2.4(3) |
| N(9) | 0.4583(9) | 0.1437(3) | 0.6005(5) | 2.6(3) |
| N(10) | 0.3674(8) | 0.1358(3) | 0.5735(5) | 2.2(3) |

Table SI.II Atomic positional parameters for complex (37)

| atom | x | y | z |
|---|---|---|---|
| Cu(1) | 0.60438(9) | 0.1694(1) | 1.0358(2) |
| Cu(2) | 0.53875(9) | 0.2451(1) | 1.0057(2) |
| Cu(3) | 0.75531(8) | 0.06527(8) | 0.5505(2) |
| Cu(4) | 0.85349(8) | 0.07970(8) | 0.5302(2) |
| O(1) | .5502(4) | 0.1873(5) | 0.977(1) |
| O(2) | 0.5798(5) | 0.1118(5) | 1.077(1) |
| O(3) | 0.4764(4) | 0.2315(5) | 1.002(1) |
| O(4) | 0.8110(4) | 0.0503(4) | 0.601(1) |
| O(5) | 0.7363(5) | 0.0062(4) | 0.580(1) |
| O(6) | 0.8894(5) | 0.0277(5) | 0.552(2) |
| O(7) | 0.7443(4) | 0.3084(4) | 0.697(1) |
| N(1) | 0.6623(5) | 0.1512(5) | 1.086(1) |
| N(2) | 0.6918(5) | 0.1963(5) | 0.960(1) |
| N(3) | 0.6266(5) | 0.2266(5) | 0.988(1) |
| N(4) | 0.5989(5) | 0.2611(5) | 0.985(1) |

| | | | |
|---|---|---|---|
| N(5) | 0.5840(6) | 0.3318(6) | 0.950(1) |
| N(6) | 0.5296(5) | 0.3033(6) | 1.044(1) |
| N(7) | 0.8933(5) | 0.1130(6) | 0.448(1) |
| N(8) | 0.8726(5) | 0.1805(5) | 0.504(1) |
| N(9) | 0.8162(4) | 0.1342(5) | 0.527(1) |
| N(10) | 0.7737(5) | 0.1274(5) | 0.541(1) |
| N(11) | 0.7089(5) | 0.1533(5) | 0.560(1) |
| N(12) | 0.6998(5) | 0.0826(5) | 0.487(1) |
| C(1) | 0.6684(8) | 0.1212(8) | 1.163(2) |
| C(2) | 0.706(1) | 0.1007(7) | 1.181(2) |
| C(3) | 0.7391(7) | 0.1091(7) | 1.120(2) |
| C(4) | 0.7337(7) | 0.1417(7) | 1.049(2) |
| C(5) | 0.6960(6) | 0.1627(7) | 1.033(2) |
| C(6) | 0.6628(6) | 0.2283(6) | 0.945(1) |
| C(7) | 0.6725(6) | 0.2656(6) | 0.884(1) |
| C(8) | 0.7077(5) | 0.2675(6) | 0.826(1) |
| C(9) | 0.7111(6) | 0.3036(7) | 0.761(1) |
| C(10) | 0.6832(6) | 0.3374(6) | 0.755(1) |
| C(11) | 0.6511(6) | 0.3363(7) | 0.815(2) |

| | | | |
|---|---|---|---|
| C(12) | 0.6448(6) | 0.3013(6) | 0.881(1) |
| C(13) | 0.6089(6) | 0.2962(7) | 0.944(2) |
| C(14) | 0.5487(7) | 0.3368(9) | 1.010(2) |
| C(15) | 0.5368(7) | 0.3833(8) | 1.025(2) |
| C(16) | 0.5018(9) | 0.387(1) | 1.086(2) |
| C(17) | 0.488(1) | 0.346(1) | 1.114(3) |
| C(18) | 0.498(1) | 0.307(1) | 1.101(3) |
| C(19) | 0.9174(8) | 0.0892(8) | 0.383(2) |
| C(20) | 0.9453(7) | 0.113(1) | 0.326(2) |
| C(21) | 0.948(1) | 0.156(1) | 0.335(3) |
| C(22) | 0.9252(6) | 0.1793(7) | 0.391(2) |
| C(23) | 0.8963(7) | 0.1569(7) | 0.445(2) |
| C(24) | 0.8331(6) | 0.1722(6) | 0.535(1) |
| C(25) | 0.8106(6) | 0.2076(6) | 0.579(1) |
| C(26) | 0.8303(6) | 0.2476(7) | 0.613(1) |
| C(27) | 0.8077(6) | 0.2793(6) | 0.656(1) |
| C(29) | 0.7453(5) | 0.2351(6) | 0.628(1) |
| C(30) | 0.7677(6) | 0.2003(6) | 0.586(1) |
| C(31) | 0.7503(5) | 0.1593(6) | 0.561(1) |
| C(32) | 0.6840(6) | 0.1239(7) | 0.505(2) |

| | | | |
|---|---|---|---|
| C(33) | 0.6418(6) | 0.1329(6) | 0.469(2) |